Stock Assessment of kingclip (*Genypterus blacodes*) in the Falkland Islands using *JABBA*

SA - 2024 - KIN

Daniel García

Natural Resources - Fisheries
Falkland Islands Government
Stanley, Falkland Islands

November 2024

García, D. (2024). Stock assessment of kingclip (*Genypterus blacodes*) in the Falkland Islands using *JABBA*. SA–2024–KIN. *Fisheries Department, Directorate of Natural Resources, Falkland Islands Government.* Stanley, Falkland Islands. 69 p.

Acknowledgements

Special thanks go to Jorge Ramos, Toni Trevizan, Erwan Saulnier, and specially to Frane Skeljo for comments, suggestions and discussions that helped to understand the fisheries of this species and improve the methodology and the final version of the report.

Distribution: Public Domain

Table of Contents

Stock assessment of kingclip (*Genypterus blacodes*) in the Falkland Islands using *JABBA*

Daniel García*

Fisheries Department, Directorate of Natural Resources, Falkland Islands Government, Bypass Road, Stanley FIQQ 1ZZ, Falkland Islands

*dgarcia@naturalresources.gov.fk

Summary

Kingclip (*Genypterus blacodes*) is a benthic demersal species found throughout the Southern Hemisphere. In the Southwest Atlantic it is found between 34°S and 55°S (Uruguayan, Argentine and Falklands Islands waters) and at depths between 50 m and 300 m. This top predator has low resilience and is therefore vulnerable to overexploitation. The recent assessment of the kingclip stock (Di Marco, 2022) showed low abundance, below the limit reference point. In this report, an assessment was conducted for the Falkland Islands waters fraction of the kingclip stock and for the entire stock, testing a range of abundance indices and their combinations (both fisheries dependant and independent) across successive model runs. The assessment was carried out using a Bayesian framework surplus production model in the *JABBA* package. The model estimates strongly depended on the abundance index used, underlining the need for a reliable abundance index when using a surplus production model. Different abundance indices led to contradictory estimates of stock status; therefore, the results of this study should be treated with caution. For a bycatch species such as kingclip, other approaches such as length-based methods should be assessed for comparison. Given its vulnerability to fishing pressure, precautionary management measures should be considered.

Introduction

Kingclip (*Genypterus blacodes*) is a benthic demersal species distributed throughout the southern hemisphere. It is an important component of fisheries in Australia, New Zealand, Chile and Argentina (Ward *et al.*, 2001). In the Southwest Atlantic, it is distributed between 34°S and 55°S and at depths of between 50 and 300 m (Cordo, 2004). During summer, kingclip shows strong aggregations off the Gulf of San Jorge (45°S - 47°S) and around the 100 m isobath (Villarino, 1998), where individuals congregate for reproduction (Sammarone, 2019). During cold months, spawning aggregations disappear and individuals disperse, with some concentrations at higher depths (Sammarone, 2023) and reaching Falkland Islands (FI) waters (Ramos & Winter, 2021).

Kingclip is a slow-growing and long-lived species; individuals as old as 30 years have been aged in the Southwest Atlantic (Cordo, 2004). Similar ages have been estimated for this species in New Zealand waters, with a maximum age of 35 years (Horn, 1993). Kingclip has a low resilience (slow growth, late maturation) to exploitation (Froese & Pauly, 2024), making it vulnerable to overexploitation.

Kingclip is an opportunistic top predator (trophic level ~4) that feeds on other benthic and demersal species, mainly fish and crustaceans. It shows an ontogenetic shift in diet with an increase in fish consumption and decrease in crustacean consumption (Bellegia *et al.*, 2023).

The L50% (length at which 50% of individuals are mature) for this species has been estimated to be 67.7 ± 0.43 cm total length for females and 66.2 ± 0.25 cm total length for males in the FI waters (Ramos & Winter, 2022), 70.5 cm for the Argentine waters (Cordo *et al.*, 2002), and in a range between 86 cm and 95 cm in the Southeast Pacific (Baker *et al.*, 2014), indicating variability due to environmental conditions or differences in historical fishing pressures.

In the Southwest Atlantic, the spawning season is from December to March, between 44°S and 48° S, and between 75 and 130 m depth (Sammarone, 2019). High concentrations of larvae and juveniles in the Gulf of San Jorge towards the end of the spawning period suggest it could be a nursery area (Sammarone, 2019). In the FI waters, the highest concentrations of kingclip are found in the north-west. During the reproductive season, about two thirds of the stock found in the FI waters moves to the spawning grounds in Argentine waters (Arkhipkin *et al.*, 2012). These migratory characteristics led to the assumption that the FI and Argentine stocks are the same (Ramos & Winter, 2022).

The biomass of kingclip is higher in the Argentine waters than in FI waters (Di Marco, 2022; Ramos & Winter, 2024). Catches from Argentina increased between 1985 and 2012, reached a maximum of 34,775 t in 1990, and steeply decreased from 2012 reaching about 2,000 t in 2019, indicating past overfishing and the inclusion of fishing restrictions since 2012 by the Argentine government (Figure 1). Catches in FI waters have been recorded since 1987 and have averaged 2,180 t per year (1987-2023), with a peak of 4,242 t in 2013 (Figure 1). Di Marco (2022) estimated that the total biomass of the Southwest Atlantic stock is close to the limit biomass reference point, and the reproductive biomass is below the limit reference point. A total catch limit of 3,821 t for

the entire Southwest Atlantic stock, including catches in FI waters, and a total catch limit of 10 t per vessel/trip or 3% of the total catch, whichever is lower, was proposed for the Argentine industrial fishery (Di Marco, 2022). Such restrictions highlight the concern about the state of the Southwest Atlantic kingclip stock.

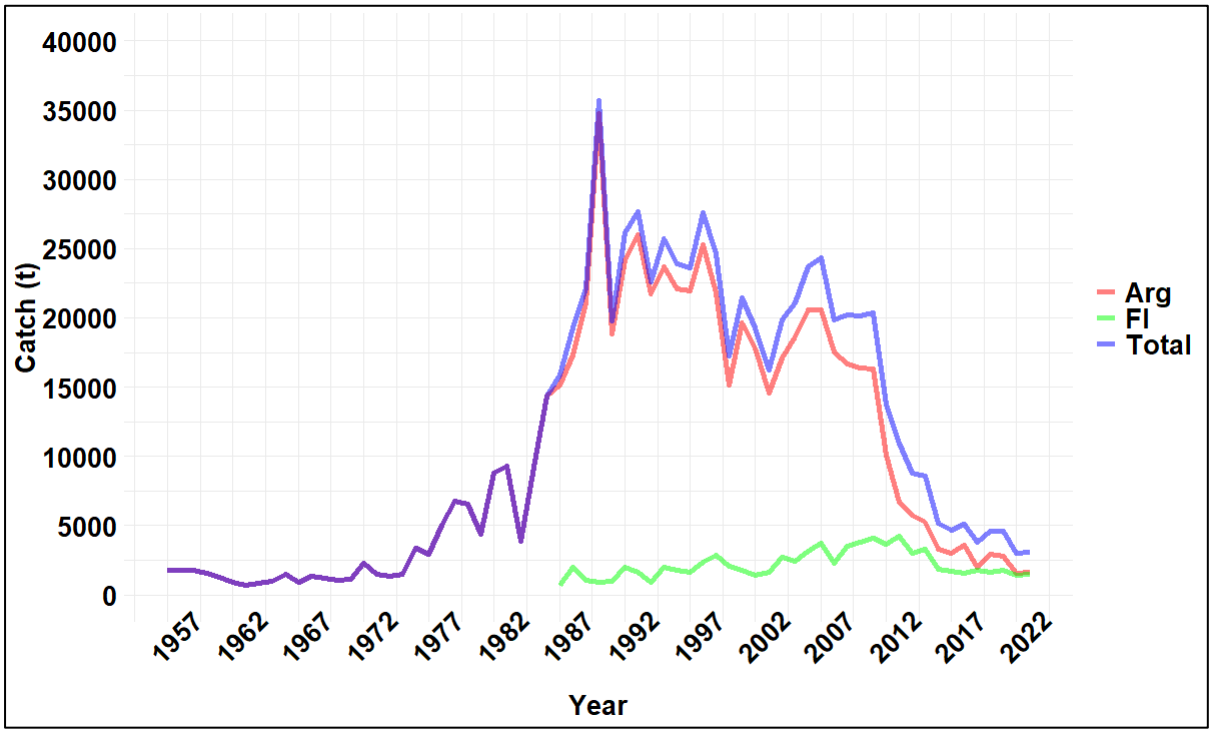

Figure 1. Catch (tonnes) of *Genypterus blacodes* in the Southwest Atlantic. Arg: Argentina, FI: Falkland Islands, Total: Total catch. Period 1957-2023.

In this report, a Bayesian surplus production model (SPM; Schaefer, 1954) was used to estimate the kingclip stock in the Southwest Atlantic, and in the Falkland Islands waters. SPMs are based on the ecological theory of density-dependent population growth with exponential population growth at low abundance and low population growth when abundance is close to the stock carrying capacity (K). SPMs rely on the assumptions that the modelled biomass belongs to a closed population (no inmigration or emigration), only the part of the population that is vulnerable to fishing fleet is modelled (exploitable biomass), there are no lag effects between the fish entering the stock and becoming vulnerable to fishing, and estimated variables are constant throughout the extent of the available data. The SPMs models were performed using the *JABBA* package (Just Another Bayesian Biomass Assessment; Winker *et al.*, 2018) For this purpose, catch per unit effort (CPUE) of the commercial fishing fleet was standardised using Generalised Additive Modelling approach (GAM; Hastie & Tibshirani, 1986). A range of alternative CPUE indices and standardisation approaches were compared in the first part of the report. Selected CPUE indices, and combinations thereof, were used to fit and compare alternative SPM models in the second part of the report. The SPM runs using only FI data (*i.e.* limited to the FI share of the stock) were compared to the model

runs using both FI and Argentine catch and CPUE data extracted from Di Marco (2022), for the entire Southwest Atlantic Stock.

Methods

Commercial catch

Kingclip catch data from the FI waters have only been systematically recorded since 1987 (Falkland Islands Government 1989). Therefore, total FI kingclip catch data from 1988 to 2023 were extracted from the Falkland Islands Fisheries Department (FIFD) database (Falkland Islands Government 2023). As kingclip is assumed to be a shared stock, Argentine catch data from 1957 onwards was examined and extracted from the Argentine Ministry of Agriculture, Livestock and Fisheries website (https://www.magyp.gob.ar/sitio/areas/pesca_maritima/desembarques/). Catch data is detailed in Table A1.

CPUE from FI commercial fisheries

Several nominal CPUE indices (kg/h) were constructed using different data subsets (according to the type of licence/s used), using daily catch and effort data of the commercial fleet:

1) Including all finfish licences (Y, A, Z, W and G).

2) Including only the calamari licences (C and X). These licences were included with the aim to include all the fleets operating in the FICZ.

3) Including each finfish licence separately; as the Y licence was replaced by the A licence, and the Z licence was replaced by the W licence, three further datasets were selected for this standardisation:

   3.1) For the Y and A licences,

   3.2) For the Z and W licences, and

   3.3) For the G licence.

4) Including the finfish licences separated by national flag. Only the flags with the largest catches were included in this set, namely Spain (ES) and the Falkland Islands (FI).

For the finfish licences, catches inside the 'Loligo Box' were excluded. For the calamari licences, catches outside the 'Loligo Box' were excluded. For all the datasets, the nominal CPUE was calculated as the total catch per year divided by the total effort per year (kg/h).

CPUE standardisation was done for each data subset. Four GAM models of increasing complexity were fitted (Table 1), and compared using the Akaike Information Criterion (AIC; Akaike, 2011). The year effect belonging to the model with the lowest AIC was used as the standardised CPUE index to inform the SPM. In all models, the response variable was kingclip CPUE (kincpue).

Only the information with grid depths up to 550 m was included in the dataset. Each grid is a square of 0.5 degrees of latitude by 0.25 degrees of longitude. The grid depth is located in the middle of each square. The first and simplest model (GAM1) included explanatory variables: latitude/longitude interaction, month as a cyclic variable, year as a factor, and vessel as a random effect. The second model (GAM2) added licence as a factor. The third model (GAM3) added the grid depth, and the fourth model (GAM4) added hake and rock cod CPUE to assess the effect of these target species on kingclip CPUE (Table 1). For the single-licence data subsets, the licence was not included as a factor, and only models GAM1, GAM3 and GAM4 were evaluated. Due to the presence of zeros (~14%), all standardisations were modelled with a Tweedie distribution with a logarithmic link function.

Table 1. Structure of the models evaluated for all the sets of standardisations. Kincpue: kingclip CPUE; LonMid/LatMid: longitude and latitude at the middle of the grid square; GridDepth: depth at the middle of the grid square; hakcpue/parcpue: cpue of hake and rock cod, respectively. *The factor "licence" was not included in standardisations by licence.

Model	Equation	Random effect	Distribution
GAM1	kincpue ~ s(LonMid, LatMid) + s(month, bs="cc") + factor(year)	vessel	tw(link="log")
GAM2	kincpue ~ s(LonMid, LatMid) + s(month, bs="cc") + factor(year)+ factor(licence)*		
GAM3	kincpue ~ s(LonMid, LatMid) + s(month, bs="cc") + s(GridDepth) + factor(year) + factor(licence)*		
GAM4	kincpue ~ s(LonMid, LatMid) + s(month, bs="cc") + s(GridDepth) + s(hakcpue) + s(parcpue) + factor(year) + factor(licence)*		

The GAM models were implemented in R (R Core Team, 2022) and R Studio (Posit team, 2023) using the package *mgcv* (Wood, 2017). Visualizations were done with the packages *ggplot2* (Wickham, 2016) and *gratia* (Simpson, 2024).

Abundance index from FI surveys

A Survey Abundance Index (SAI) was constructed from FI bottom trawl survey data. Two kind of surveys are performed twice a year, during the months of February and July. The groundfish survey aims to estimate the abundance of finfish species, and the Loligo pre-season survey aims to estimate the abundance of *Doryteuthis gahi*. The index was standardised using a GAM model with density (kg/km^2) as the response variable. The interaction between latitude and longitude, bottom temperature and depth were included as smooth explanatory variables. Month (February/July), year and survey type (finfish/Loligo) were included as factors, and the vessel as a random effect. Two models were evaluated: AM1) Included the interaction between latitude and longitude for the

whole dataset, and AM2) evaluated the interaction with different smoothers for the first season (February) and for the second season (July). The structure of both models is detailed in Table 2. The models were then compared using AIC and the standardised abundance index belonging to the model with the lower AIC was used to inform the SPM.

Table 2. Structure of the models evaluated for the abundance index standardisation. Density: kingclip density per survey station; MeanLon / MeanLat: mean longitude and latitude of survey trawls; MeanDepth: mean depth of the survey trawl; temp: bottom water temperature of each trawl; month: factor with two levels (February/July); Survey: factor with two levels (finfish/Loligo preseason); year: factor corresponding to the year of the survey. The vessel is included as a random effect.

Model	Equation	Random effect	Distribution
AM1	Density ~ s(MeanLon, MeanLat) + s(MeanDepth) + s(temp) + factor(month) + factor(year) + Survey	vessel	tw(link="log")
AM2	Density ~ s(MeanLon, MeanLat, by=month) + s(MeanDepth) + s(temp) + factor(month) + factor(year) + Survey		

Surplus Production Models with *JABBA*

The *JABBA* package (Winker *et al.*, 2018) was used to implement Schaeffer SPM for kingclip. This tool allows the evaluation of space state Bayesian SPM with process and observation errors, and has the advantage of generating a friendly and reproducible interface for stock assessment, while maintaining the necessary flexibility to evaluate different scenarios. *JABBA* is run in JAGS (Plummer, 2003) to estimate the Bayesian posterior distributions of all quantities of interest by means of a Markov Chains Monte Carlo (MCMC) simulation.

In *JABBA*, surplus production at time *t* (**SP$_t$**) is obtained from the generalised Pella-Tomlinson formula (Pella & Tomlinson, 1969):

$$\mathrm{SP}_t = \frac{r}{m-1}\mathrm{B}_t\left(1-\left(\frac{\mathrm{B}_t}{\mathrm{K}}\right)^{(m-1)}\right)$$

Where ***r*** is the intrinsic population growth rate at time *t*, **K** is the carrying capacity of the population, **B** is the biomass at time *t*, and ***m*** is the shape parameter of the function. When *m*=2, the model is reduced to the Schaefer form, with maximum sustainable yield (MSY) at B_t = K/2.

The general Schaefer equation is:

$$\mathrm{B}_{(t+1)} = \mathrm{B}_t + r\,\mathrm{B}_t\left(1-\left(\frac{\mathrm{B}_t}{\mathrm{K}}\right)\right) - \mathrm{C}_t$$

Where $\mathbf{B_{(t+1)}}$ is the biomass at time *t+1*, $\mathbf{B_t}$ is the biomass at time *t*, the second term in the equation is the SP, and $\mathbf{C_t}$ is the catch at time *t*. This means that the biomass of a population at a given time depends on the biomass at the previous time, plus the surplus production of the population, minus the fishing pressure on the population at that previous time.

JABBA also has the advantage of allowing the inclusion of several abundance indices with an associated standard error (or coefficient of variation, CV). It also includes a parameter ***psi*** that scales the initial biomass, with the possibility to act as a reproductive biomass or as an initial biomass depletion.

The models are informed by the catch and CPUE data, and by priors (Bayesian framework). At least three priors should be provided for the model to work: carrying capacity (**K**), intrinsic population growth rate (***r***), and initial depletion (or proportion of reproductive biomass, ***psi***). To assess the relative influence of the data vs. priors on model outcomes, the posterior to prior median (PPMR) and the posterior to prior variance (PPVR) ratios were used. Values near 1 indicate that the posterior is mostly influenced by the prior and values far from 1 indicate that the posterior is mostly influenced by the data.

Cordo (2001) estimated the K of the entire Southwest Atlantic kingclip stock from a Surplus Production model at 302,800 tons (CI 90%: 240,200 - 391,200) and a spawning stock biomass carrying capacity from an age-structured model at 501,100 tons (CI 90%: 321,500 - 784,800), with natural mortality fixed at M=0.2. The two different types of models produced very different estimates of the carrying capacity of the population. Given that the proportion of kingclip stock reaching FI waters is assumed to be a small fraction of the total stock (Ramos & Winter, 2022), a fraction of K was set as a prior for the model for the FI stock assessment. For the evaluations, the parameter was set at 300,000 tons when the whole stock was assessed (Arg + FI), and at 30,000 tons when only the FI share of the stock was assessed (Table 3). The K for the FI share of the stock was determined based on the estimated average biomass from the groundfish and calamari pre-season surveys (Ramos & Winter, 2024).

The estimated *r* for the Southwest Atlantic stock was 0.23 (Cordo, 2001) with a CV of 23.6% and a 90% CI between 0.15 and 0.34. These values are quite different from those estimated by the *FishLife* package (Thorson *et al.*, 2023) of 0.1 at the species level. The *r* prior was thus set to a range between 0.1 and 0.23 (Table 3).

At the beginning of the catch timeseries (1957) the stock was assumed to be barely exploited and the biomass close to the virgin biomass. Thus, when including the total catch timeseries, the initial depletion prior was set to 0.9. On the other hand, when the short FI catch timeseries was included, starting at 1988, the resource was already being exploited and, in this scenario, an initial depletion prior of 0.7 was selected. In both scenarios, an error of 0.1 was assumed for the prior (Table 3).

A total of 26 models were run with different combinations of catch and CPUE indices time-series:

1) 18 models were assumed to assess the whole Southwest Atlantic kingclip stock; these models used the long (1957-2023) FI + Arg catch time-series, and different

combinations of FI CPUE indices, Arg CPUE index, and FI survey index. The inclusion of Arg data was crucial to this approach, as Arg waters hold most of the stock.

2) 8 models were assumed to assess the FI share of the kingclip stock; these models used the short (1988-2023) FI only catch time-series, and different combinations of FI CPUE indices and FI survey index.

The complete list of models with different combinations of data (catch and CPUE indices) and assumed priors is given in Table 2.

The Argentine standardised CPUE consists of three CPUE time series with no overlapping years. All the standardised CPUE series are shown in Table A2. The models constructed only with the FI CPUE indices included the standard error estimated by the GAM models in the standardisations (Table A3). Given that the Argentine CPUE was accompanied by a Coefficient of Variation (CV) that averaged 0.3 for each CPUE, the CV was calculated in the same sense for the FI CPUEs when both FI and Argentine indices were included in the models. The CV of the FI CPUEs were calculated and scaled to average 0.3 (as done for the Argentine CPUEs) and for the SAI, the CV was scaled to average 0.2 to give it a higher weight in the model (Table A4).

To evaluate CPUE fits, the model compares predicted CPUE indices to the observed CPUE. *JABBA*-residual plots were also used to examine boxplots indicating the median and quantiles of all residuals available for any given year. The area of each box indicates the strength of the discrepancy between each CPUE series (larger box means higher degree of conflicting information), and a loess smoother through all residuals aids to detect the presence systematic residual patterns. In addition, *JABBA* also calculates the root-mean-squared-error (RMSE) as a goodness-of-fit statistic which describes de standard deviation of residuals, with a RMSE below 30% indicating a reasonably precise model fit to relative abundance indices (Carvalho *et al.*, 2021). Moreover, a Deviance Information Criterion (DIC) is also provided. Supporting goodness-of-fit statistics, provided in the form of the RMSE, is a good measure of how precisely the model predicts the response and is the most important criterion in evaluating model fit if the purpose of the model is prediction. However, the best measure of model fit ultimately depends on the analyst's objectives and there is no guarantee, neither by *JABBA* nor by any stock assessment model, that a model with a great goodness-of-fit score adequately reflects the population dynamics of the stock (Winker *et al.*, 2018).

Runs test were conducted to quantitatively evaluate the randomness of residuals (Carvalho *et al.*, 2017). The runs test diagnostic was applied to residuals of the CPUE fit on log-scale. The runs test results can be visualized within *JABBA* using a specifically designed plot function that illustrates which time series passed or failed the runs test and highlights individual data points that fall outside the three-sigma limits (Winker *et al.*, 2018). All the MCMC simulations performed consisted of two chains with 100,000 iterations, and a burn-in of 5,000 iterations. The thinning rate of saved intervals was left as default (5 intervals).

Table 3. Catch series, abundance indices and priors used to inform different models. The prior information was provided to the model either as a Log-normal distribution defined by a central tendency and variation, or as a range defined by the minimum and maximum. K: carrying capacity; *r*: population growth rate; *Psi*: initial depletion. CPUE_ff: CPUE for vessels with finfish licence; CPUE_ES: CPUE for vessels with Spanish flag; CPUE_FK: CPUE for vessels with Falklands flag; CPUE_LOL: CPUE for vessels with Loligo licence; CPUE_AY: CPUE for vessels with A and Y licence; CPUE_WZ: CPUE for vessels with W and Z licence; CPUE_G: CPUE for vessels with G licence. SAI: Surveys Abundance Index; Arg_CPUEs: CPUEs extracted from Di Marco, 2022 for Argentinian bottom trawlers.

MODEL	CATCH SERIES	ABUNDANCE INDEX	K DIST.	K PRIOR	*r* DIST.	*r* PRIOR	*Psi* DIST.	*Psi* PRIOR
M1	1957	CPUE_ff	Log-normal	300000, 0.25	range	0.1, 0.23	Log-normal	0.9, 0.1
M2	1957	CPUE_ff; Arg_CPUEs	Log-normal	300000, 0.25	range	0.1, 0.23	Log-normal	0.9, 0.1
M3	1957	CPUE_ff; Arg_CPUEs; SAI	Log-normal	300000, 0.25	range	0.1, 0.23	Log-normal	0.9, 0.1
M4	1957	CPUE_LOL	Log-normal	300000, 0.25	range	0.1, 0.23	Log-normal	0.9, 0.1
M5	1957	CPUE_LOL; Arg_CPUEs	Log-normal	300000, 0.25	range	0.1, 0.23	Log-normal	0.9, 0.1
M6	1957	CPUE_LOL; Arg_CPUEs; SAI	Log-normal	300000, 0.25	range	0.1, 0.23	Log-normal	0.9, 0.1
M7	1957	CPUE_ES; CPUE_FK	Log-normal	300000, 0.25	range	0.1, 0.23	Log-normal	0.9, 0.1
M8	1957	CPUE_ES; CPUE_FK; Arg_CPUEs	Log-normal	300000, 0.25	range	0.1, 0.23	Log-normal	0.9, 0.1
M9	1957	CPUE_ES; CPUE_FK; Arg_CPUEs; SAI	Log-normal	300000, 0.25	range	0.1, 0.23	Log-normal	0.9, 0.1
M10	1957	CPUE_AY; CPUE_WZ; CPUE_G	Log-normal	300000, 0.25	range	0.1, 0.23	Log-normal	0.9, 0.1
M11	1957	CPUE_AY; CPUE_WZ; CPUE_G; Arg_CPUEs	Log-normal	300000, 0.25	range	0.1, 0.23	Log-normal	0.9, 0.1
M12	1957	CPUE_AY; CPUE_WZ; CPUE_G; Arg_CPUEs; SAI	Log-normal	300000, 0.25	range	0.1, 0.23	Log-normal	0.9, 0.1
M13	1957	CPUE_ff; CPUE_LOL	Log-normal	300000, 0.25	range	0.1, 0.23	Log-normal	0.9, 0.1
M14	1957	CPUE_ff; CPUE_LOL; Arg_CPUEs	Log-normal	300000, 0.25	range	0.1, 0.23	Log-normal	0.9, 0.1
M15	1957	CPUE_ff; CPUE_LOL; Arg_CPUEs; SAI	Log-normal	300000, 0.25	range	0.1, 0.23	Log-normal	0.9, 0.1
M16	1957	SAI	Log-normal	300000, 0.25	range	0.1, 0.23	Log-normal	0.9, 0.1
M17	1957	Arg_CPUEs	Log-normal	300000, 0.25	range	0.1, 0.23	Log-normal	0.9, 0.1
M18	1957	SAI; Arg_CPUEs	Log-normal	300000, 0.25	range	0.1, 0.23	Log-normal	0.9, 0.1
M19	1988	CPUE_ff	Log-normal	30000, 0.25	range	0.1, 0.23	Log-normal	0.7, 0.1
M20	1988	CPUE_LOL	Log-normal	30000, 0.25	range	0.1, 0.23	Log-normal	0.7, 0.1
M21	1988	CPUE_ff; CPUE_LOL	Log-normal	30000, 0.25	range	0.1, 0.23	Log-normal	0.7, 0.1
M22	1988	CPUE_ES; CPUE_FK	Log-normal	30000, 0.25	range	0.1, 0.23	Log-normal	0.7, 0.1
M23	1988	CPUE_AY; CPUE_WZ; CPUE_G	Log-normal	30000, 0.25	range	0.1, 0.23	Log-normal	0.7, 0.1
M24	1988	SAI	Log-normal	30000, 0.25	range	0.1, 0.23	Log-normal	0.7, 0.1
M25	1988	SAI; CPUE_ff	Log-normal	30000, 0.25	range	0.1, 0.23	Log-normal	0.7, 0.1
M26	1988	SAI; CPUE_ff; CPUE_LOL	Log-normal	30000, 0.25	range	0.1, 0.23	Log-normal	0.7, 0.1

Results

CPUE Standardisations

Pooled finfish licences

For pooled finfish licences (A, G, W, Y, Z), model GAM4 had the lowest AIC and was later used to provide the relative abundance index for the SPM (Table 4). Model diagnostics are shown in Figure A1, A.

Table 4. Akaike Information Criterion (AIC) for models fitted to pooled finfish licences. The structure of the models is indicated in Table 1. d.f.: degrees of freedom of the model.

Model	d.f.	AIC
GAM1	324.21	890,073
GAM2	326.61	889,805
GAM3	334.89	889,747
GAM4	351.17	888,754

The partial effect of the interaction between latitude and longitude estimates a higher CPUE in the north-west of the fishing area and a secondary, much lower, peak in the south-east (Figure 2). For the monthly smooth partial effect, CPUE was lower during summer, increased towards autumn, and was higher in April and August (Figure 2). The partial effect for grid depth (depth in the middle of the grid) showed that between 100m and 400m, the highest CPUE was at 200m. Depths above 100m and below 400m show a wide confidence interval due to the small number of data points and are therefore considered unreliable (Figure 2). The partial effects of hake CPUE and rock cod CPUE shows that up to 2.5 t/h, there is an initial tendency for the kingclip CPUE to decrease but then the trend is reversed and the trend is to increase until close to 10t/h for the hake CPUE and until 20t/h for the rock cod CPUE. For the hake CPUE, the trend decreases again until 20 t/h and increases thereafter. For the rock cod CPUE, after 20 t/h there is another reversal where the kingclip CPUE decrease but the confidence intervals become much wider and the trend increases after 30 t/h (Figure 2). The nominal CPUE showed a similar trend to that of the standardised CPUEs (Figure 3).

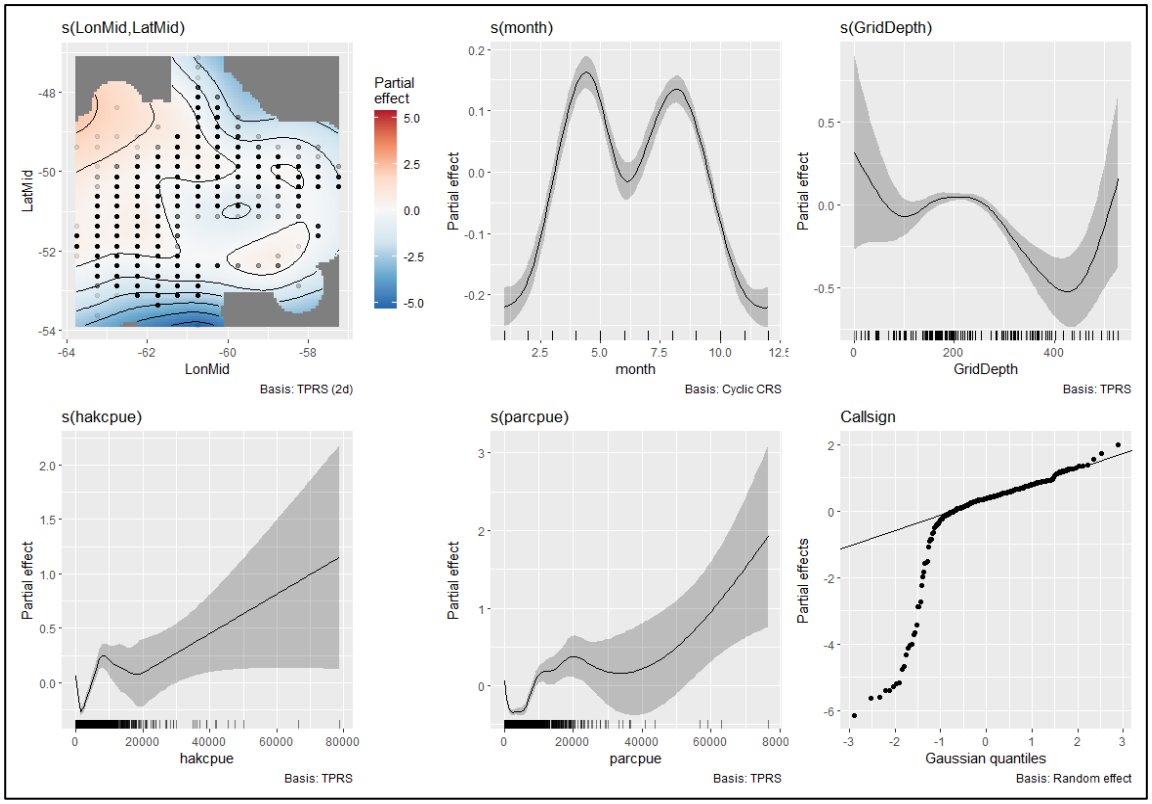

Figure 2. Partial effects of the smooth terms of the GAM4 model for the pooled finfish licences. s(LonMid, LatMid): smooth term of the interaction between the longitude and latitude of the middle point of each grid; s(month): smooth term of the month; s(GridDepth): smooth term of the depth at the middle of each grid; s(hakcpue): smooth term of the hake CPUE; s(parcpue): smooth term of the rock cod CPUE; Callsign: random effect of the factor(vessel).

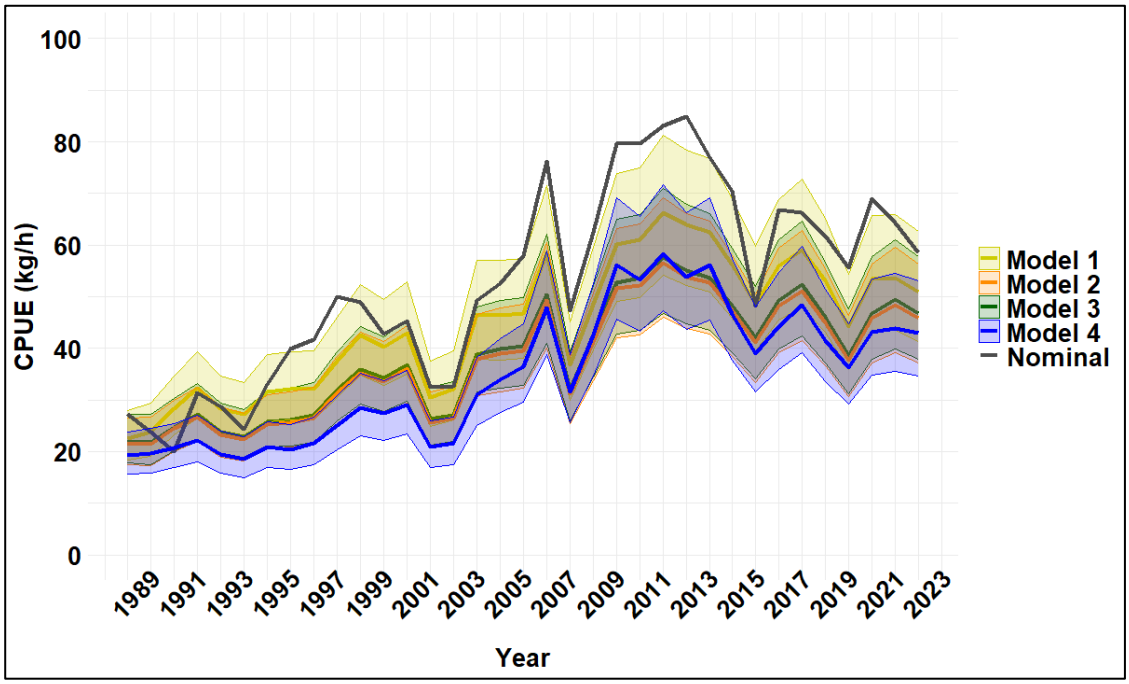

Figure 3. Yearly trend of the Nominal CPUE and standardised CPUE (models 1-4 with their respective 95% CI) for pooled finfish licences.

Calamari (Loligo) licences (C, X)

The same set of models was run for calamari licences and again model GAM4 showed the lowest AIC (Table 5). Model diagnostics are shown in Figure A1, B.

Table 5. Akaike Information Criterion (AIC) for models fitted to calamari licences. The structure of the models is indicated in Table 1. d.f.: degrees of freedom of the model.

Model	d.f.	AIC
GAM1	154.85	53,058
GAM2	154.75	53,018
GAM3	155.04	53,018
GAM4	165.92	52,791

The partial effect of the interaction between latitude and longitude estimated a higher CPUE in the south-east of the fishing area and a secondary peak in the south-west (Figure 4). Note that this information was restricted to the "Loligo box". For the monthly smooth partial effect, the lowest CPUE was estimated in September and the highest in April, with a secondary peak between June and July (Figure 4). The partial effect for grid depth (depth at the centre of the grid) showed a linear increasing trend with increasing depth, but depths above 150m and below 350m showed a wide confidence interval adding uncertainty (Figure 4). The partial effect of the hake CPUE shows an increasing trend until 500 kg/h and a decreasing trend afterwards. For the rock cod CPUE, the initial trend is to decrease until 2,000 kg/h, then the partial effect fluctuates until 5,000 kg/h where the effect increases. After 7,500 kg/h the trend is reversed again with a less steep decrease (Figure 4). The annual trend of the models was similar to the trend of the nominal CPUE (Figure 5).

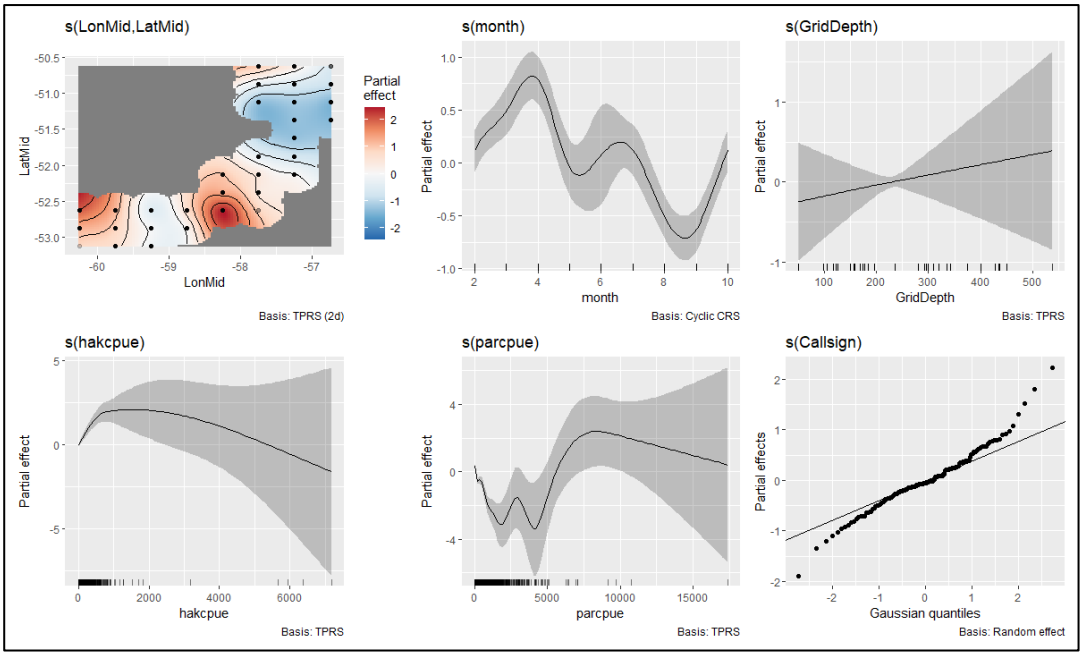

Figure 4. Partial effects of the smooth terms of the GAM4 model for the calamari (Loligo) licences. S(LonMid, LatMid): smooth term of the interaction between the longitude and latitude of the middle point of each grid; s(month): smooth term of the month; s(GridDepth): smooth term of the depth at the middle of each grid; s(hakcpue): smooth term of the hake CPUE; s(parcpue): smooth term of the rock cod CPUE; Callsign: random effect of the vessel.

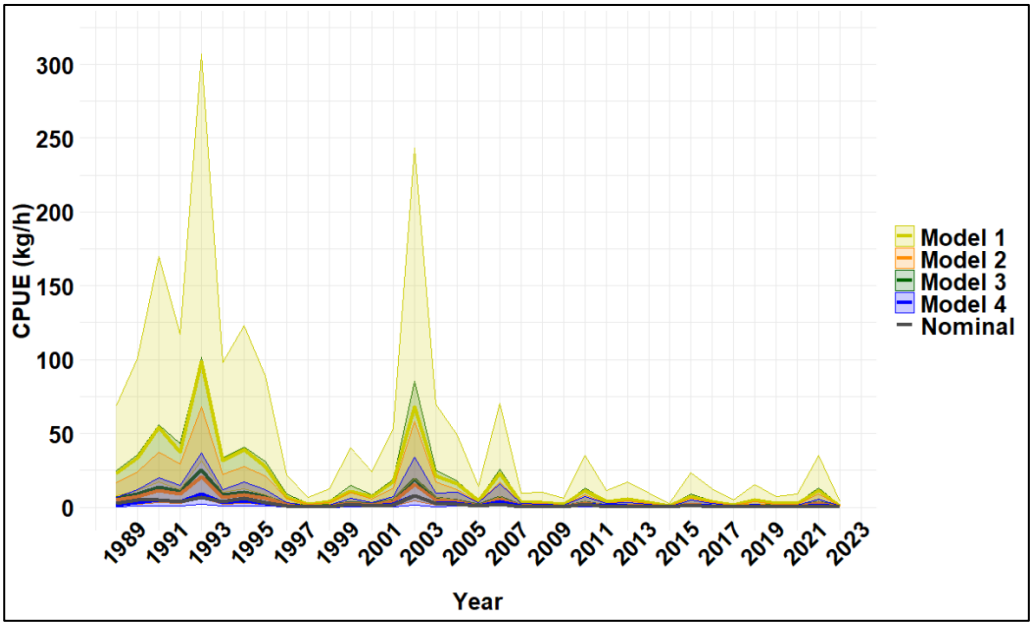

Figure 5. Yearly trend of the Nominal and standardised CPUE (models 1-4 with their respective 95% CI) for the calamari (Loligo) licences.

Standardisation by separate licences

A-Y licences

Model GAM4 showed the lowest AIC (Table 6). Model diagnostics were considered acceptable (Fig. A1-C).

Table 6. Akaike Information Criterion (AIC) for models fitted to A-Y licences. The structure of the models is indicated in Table 1. d.f.: degrees of freedom of the model.

Model	d.f.	AIC
GAM1	206.05	257,058
GAM3	213.82	257,031
GAM4	231.34	256,606

The partial effect of latitude and longitude showed a peak of CPUE in the north-west, a second and smaller peak in the south-east, and the lowest estimate in the south. The monthly estimation showed the highest estimation in April, two secondary peaks in July-August and October-November, and the lowest estimates in summer months. The partial effect of depth showed higher CPUE between 150-200m and between 250-300m. Considering the effect of hake CPUE and rock cod CPUE up to 20 t/h, there is an initial tendency for the kingclip CPUE to decrease but then the trend is reversed and tends to increase. After 20 t/h there is another reversal and the trend decrease but the confidence intervals become much wider (Figure 6). The annual trend shows an increasing CPUE until 2012 and decreasing afterwards, but not reaching the levels from the beginning of the time-series (Figure 7)

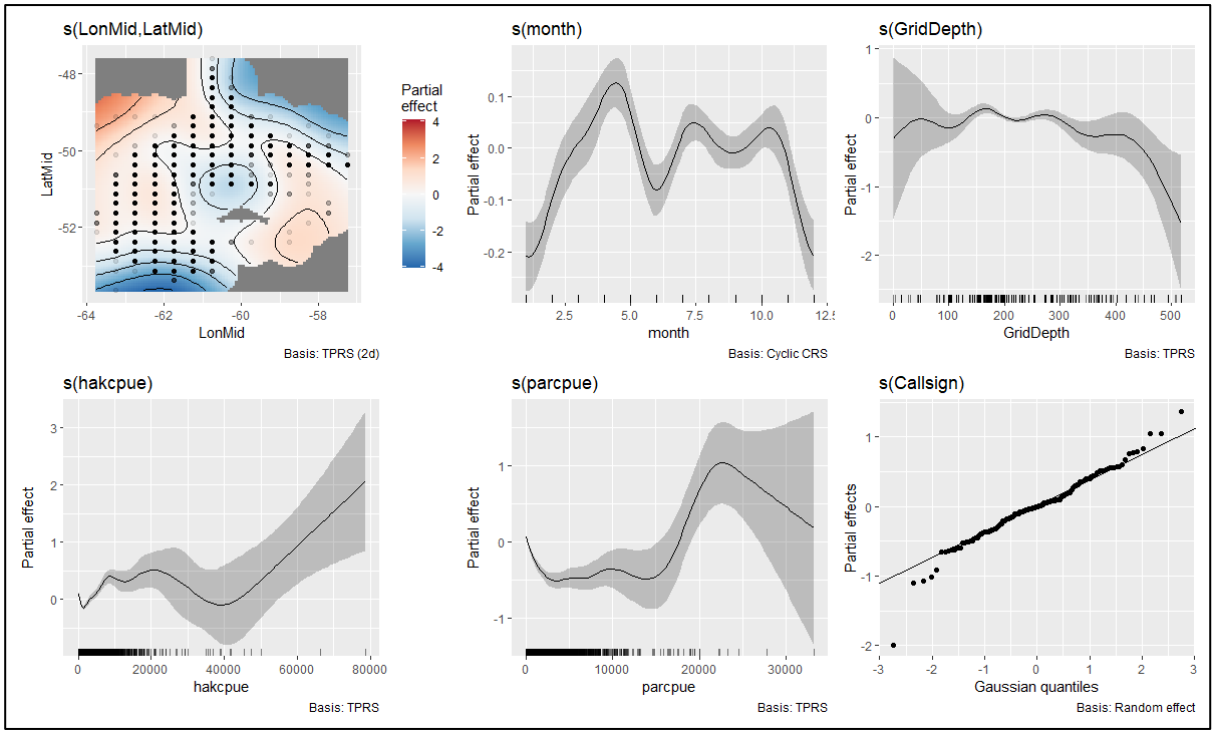

Figure 6. Partial effects of the smooth terms of the GAM4 model for the A and Y licences. S(LonMid, LatMid): smooth term of the interaction between the longitude and latitude of the middle point of each grid; s(month): smooth term of the month; s(GridDepth): smooth term of the depth at the middle of each grid; s(hakcpue): smooth term of the hake CPUE; s(parcpue): smooth term of the rock cod CPUE; Callsign: random effect of the vessel.

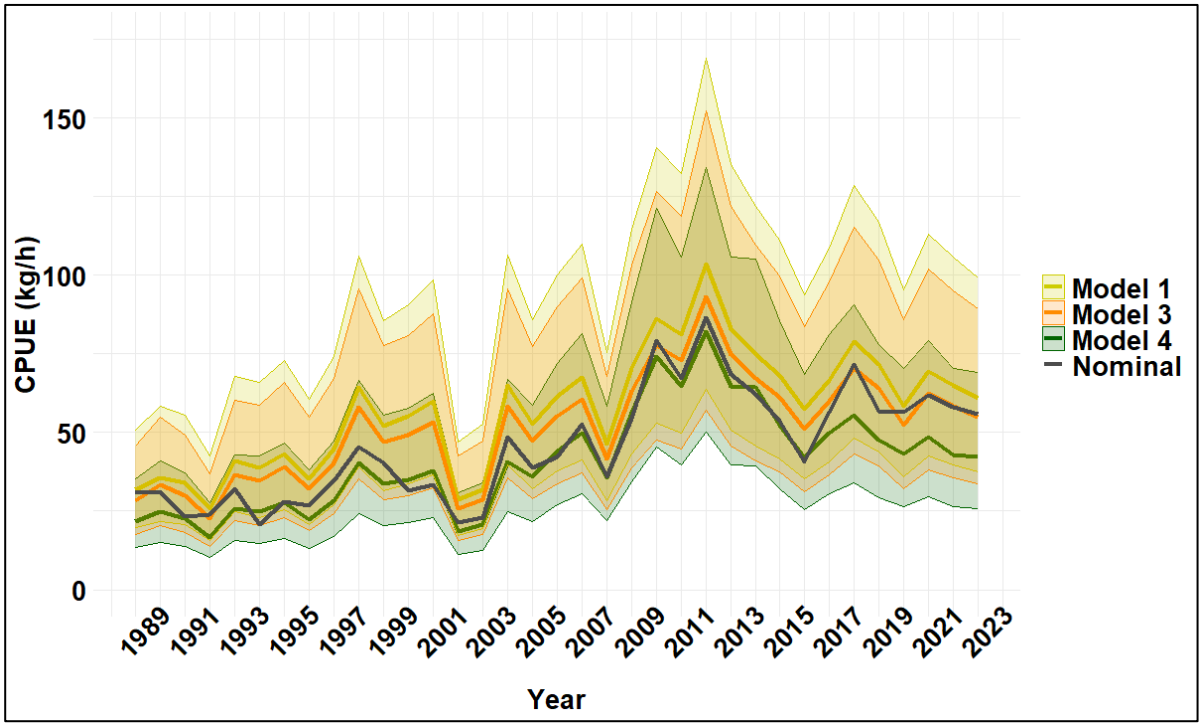

Figure 7. Yearly trend of the Nominal and standardised CPUE (models 1-4 with their respective 95% CI) for the finfish licences A and Y.

W-Z licences

Once again, the model GAM4 exhibited the lowest AIC (Table 7). Model diagnostics are shown in Figure A1, D.

Table 7. Akaike Information Criterion (AIC) for models fitted to W-Z licences. The structure of the models is showed in Table 1. d.f.: degrees of freedom of the model.

Model	d.f.	AIC
GAM1	264.97	450,956
GAM3	271.64	450,811
GAM4	289.10	450,294

The partial effects of the smooth terms showed higher CPUE to the north-west. However, the effects of month, depth, and hake CPUE exhibited a considerable degree of uncertainty, thereby impeding the formulation of definitive conclusions. No discernible trend is observed until the 30 t/h of rockcod, where a decline becomes evident (Figure 8). The yearly trend for this licence showed an upward trajectory in CPUE over time, and the trends of the models were comparable to the trend of the nominal CPUE, with the exception of the final year (Figure 9). This effect was associated with the inclusion of the vessel as a random effect (tested but not shown in the report).

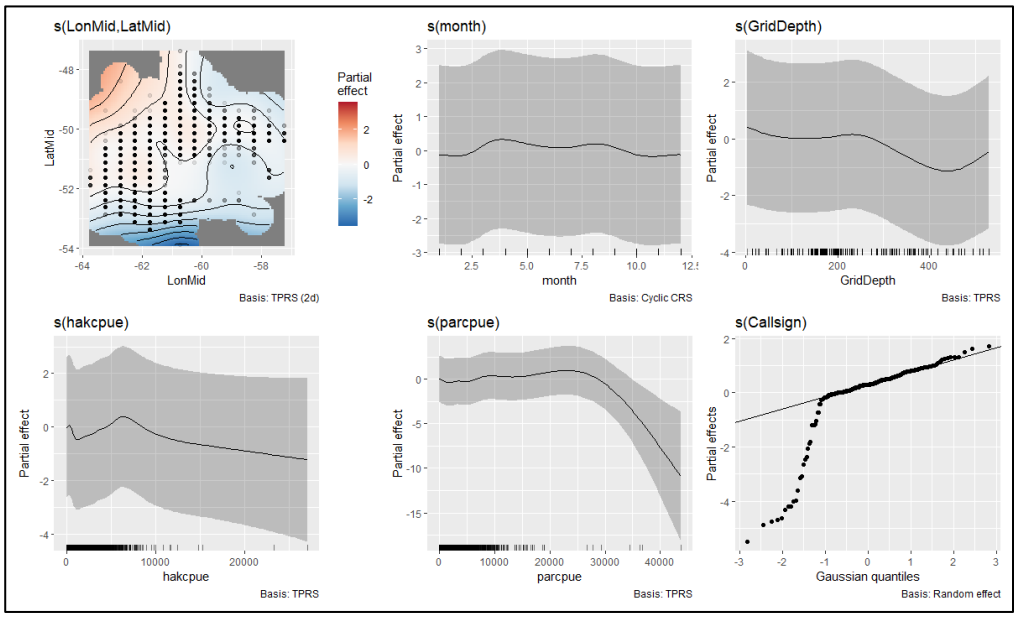

Figure 8. Partial effects of the smooth terms of the GAM4 model for the W and Z licences. S(LonMid, LatMid): smooth term of the interaction between the longitude and latitude of the middle point of each grid; s(month): smooth term of the month; s(GridDepth): smooth term of the depth at the middle of each grid; s(hakcpue): smooth term of the hake CPUE; s(parcpue): smooth term of the rock cod CPUE; Callsign: random effect of the vessel.

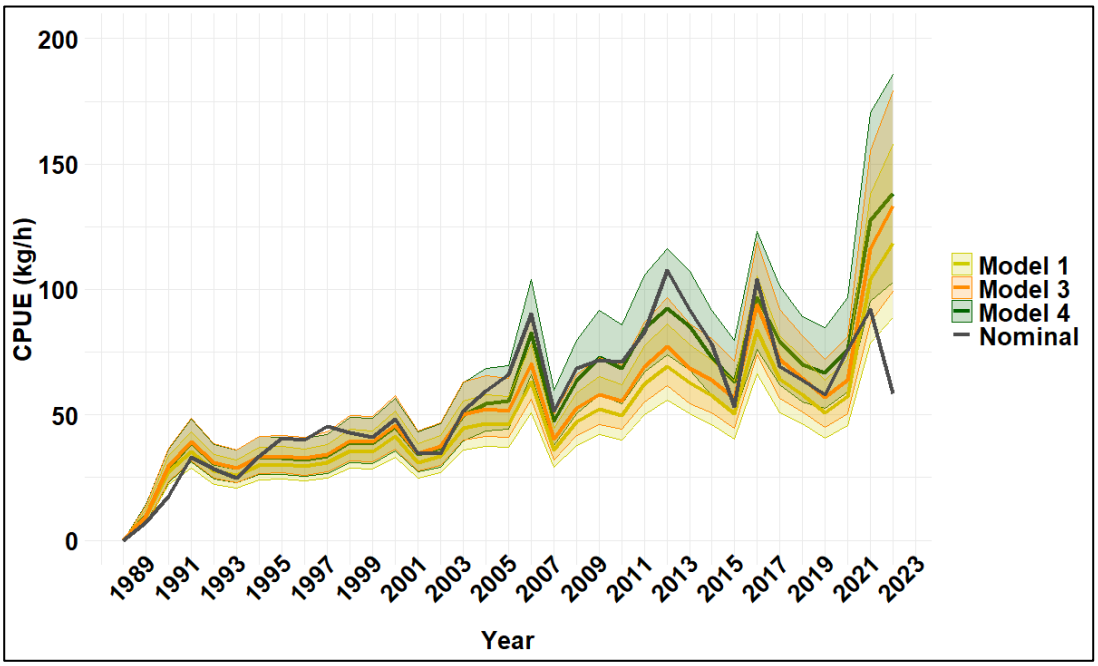

Figure 9. Yearly trend of the Nominal and standardised CPUE (models 1-4 with their respective 95% CI) for the finfish licences W and Z.

G licence

The G licence is primarily allocated to the *Illex* squid and is only operational for a portion of the year (February to May). Once again, the model GAM4 (Table 8) had the lowest AIC. Model diagnostics are shown in Figure A1, E.

Table 8. Akaike Information Criterion (AIC) for models fitted to G licence. The structure of the models is showed in Table 1. d.f.: degrees of freedom of the model.

Model	d.f.	AIC
GAM1	124.74	173,657
GAM3	123.90	173,608
GAM4	139.92	173,319

The partial effect of latitude and longitude showed higher CPUE to the north-east, with a secondary CPUE peak to the west. The monthly partial trend showed a discernible increase from February to May (the period during which this licence is operational) with a linear pattern. Depth data exhibited an almost linear pattern, with lower CPUE at increasing depth. The effect of hake CPUE and rock cod CPUE did not show a clear pattern until 5 t/h for hake and 40 t/h for rock cod, where the trend becomes linear, increasing when the CPUE of the other species increases (Figure

10). The yearly trend did not exhibit a discernible pattern, and no contrasts were evident (Figure 11).

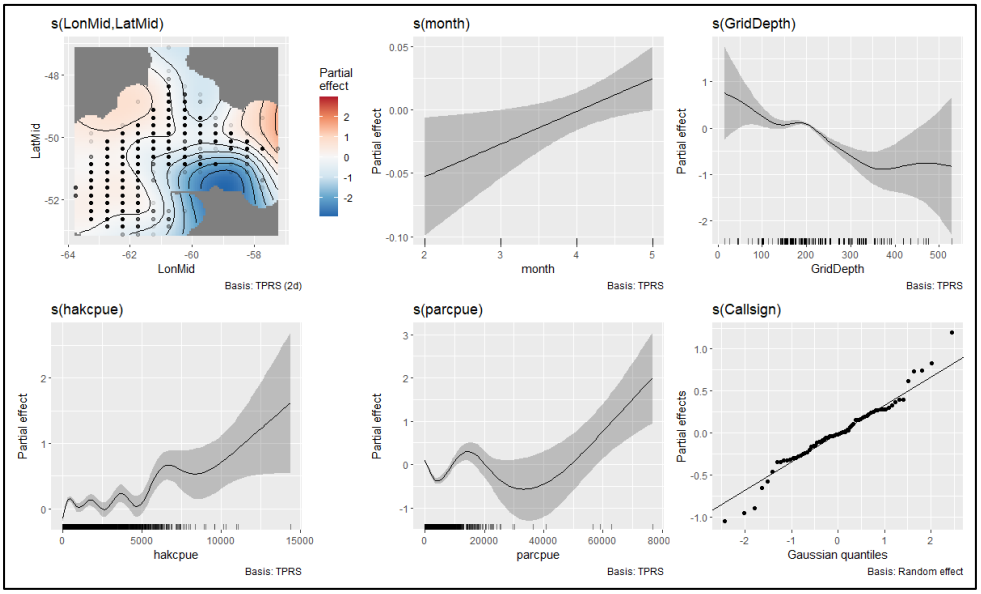

Figure 10. Partial effects of the smooth terms of the GAM4 model for the G licenced vessels. s(LonMid, LatMid): smooth term of the interaction between the longitude and latitude of the middle point of each grid; s(month): smooth term of the month; s(GridDepth): smooth term of the depth at the middle of each grid; s(hakcpue): smooth term of the hake CPUE; s(parcpue): smooth term of the rock cod CPUE; Callsign: random effect of the vessel.

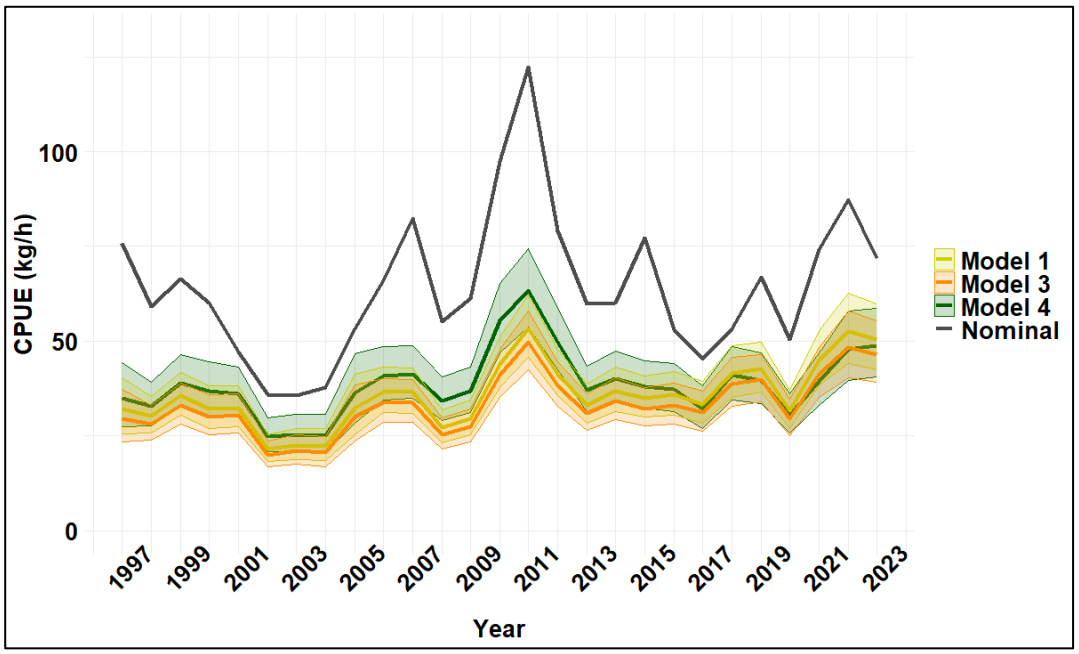

Figure 11. Yearly trend of the Nominal and standardised CPUE (models 1-4 with their respective 95% CI) for the finfish licence G.

Standardisation by nation flag

The most consistent catches were reported under the Spanish (ES) and Falkland Islands (FK) flags.

Spanish flag (ES)

Model GAM4 was the model with the lowest AIC for standardising the CPUE of vessels under Spanish flag (Table 9). Model diagnostics are shown in Figure A1-F.

Table 9. Akaike Information Criterion (AIC) for models fitted to the Spanish flag vessels. The structure of the models is showed in Table 1. D.f.: degrees of freedom of the model.

Model	d.f.	AIC
GAM1	179.49	628,761
GAM2	181.39	628,472
GAM3	188.50	628,422
GAM4	205.90	627,699

The partial effects for this model indicated higher CPUE in the north-west and south-east. The highest partial estimation was observed in April and October. The partial effect of depth demonstrated a consistent decline with increasing depth until 400 m, where the trend reversed. No discernible correlation was evident for the other species partial effects until a CPUE of 30 t/h, where the relation became direct. However, the confidence intervals from the 20t/h are substantial due to the limited data set (Figure 12). Furthermore, the yearly trend estimation demonstrated a notable increase in CPUE over time (Figure 13).

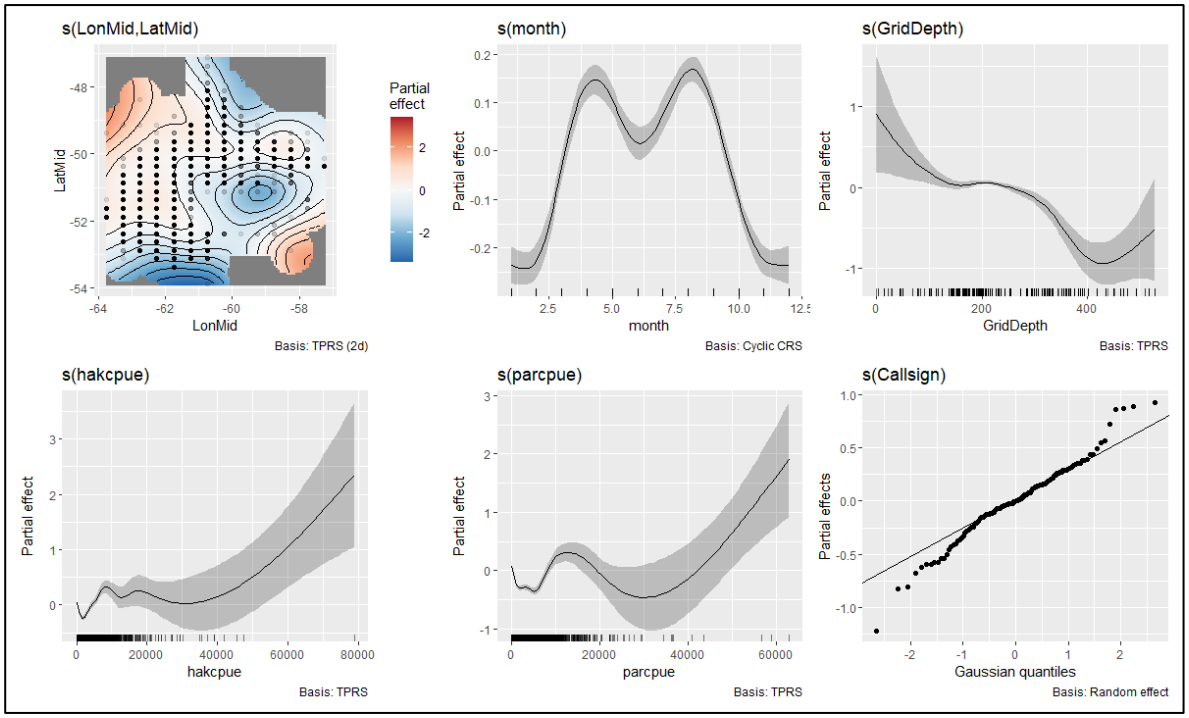

Figure 12. Partial effects of the smooth terms of the GAM4 model for the ES flag. S(LonMid, LatMid): smooth term of the interaction between the longitude and latitude of the middle point of each grid; s(month): smooth term of the month; s(GridDepth): smooth term of the depth at the middle of each grid; s(hakcpue): smooth term of the hake CPUE; s(parcpue): smooth term of the rock cod CPUE; Callsign: random effect of the vessel.

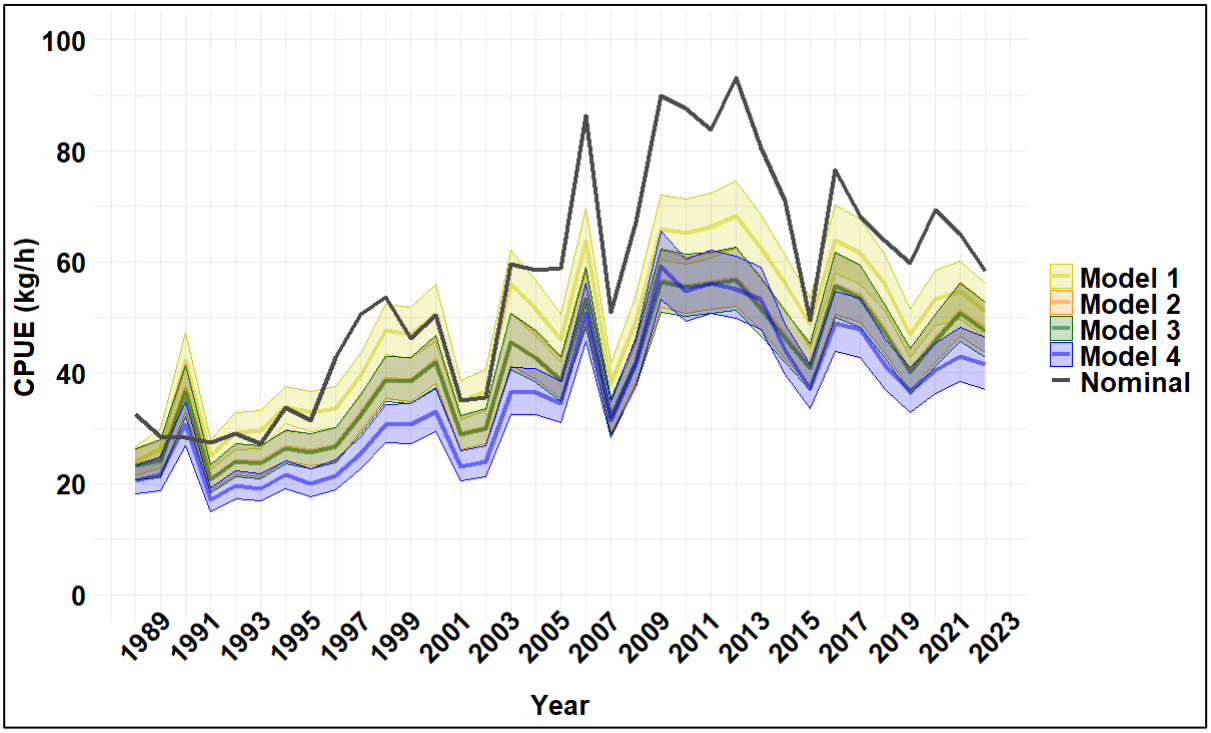

Figure 13. Yearly trend of the Nominal and standardised CPUE (models 1-4 with their respective 95% CI) for the finfish flag ES (Spain).

Falkland Islands flag (FI)

The model with the lowest AIC for standardising the CPUE of vessels under the Falkland Islands flag was identified as model GAM4 (Table 10). Model diagnostics are shown in Figure A1, G.

Table 10. Akaike Information Criterion (AIC) for models fitted to the FI flag vessels. The structure of the models is showed in Table 1. D.f.: degrees of freedom of the model.

Model	d.f.	AIC
GAM1	89.17	173,231
GAM2	90.99	173,224
GAM3	98.91	173,166
GAM4	115.41	172,895

The partial effects estimations indicate higher CPUE to the north-west and a secondary peak in the north-east. The monthly effect demonstrates the presence of two peaks in the estimated high values. These were observed in April and August, respectively. The lowest estimation was observed in November. The partial effect for depth demonstrated a decline in CPUE with depth, with a plateau observed between 150m and 250m, where the confidence interval was smaller. The CPUE of hake and rock cod exhibited no discernible trend until reaching 20t/h for hake and 25t/h for rock cod, where a decline in kingclip CPUE was observed alongside an increase in other species (Figure 14). The yearly trend exhibited no discernible pattern, with a slight tendency towards an increase over time (Figure 15).

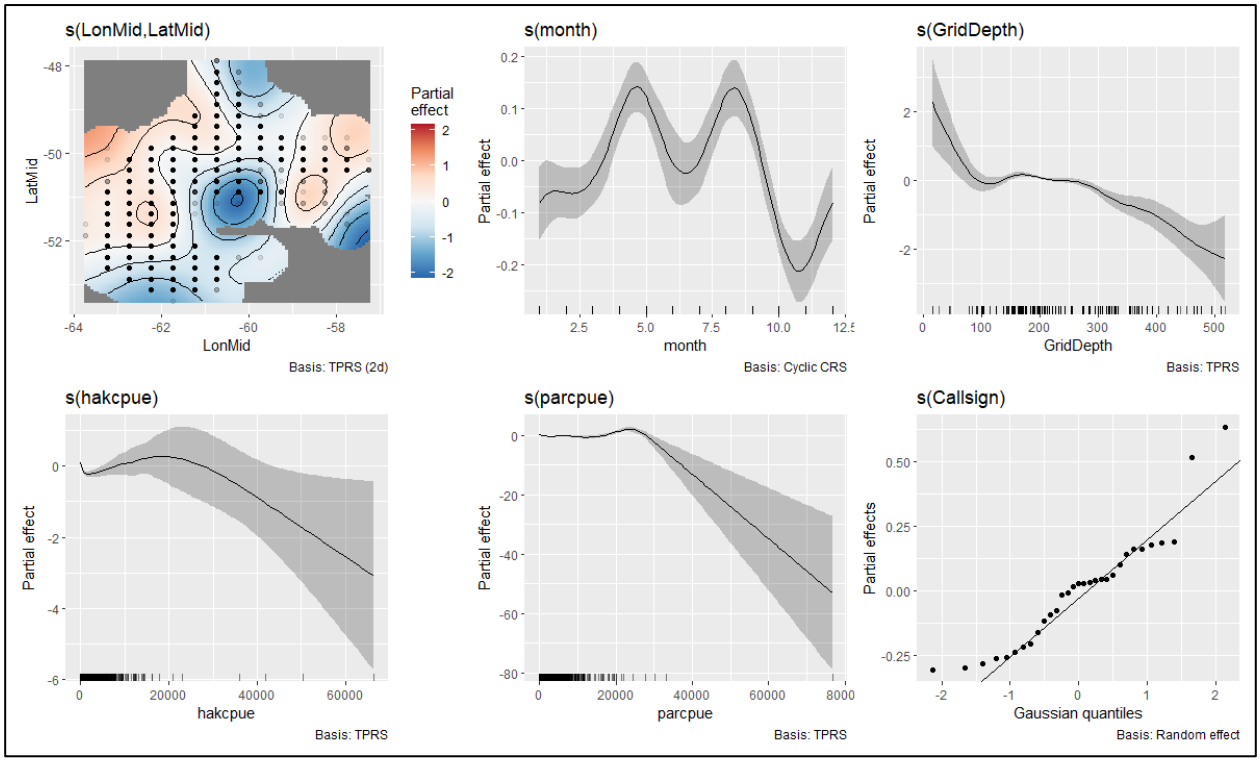

Figure 14. Partial effects of the smooth terms of the GAM4 model for the FI flag. s(LonMid, LatMid): smooth term of the interaction between the longitude and latitude of the middle point of each grid; s(month): smooth term of the month; s(GridDepth): smooth term of the depth at the middle of each grid; s(hakcpue): smooth term of the hake CPUE; s(parcpue): smooth term of the rock cod CPUE; Callsign: random effect of the vessel.

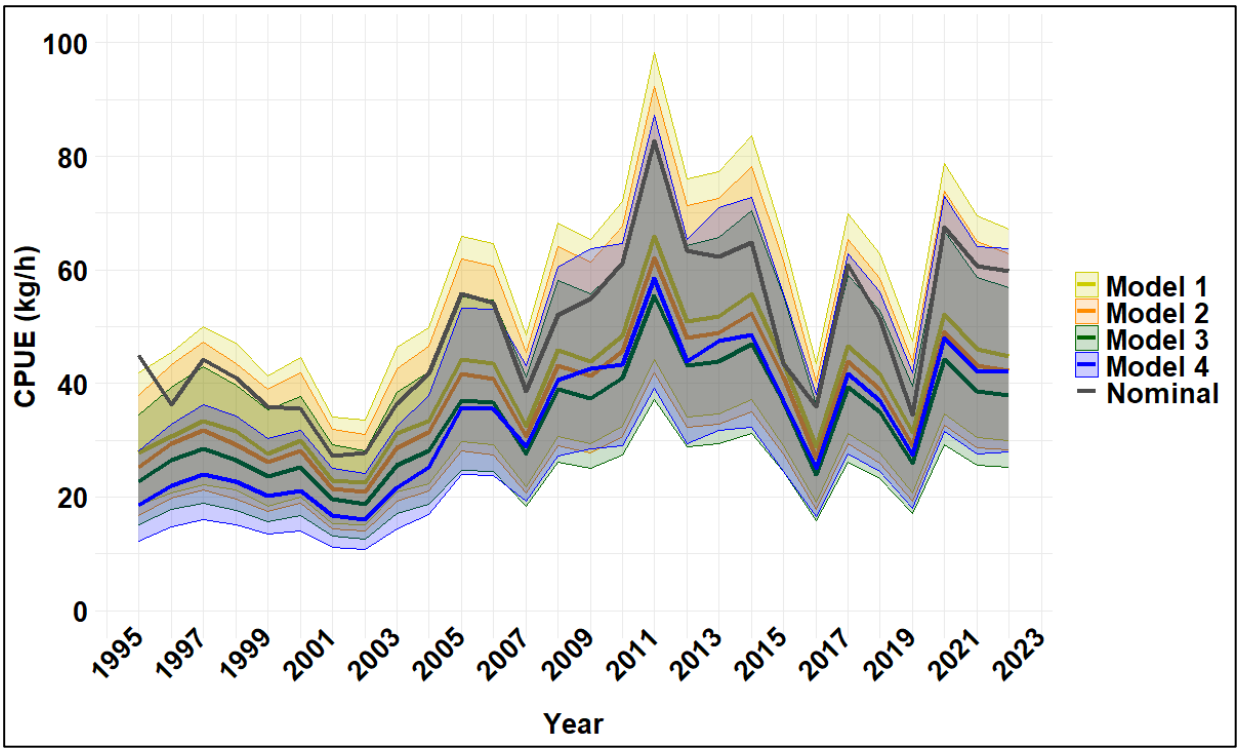

Figure 15. Yearly trend of the Nominal and standardised CPUE (models 1-4 with their respective 95% CI) for the finfish flag FK (Falkland Islands).

Abundance Index from surveys

The second model, incorporating discrete smoothers for each month factor, was preferred according to AIC (Table 11). The model demonstrated acceptable diagnostics (Figure A1-H).

Table 11. Akaike Information Criterion (AIC) for models fitted to the survey abundance index. The structure of the models is showed in Table 1. D.f.: degrees of freedom of the model.

Model	d.f.	AIC
AM1	65.43	14,398
AM2	84.46	14,378

The partial effects showed the presence of two areas of higher abundance, one to the north-west and the other to the south; a third area was also estimated to the north-east. The effect of depth shows no clear trend until 500 m, but the data thereafter are scarce, limiting the reliability of the trend estimation. The effect of temperature has a maximum estimate at 7.5°C and a secondary peak at 6°C (Figure 16). Although not significant, the partial effect of the factor "survey" was higher for the groundfish survey (p=0.2; Figure 17A) and the partial effect of the factor "month" was higher for the July surveys (p=0.13; Figure 17B). The annual trend showed a decline in abundance from 2015 to 2016 for both models, with a sustained low level thereafter (Figure 18). It should be noted that no surveys were performed from 2012 to 2014.

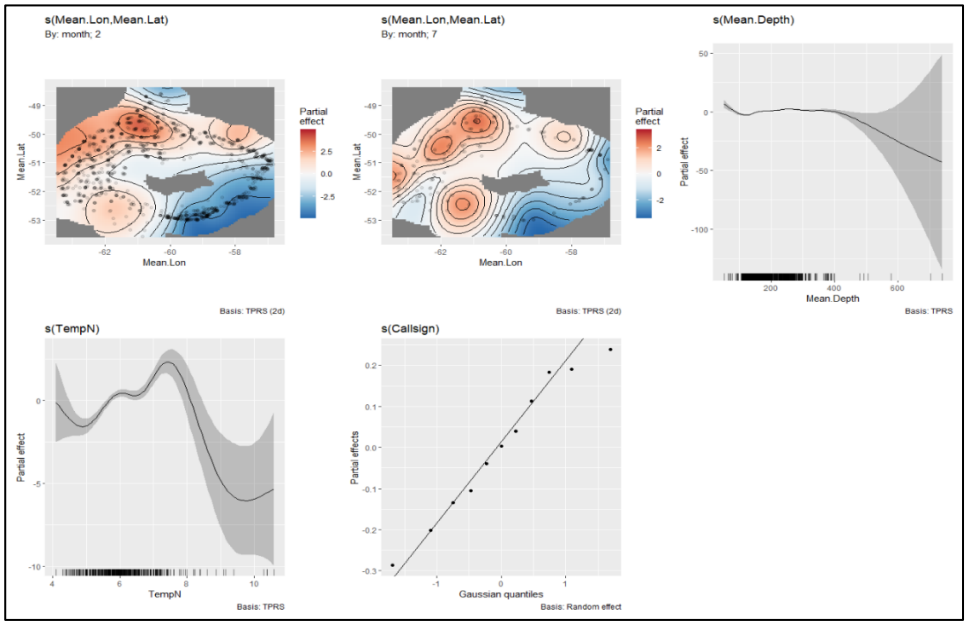

Figure 16. Partial effects of the smooth terms of the AM2 model for the Survey Abundance Index. S(Mean.Lon, Mean.Lat): smooth term of the interaction between the mean of start and end longitude and latitude of each trawl, by the factor month (2=February, 7=July); s(Mean.Depth): mean depth of each trawl; s(TempN): bottom temperature of each trawl; Callsign: random effect of the vessel.

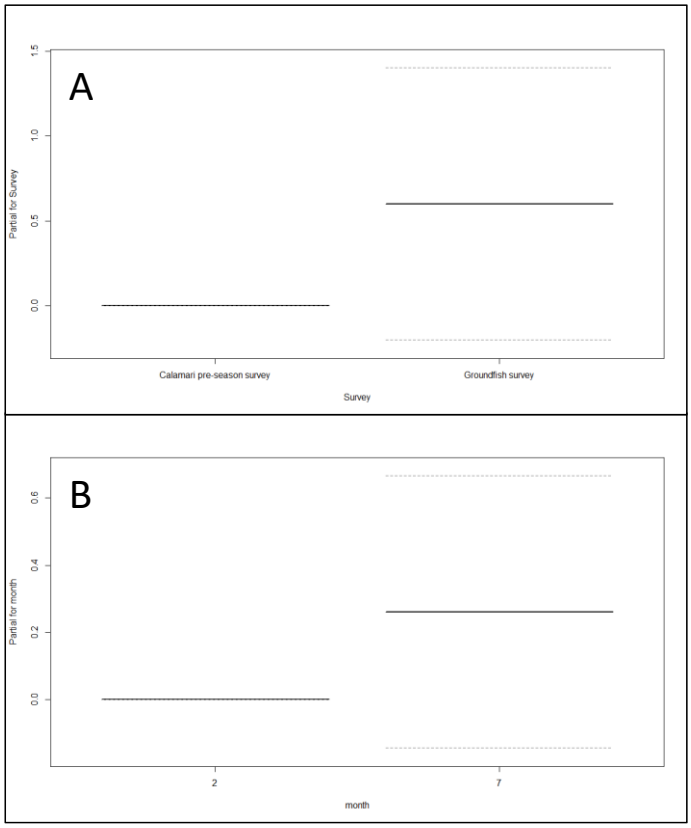

Figure 17. Partial effects of the factors Survey (A) and month (B) of the AM2 for the Survey Abundance Index. Solid lines represent the means and dashed lines the 95% Confidence Interval.

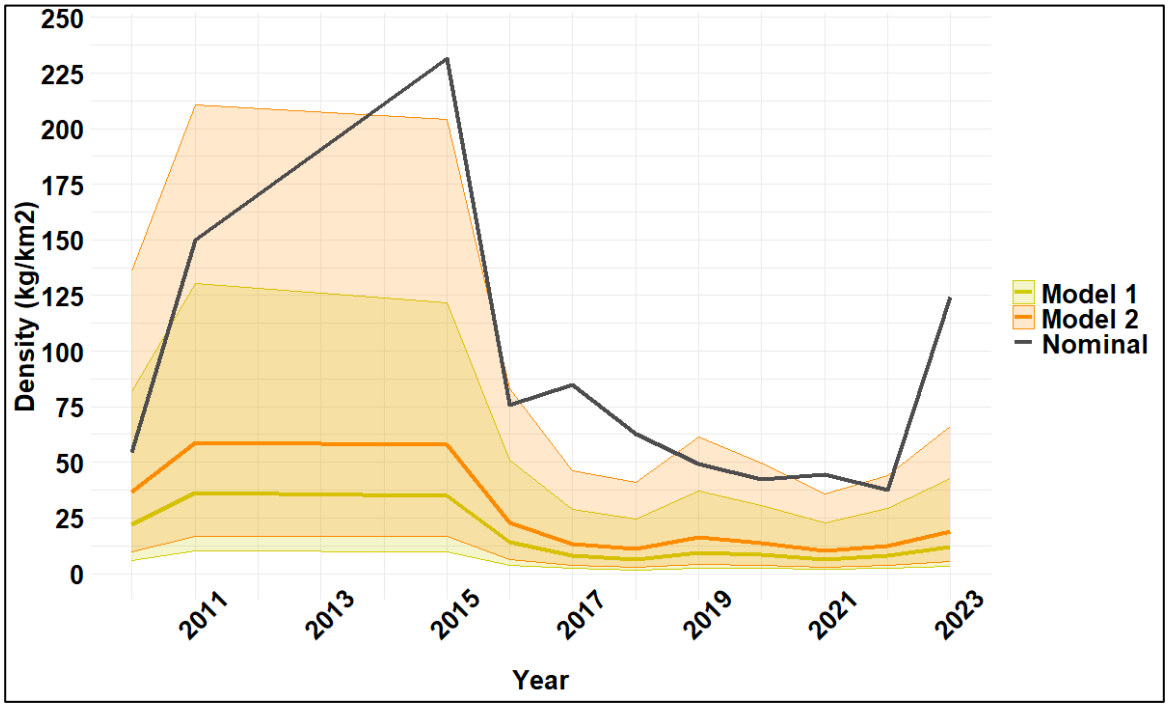

Figure 18. Yearly trend of the Nominal and standardised abundance index from surveys (models 1-2 with their respective 95% CI).

Stock assessment with *JABBA*

Posterior to prior ratios

The selected priors had different effects on the estimated model posteriors (Figures 19, A2, A3). When assessing the whole stock (models M1 to M18) the K Posterior-Prior Median Ratio (PPMR) shows values above 1, most of them above 1.2. This means that the posterior estimated median is higher than the median of the given prior. In the cases of models M1, M7 and M13, the posteriors were strongly influenced by the data. For models M2, M4, M10 and M17, the posteriors were mostly influenced by the priors. The variance ratio (PPVR) of K showed values below 1, indicating that the variance of the posteriors was smaller than those of the priors. Most of the values from the different models were below 0.6, indicating strong influence of the data on the variance of the posterior. Only models M2, M4, M10 and M17 had a higher effect of the prior on the posterior, but still not a very strong effect (Figures 19, A2). In the case of the PPMR of r, the values were also above 1 with model M2 showing the strongest influence by the data and models M4, M16 and M18 showing the strongest influence by the prior with M16 having a value of 1. The PPVR of r showed a strong influence of the priors for most of the models, except for models M4, M5 M17 and M18. The initial depletion (Psi) for both PPMR and PPVR was mostly influenced by the priors, with all the models values close to 1 (Figures 19, A2).

For the FI stock assessment, the PPMR of K showed values above 1, with models M19, M21, M22, M25 and M26 with the strongest influence given by the data (Figure 19, A3). For the PPVR, all the posteriors were mostly influenced by the data, with models M20, M23 and M24 with the weakest effect. All the values were below 1 (Figure 19, A3). The PPMR of r showed the strongest influence by the data for models M20, M23 and M24 and the PPVR showed values close to 1 for all the models (Figure 19, A3) The influence of the data on the posteriors of the Psi PPMR and the PPVR was higher than the one for the whole stock, but still close to 1 (Figure 19, A3).

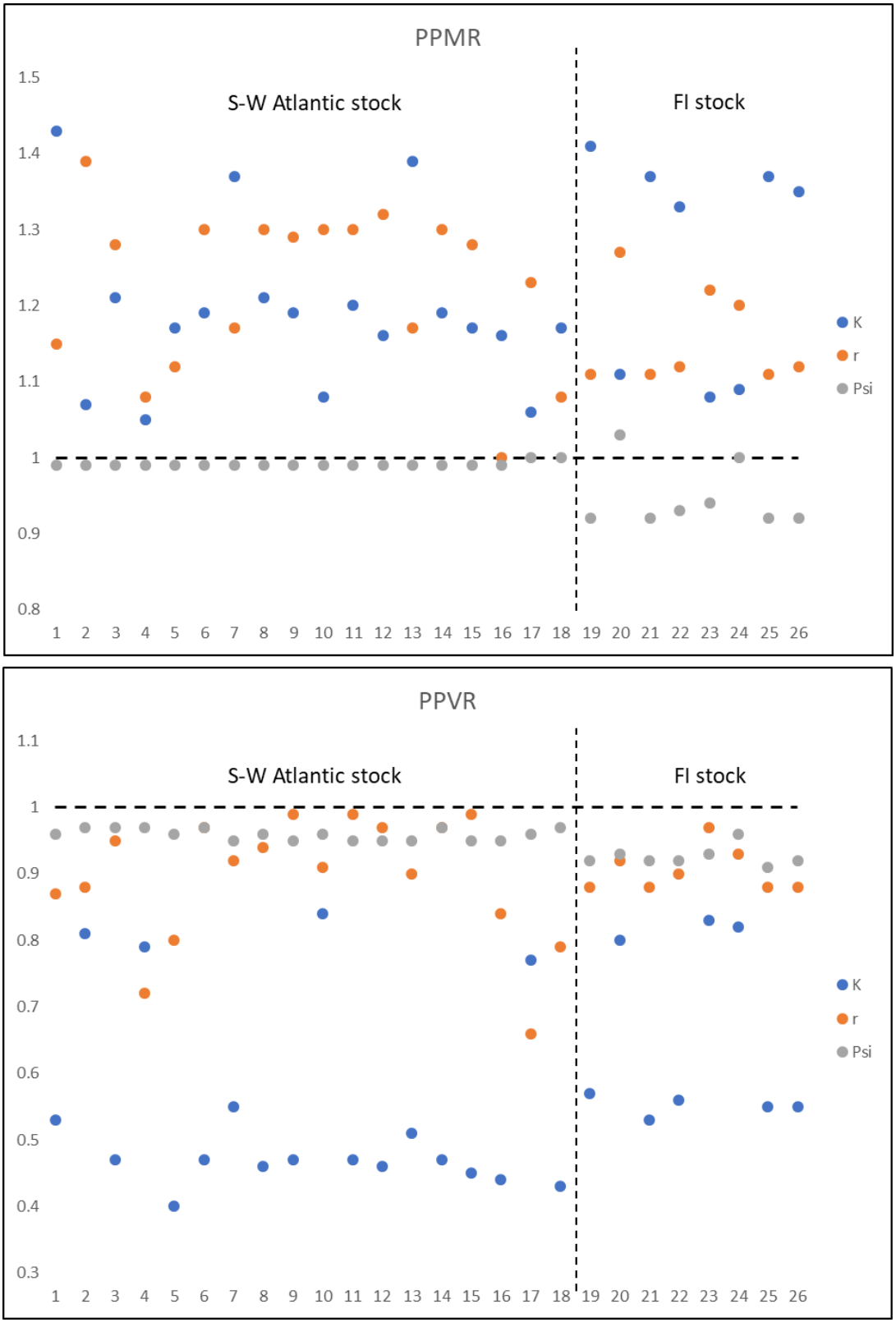

Figure 19. Posterior to Prior Median (PPMR) and Variance (PPVR) ratio of the carrying capacity (K), population growth rate (r) and initial depletion (Psi). Numbers on the x-axis correspond to the different *JABBA* models. The vertical dashed line separates the models pertaining to the Southwest Atlantic Stock (M1-M18) from the models pertaining to the FI share of the stock (M19-M26).

Abundance indices fit

For scenarios where one or more finfish licence CPUEs are included (pooled finfish CPUE, CPUE by nation flag, CPUE by finfish licence) the indices seem to be well fitted in the models. When those indices are in combination with the Argentine CPUE, or with the Argentine CPUEs plus SAI, the behaviour of the model's fits appears to be led by the pattern observed in the finfish licence indices more than the other indices (Figures 20, 21 and 22).

The pattern observed for the calamari (Loligo) licence index tends to be well interpreted by the model when modelled alone (Figures 20, 23, A4, for M4; Figures 22, 24, A5, for M20), however the fit decreases when combined with other indices (Figures20, 23, A4, for M5, M6; Figure 21, 23, A4, for M13-15; Figures 22, 24, A5, for M21, M26) and the trend tends to be guided by the other indices. Similar effects were observed for the Survey Abundance Index (Figure 20, for M3, M6, M9; Figure 21, for M12, M15, M16, M18; Figure 22, for M24-26) and for the Argentine indices (Figure 20, for M2, M8; Figure 21, for M11, M14, M17, M18).

The goodness-of-fit was higher (lower RMSE) for the models including the finfish licences only (M1, M7, M10 for the SW Atlantic stock; M19, M22, M23 for the FI share of the stock). The calamari (Loligo) licence CPUE showed the highest RMSE when included alone (M4, M20) and also in combination with other licences (M5, M6, M13-M15, M21, M26). The SAI had also a relatively high RMSE compared with the others, when included alone (M16, M24). The inclusion of the SAI with other indices decreased the goodness-of-fit in general, with the exception of the models that included also the calamari (Loligo) CPUE (Table 12, Figures 23, 24). When including the Argentine CPUE, the goodness of fit improved for models that included also the calamari (Loligo) or the SAI (M5, M14, M18), but not for the other combinations. When only including the Argentine CPUE (M17) the goodness of fit was acceptable (Table 12, Figure 23).

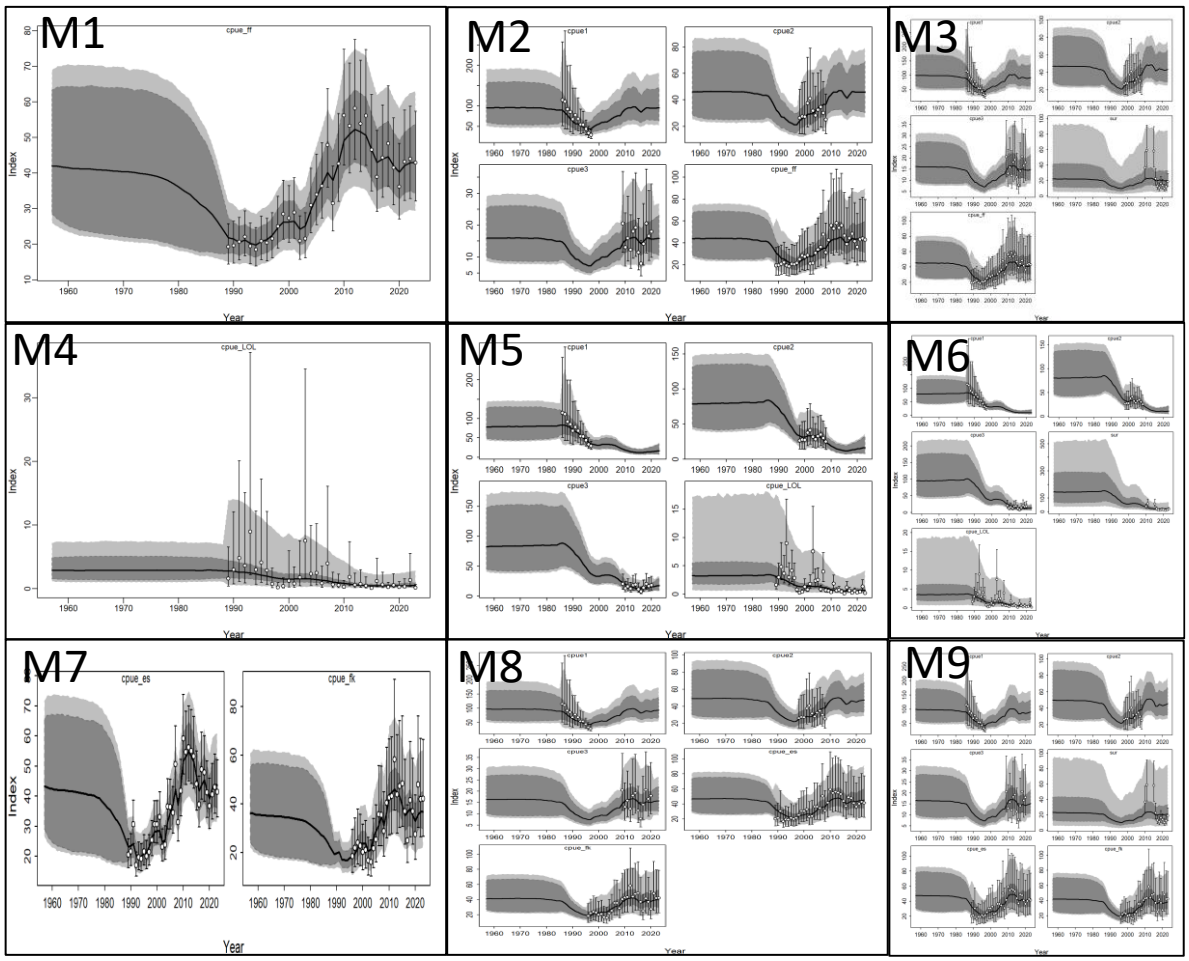

Figure 20. Observed (circle) with error 95% CIs (error bars) and predicted (solid line) CPUE for the models M1 to M9. Dark shaded area shows 95% credibility intervals of the expected mean CPUE and the light shaded area the 95% posterior predictive distribution intervals. Inner panels for each model correspond to a different CPUE: cpue_ff: CPUE of pooled finfish licence; cpue_LOL: CPUE of the calamari (Loligo) licences; cpue_es: CPUE of the vessels with Spanish flag; cpue_fk: CPUE of the vessels with Falkland Islands flag; cpue1, cpue2, cpue3: CPUEs from the Argentine fleet; sur: Survey Abundance Index.

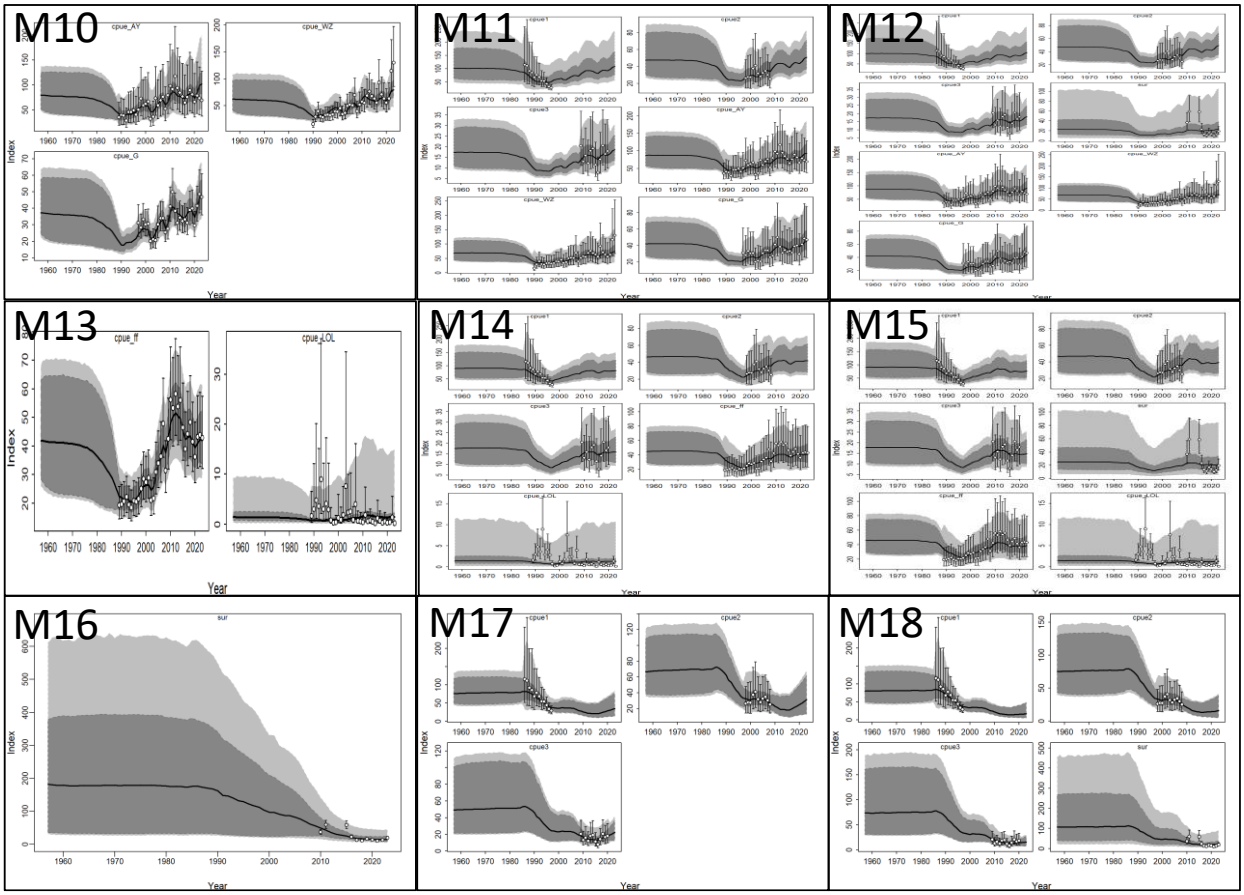

Figure 21. Observed (circle) with error 95% CIs (error bars) and predicted (solid line) CPUE for the models M10 to M18. Dark shaded area shows 95% credibility intervals of the expected mean CPUE and the light shaded area the 95% posterior predictive distribution intervals. Each model panel corresponds to a different CPUE: cpue_AY: CPUE of vessels with A or Y licence; cpue_WZ: CPUE of vessels with W or Z licence; cpue_G: CPUE of vessels with G licence; cpue_ff: CPUE of pooled finfish licence; cpue_LOL: CPUE of the calamari (Loligo) licences; cpue1, cpue2, cpue3: CPUEs from the Argentine fleet; sur: Survey Abundance Index.

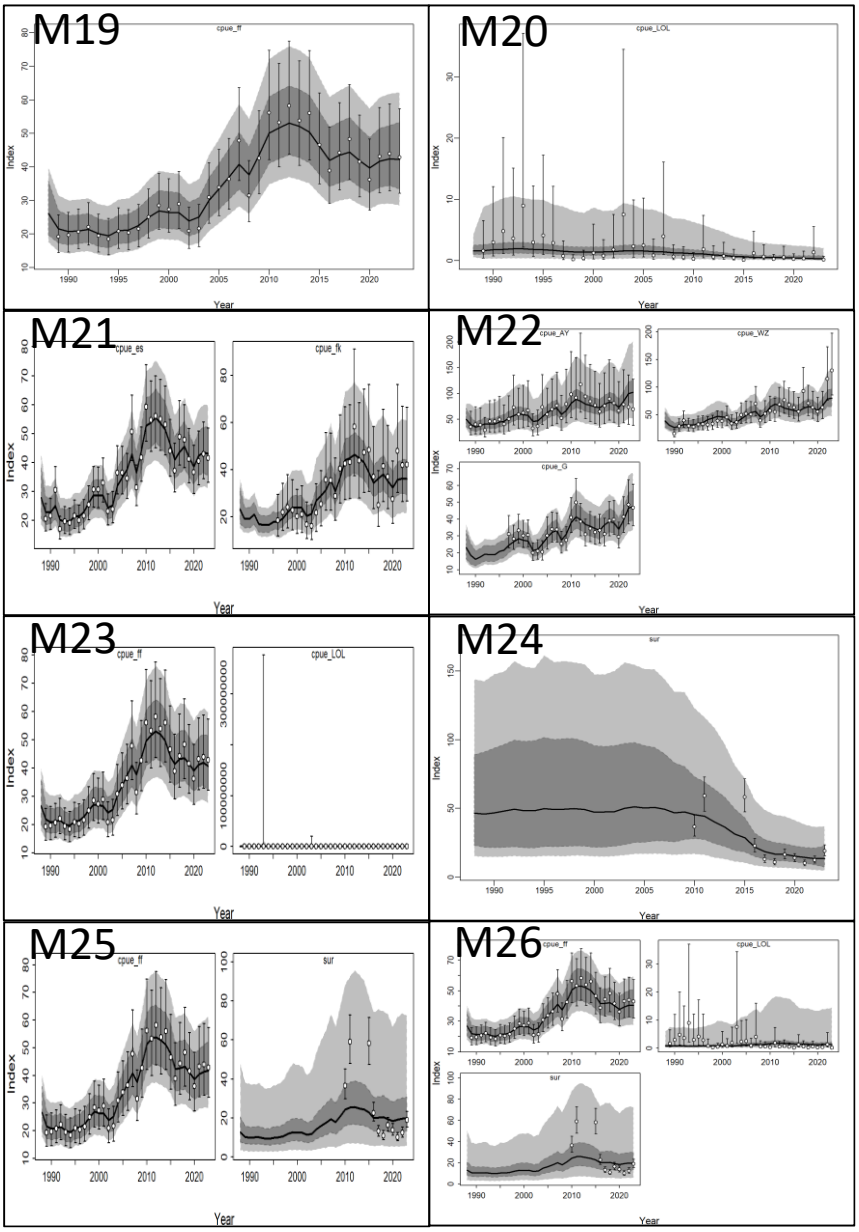

Figure 22. Observed (circle) with error 95% CIs (error bars) and predicted (solid line) CPUE for the models M19 to M26. Dark shaded area shows 95% credibility intervals of the expected mean CPUE and the light shaded area the 95% posterior predictive distribution intervals. Each model panel corresponds to a different CPUE: cpue_ff – CPUE of pooled finfish licence; cpue_LOL – CPUE of the calamari (Loligo) licences; cpue_es – CPUE of the vessels with Spanish flag; cpue_fk – CPUE of the vessels with Falkland Islands flag; cpue_AY – CPUE of vessels with A or Y licence; cpue_WZ – CPUE of vessels with W or Z licence; cpue_G – CPUE of vessels with G licence; sur – Survey Abundance Index.

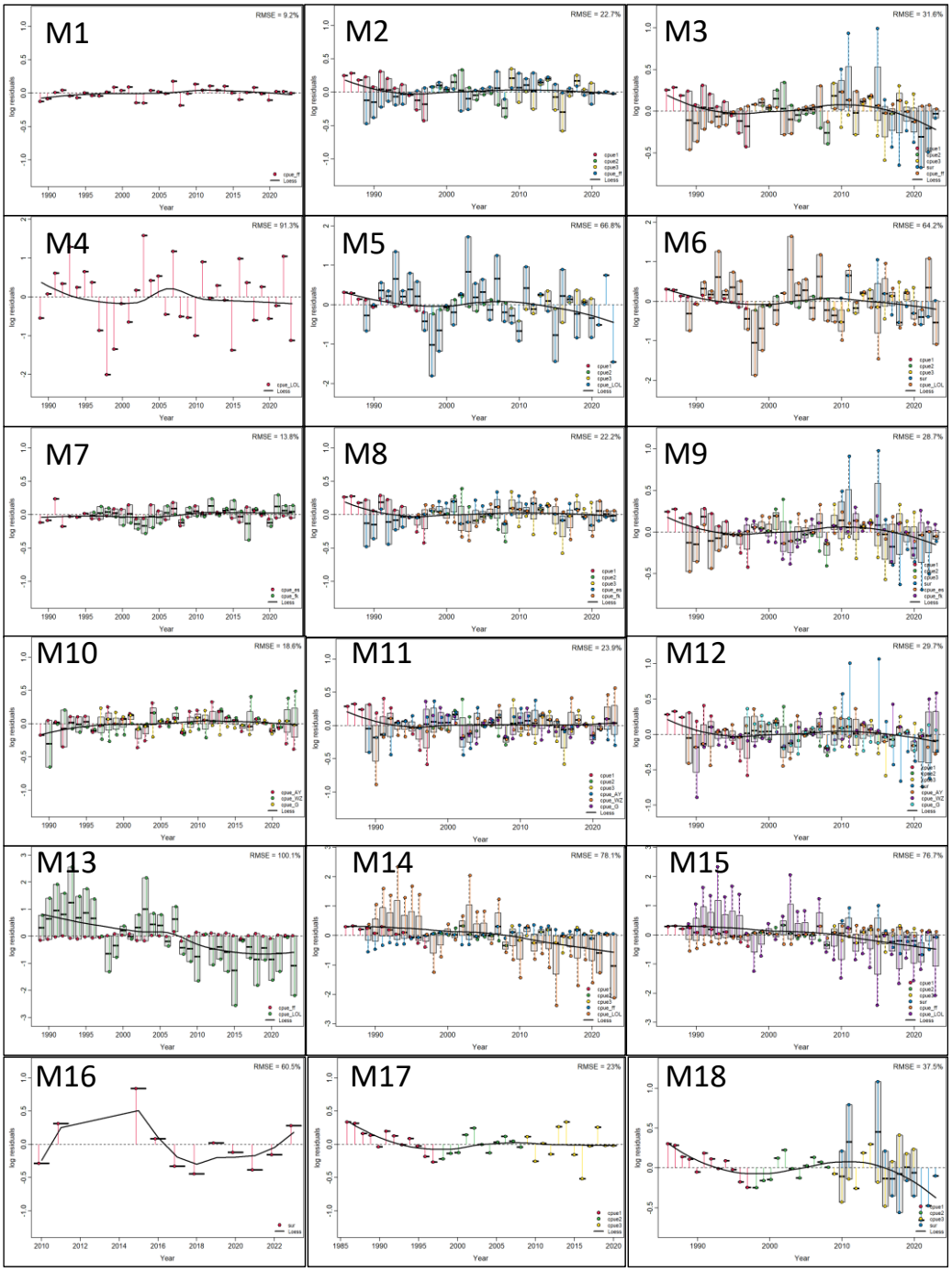

Figure 23. Residuals of the abundance indices fit. Boxplots indicate the median and quantiles of all CPUE residuals available for any given year. The size of the box indicate discrepancy between indices. Solid black lines indicate a loess smoother through all residuals. Each colour corresponds to a different index. RMSE: root-mean-squared-error. Whole SW Atlantic stock (Models 1 to 18).

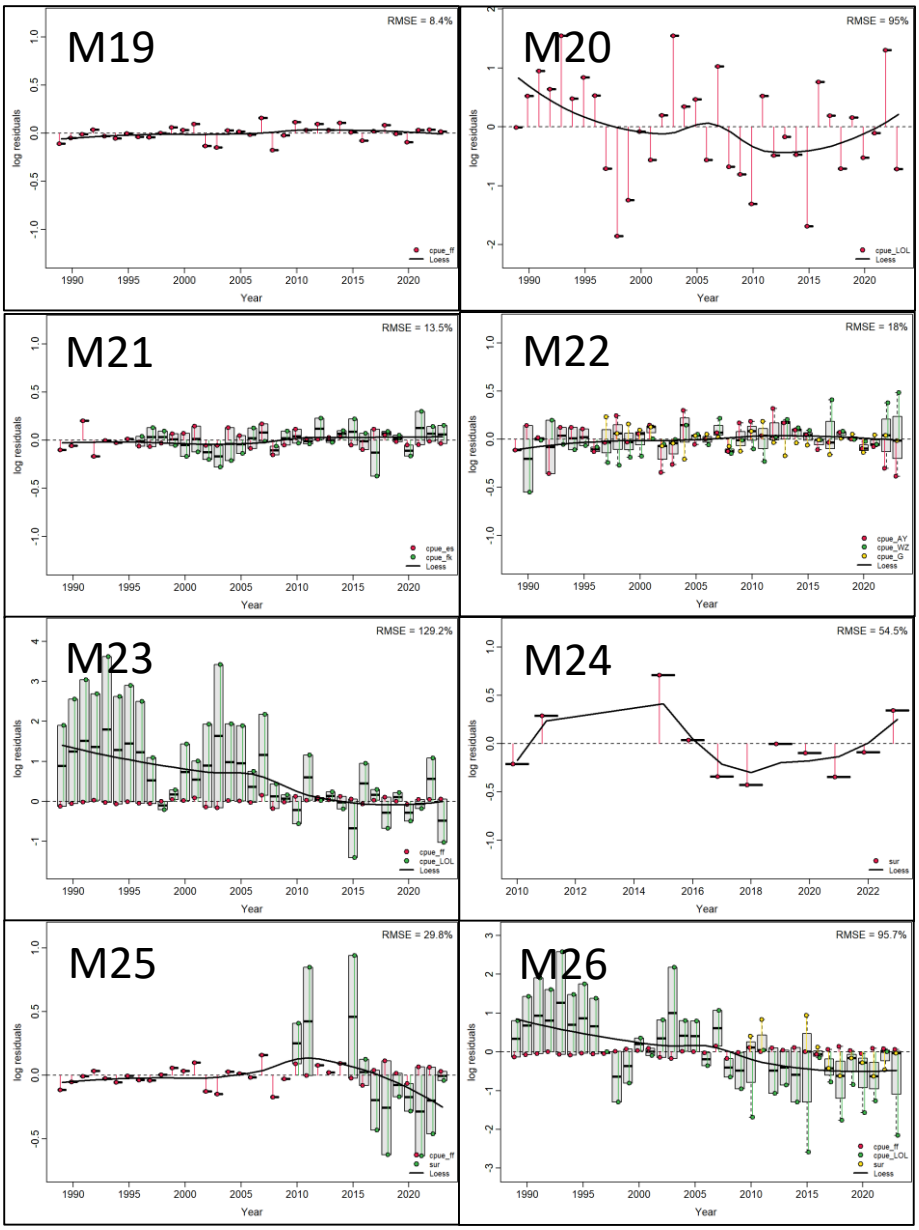

Figure 24. Boxplots indicate the median and quantiles of all CPUE residuals available for any given year. The size of the box indicate discrepancy between indices. Solid black lines indicate a loess smoother through all residuals. Each colour corresponds to a different index. RMSE: root-mean-squared-error. FI stock share (Models 19 to 26).

For the SW Atlantic stock, the model with the lowest Deviance Information Criterion (DIC) was the model M4 (-442.9) that includes only the calamari (Loligo) licences CPUE (Table 12). The second lowest DIC corresponded to the Model M1, including the CPUE of all finfish licences pooled. High DIC was observed in the models M11, M12 and M16 (Table 12). For the FI share of the stock, the model with the lowest DIC was the model M24 that includes only the SAI, and the second lowest DIC was model M20, including the calamari (Loligo) CPUE licences (Table 12). The model with the highest DIC was the model M23 (Table 12).

Table 12. Goodness of fit of the *JABBA* models. RMSE: Root Mean Squared error; DIC: Deviance Information Criterion. Models with * indicate models for the FI share of the stock.

Model	RMSE	DIC	Model	RMSE	DIC
M1	9.2	-316.1	**M14**	78.1	86.6
M2	22.7	-34.5	**M15**	76.7	171.3
M3	31.6	49.8	**M16**	60.5	451.7
M4	91.3	-442.9	**M17**	23	-291.3
M5	66.8	-199.3	**M18**	37.5	-204.2
M6	64.2	-114.9	**M19***	8.4	-74.5
M7	13.8	-117.1	**M20***	95	-194.2
M8	22.2	159.5	**M21***	129.2	44.3
M9	28.7	243.3	**M22***	13.5	118.8
M10	18	431	**M23***	18	431
M11	23.9	472.4	**M24***	54.5	-210
M12	29.7	558.1	**M25***	29.8	8.8
M13	100.1	-192.3	**M26***	95.7	132.9

If we consider both, RMSE and DIC for the SW Atlantic stock, the model with the best selection criterions is the M1 (RMSE=9.2, DIC=-316.1). This model includes only the pooled finfish licences CPUE and showed the best fit to the index. Models M7 (finfish CPUE by nation flag) and M17 (Argentine CPUE) showed also good overall fit statistics. In the same way, for the FI share of the stock, the model that includes the pooled finfish licences (M19) is the one with the overall better selection statistics (RMSE=8.4, DIC=-74.5).

Estimated parameters and trajectories of biomass and fishing mortality

For the SW Atlantic stock, the estimated K ranged between 316,573 tons (M4) and 433,570 t (M1), with a mean value across all models of 360,869 tons (Table 12). The estimated population growth rate (r) ranged from 0.15 (M16) to 0.21 (M2) with a mean across all models of 0.19 (Table 12). The MSY (Maximum Sustainable Yield) estimations ranged between 13,149 tons (M4) and 19,239 tons (M1) with an average of 16,847 tonnes across all the models (Table 12), and the ratio between the current biomass and the biomass at MSY (B_{2023}/B_{MSY}) ranged from a minimum of 0.13 (M16) to a maximum of 2.26 (M10; Table 12), with an average of 1.31 (Table 12).

For the FI share of the stock, the estimated K ranged between 32,406 tons (M23) and 42,781 tons (M19), with an average of 38,181 tons across all models (Table 13). The population growth rate (r) was estimated to be between 0.17 (M19, M21, M22, M25, M26) and 0.19 (M20, M23) with an average of 0.18 across all models (Table 13). The MSY estimations ranged between 1,503 tons (M24) and 1,825 tons (M19) with an average of 1,692 tons across all the models (Table 13). The ratio B_{2023}/B_{MSY} ranged from a minimum of 0.32 (M20) to a maximum of 2.24 (M23) with an average of 1.43 across the models (Table 13).

Table 12. Parameter estimates of Schaefer models of the SW Atlantic stock using Bayesian approach. **K**: carrying capacity. ***r***: population intrinsic growth rate. **MSY**: maximum sustainable yield. B_{MSY}: biomass corresponding to MSY. B_{2023}/B_{MSY}: ratio of biomass in 2023 to biomass MSY. B_{2023}/K: ratio of current biomass to K. F_{2023}: exploitation rate in 2023. F_{MSY}: exploitation rate corresponding to MSY. F_{2023}/F_{MSY}: ratio of exploitation rate in 2023 to exploitation rate MSY. The mean is shown in bold and credible interval is given in brackets.

	M1	M2	M3	M4	M5	M6	M7	M8	M9
K	**433,570** (309,520–622,419)	**321,062** (269,767–373,101)	**368,229** (269,842–520,319)	**316,573** (265,694–376,380)	**356,915** (266,345–493,113)	**351,676** (262,497–482,406)	**415,667** (292,325–601,202)	**369,765** (268,703–517,882)	**361,460** (264,080–512,082)
r	**0.18** (0.12–0.26)	**0.21** (0.14–0.31)	**0.20** (0.13–0.29)	**0.17** (0.11–0.25)	**0.17** (0.12–0.26)	**0.17** (0.12–0.24)	**0.18** (0.12–0.26)	**0.20** (0.13–0.29)	**0.20** (0.13–0.29)
MSY	**19,239** (12,419–28,990)	**17,210** (11,216–24,477)	**18,169** (11,710–26,524)	**13,149** (8,941–17,985)	**15,346** (10,681–21,444)	**14,795** (10,231–20,798)	**18,703** (11,895–28,614)	**18,424** (12,064–26,626)	**17,941** (11,617–25,979)
B_{MSY}	**216,785** (154,760-311,210)	**160,531** (134,883–191,550)	**184,115** (134,921–260,159)	**158,287** (132,847-188,190)	**178,458** (133,172–246,557)	**175,838** (131,249–241,203)	**207,833** (146,162-300,601)	**184,883** (134,352–258,941)	**180,730** (132,040–256,041)
B_{1957}	**381,937** (233,306–612,133)	**283,763** (193,518–402,615)	**325,102** (203,342–512,181)	**280,723** (194,885–391,926)	**315,839** (207,248–485,151)	**311,529** (203,377–477,544)	**363,862** (220,297–588,615)	**326,482** (204,826–509,850)	**319,211** (199,745–503,941)
B_{2023}	**388,697** (246,254–611,903)	**283,516** (184,588–408,159)	**298,921** (180,542–485,706)	**48,371** (17,564–124,153)	**67,280** (29,730–140,179)	**41,677** (18,250–90,973)	**364,966** (232,813–575,239)	**313,874** (195,811–503,049)	**291,420** (180,413–468,149)
B_{2023}/B_{MSY}	**1.802** (1.278–2.371)	**1.771** (1.185–2.442)	**1.636** (1.036–2.332)	**0.305** (0.111–0.784)	**0.376** (0.163–0.791)	**0.237** (0.101–0.517)	**1.77** (1.272–2.293)	**1.714** (1.145–2.358)	**1.628** (1.033–2.271)
B_{2023}/K	**0.901** (0.639–1.185)	**0.885** (0.592–1.221)	**0.818** (0.518–1.166)	**0.152** (0.055–0.392)	**0.188** (0.081–0.396)	**0.118** (0.051–0.259)	**0.885** (0.636–1.147)	**0.857** (0.573–1.179)	**0.814** (0.516–1.136)
F_{2023}	**0.011** (0.007–0.017)	**0.015** (0.011–0.023)	**0.014** (0.009–0.024)	**0.089** (0.034–0.245)	**0.064** (0.031–0.145)	**0.103** (0.047–0.236)	**0.012** (0.007–0.018)	**0.014** (0.009–0.022)	**0.015** (0.009–0.024)
F_{MSY}	**0.088** (0.059–0.129)	**0.107** (0.07–0.154)	**0.098** (0.064–0.145)	**0.083** (0.057–0.116)	**0.086** (0.058–0.123)	**0.084** (0.057–0.12)	**0.09** (0.06–0.132)	**0.099** (0.066–0.147)	**0.098** (0.065–0.145)
F_{2023}/F_{MSY}	**0.125** (0.075–0.213)	**0.142** (0.087-0.255)	**0.146** (0.085-0.273)	**1.085** (0.4–3.12)	**0.748** (0.342-1.794)	**1.237** (0.545-2.903)	**0.131** (0.079 – 0.222)	**0.138** (0.082-0.243)	**0.149** (0.088-0.27)

Table 12. (Cont.)

	M10	M11	M12	M13	M14	M15	M16	M17	M18
K	**324,011** (270,686–388,521)	**364,049** (263,502–511,956)	**351,150** (255,379–492,364)	**419,098** (300,989–601,458)	**361,291** (263,866–506,987)	**355,780** (258,722–499,059)	**352,356** (258,153–491,612)	**318,043** (268,195–378,003)	**354,951** (263,922–496,377)
r	**0.2** (0.13–0.29)	**0.2** (0.13–0.29)	**0.2** (0.13–0.3)	**0.18** (0.12–0.26)	**0.2** (0.13–0.29)	**0.2** (0.13–0.29)	**0.15** (0.1–0.22)	**0.19** (0.13–0.26)	**0.17** (0.11–0.24)
MSY	**16,202** (10,604–23,556)	**18,277** (11,904–26,061)	**17,888** (11,650–25,706)	**18,929** (12,182–28,448)	**18,013** (11,740–26,130)	**17,528** (11,375–25,599)	**13,582** (8,978–19,887)	**15,090** (10,530–20,205)	**14,765** (10,157–20,866)
B_{MSY}	**162,005** (135,343–194,261)	**182,024** (131,751–255,978)	**175,575** (127,689–246,182)	**209,549** (150,494–300,729)	**180,646** (131,933–253,494)	**177,890** (129,361–249,530)	**176,178** (129,077–245,806)	**159,021** (134,097–189,001)	**177,475** (131,961–248,188)
B_{1957}	**283,429** (188,284–409,874)	**322,017** (203,359–505,833)	**311,251** (196,673–487,082)	**369,775** (228.774–585.459)	**320,268** (203,992–498,296)	**315,516** (198,898–490,782)	**311,488** (196,922–482,204)	**183,384** (201,011–390,802)	**316,767** (206,540–484,511)
B_{2023}	**363,070** (257,020–471,164)	**343,831** (220,589–534,694)	**323,760** (209,262–505,393)	**369,731** (232,448–582,905)	**289,309** (172,893–471,312)	**264,859** (155,789–434,414)	**23,216** (8,970–173,336)	**134,348** (52,520–283,187)	**67,291** (19,228–197,559)
B_{2023}/B_{MSY}	**2.259** (1.637–2.678)	**1.91** (1.297–2.533)	**1.864** (1.266–2.499)	**1.767** (1.256–2.325)	**1.6181** (1.027–2.264)	**1.502** (0.917–2.145)	**0.133** (0.05–0.91)	**0.849** (0.331–1.753)	**0.384** (0.102–1.1)
B_{2023}/K	**1.129** (0.819–1.339)	**0.955** (0.648–1.267)	**0.932** (0.633–1.249)	**0.884** (0.628–1.163)	**0.809** (0.513–1.132)	**0.751** (0.459–1.072)	**0.066** (0.025–0.455)	**0.424** (0.166–0.877)	**0.192** (0.051–0.55)
F_{2023}	**0.012** (0.009–0.017)	**0.013** (0.008–0.019)	**0.013** (0.009–0.205)	**0.012** (0.0074–0.018)	**0.015** (0.009–0.025)	**0.016** (0.01–0.028)	**0.185** (0.025–0.479)	**0.032** (0.015–0.082)	**0.064** (0.022–0.224)
F_{MSY}	**0.1** (0.066–0.145)	**0.099** (0.066–0.147)	**0.101** (0.066–0.15)	**0.09** (0.06–0.131)	**0.099** (0.065–0.147)	**0.098** (0.065–0.145)	**0.077** (0.052–0.111)	**0.095** (0.066–0.13)	**0.083** (0.057–0.118)
F_{2023}/F_{MSY}	**0.12** (0.078-0.192)	**0.125** (0.078-0.214)	**0.13** (0.08-0.224)	**0.13** (0.078-0.223)	**0.149** (0.087-0.282)	**0.165** (0.093-0.319)	**2.415** (0.308-6.322)	**0.343** (0.143-0.944)	**0.78** (0.25-2.762)

Table 13. Parameter estimates of Schaefer models M19 to M26 of the FI share of the stock using Bayesian approach. carrying capacity. ***r***: population intrinsic growth rate. **MSY**: maximum sustainable yield. B_{MSY}: biomass corresponding to MSY. B_{2023}/B_{MSY}: ratio of biomass in 2023 to biomass MSY. B_{2023}/K: ratio of current biomass to K. F_{2023}: exploitation rate in 2023. F_{MSY}: exploitation rate corresponding to MSY. F_{2023}/F_{MSY}: ratio of exploitation rate in 2023 to exploitation rate MSY. The mean is shown in bold and credible interval is given in brackets.

	M19	M20	M21	M22	M23	M24	M25	M26
K	**42,781** (30,267–62,128)	**33,322** (27,983–39,822)	**41,653** (29,984–59,762)	**40,311** (28,700–58,541)	**32,406** (27,154–38,824)	**32,604** (27,347–38,985)	**41,571** (29,539–60,209)	**40,801** (28,759–58,602)
r	**0.17** (0.11–0.25)	**0.19** (0.13–0.28)	**0.17** (0.11–0.25)	**0.17** (0.11–0.25)	**0.19** (0.12–0.28)	**0.18** (0.12–0.27)	**0.17** (0.11–0.25)	**0.17** (0.11–0.25)
MSY	**1,825** (1,122–2,880)	**1,633** (1,046–2,338)	**1,785** (1,102–2,793)	**1,743** (12,182–28,448)	**1,511** (970–2,272)	**1,503** (968–2,190)	**1,777** (1,094–2,803)	**1,755** (1,083–2,750)
B_{MSY}	**21,391** (15,138–31,064)	**16,661** (13,991–19,911)	**20,827** (14,892–29,881)	**20,155** (14,350–29,270)	**16,203** (13,577–19,412)	**16,302** (13,673–19,492)	**20,786** (14,769–30,104)	**20,401** (14,379–29,301)
B_{1988}	**23,095** (14,602–36,456)	**25,531** (17,756–36,387)	**22,516** (14,495–35,565)	**22,004** (13,899–35,275)	**17,446** (12,033–25,377)	**23,392** (15,675–34,040)	**22,354** (14,204–35,312)	**22,066** (13,938–34,651)
B_{2023}	**37,097** (22,561–60,848)	**5,336** (1,515–14,555)	**34,503** (21,233–55,870)	**34,061** (31,148–55,393)	**36,033** (25,216–47,226)	**6,667** (2,674–15,823)	**35,076** (21,479–56,938)	**33,204** (20,275–54,331)
B_{2023}/B_{MSY}	**1.742** (1.237–2.326)	**0.32** (0.093–0.861)	**1.662** (1.177–2.231)	**1.701** (1.198–2.231)	**2.239** (1.613–2.676)	**0.41** (0.162–0.964)	**1.69** (1.2–2.264)	**1.637** (1.15–2.208)
B_{2023}/K	**0.871** (0.619–1.163)	**0.16** (0.046–0.431)	**0.831** (0.589–1.115)	**0.85** (0.599–1.115)	**1.12** (0.806–1.338)	**0.205** (0.081–0.482)	**0.845** (0.6–1.132)	**0.818** (0.575–1.104)
F_{2023}	**0.040** (0.024–0.065)	**0.275** (0.101–0.970)	**0.043** (0.026–0.069)	**0.043** (0.027–0.069)	**0.041** (0.031–0.058)	**0.22** (0.093–0.549)	**0.042** (0.026–0.068)	**0.044** (0.027–0.072)
F_{MSY}	**0.085** (0.057–0.124)	**0.097** (0.064–0.142)	**0.085** (0.057–0.124)	**0.086** (0.057–0.125)	**0.093** (0.061–0.138)	**0.092** (0.061–0.134)	**0.085** (0.057–0.124)	**0.086** (0.057–0.125)
F_{2023}/F_{MSY}	**0.467** (0.268-0.831)	**2.853** (0.944-10.878)	**0.501** (0.287-0.881)	**0.503** (0.289-0.874)	**0.444** (0.284-0.718)	**2.411** (0.958-6.252)	**0.494** (0.283-0.864)	**0.515** (0.294-0.909)

The biomass trend estimates derived from the SW Atlantic stock indicate biomass values near the carrying capacity until mid-1980s (Figure 25), when the fishing mortality increases (Figure 26). A decreasing trend in biomass is evident for all the models from mid-1980s until mid-1990s. From mid-1990s onwards, models produced two main trends depending on the CPUE index used in model fitting.

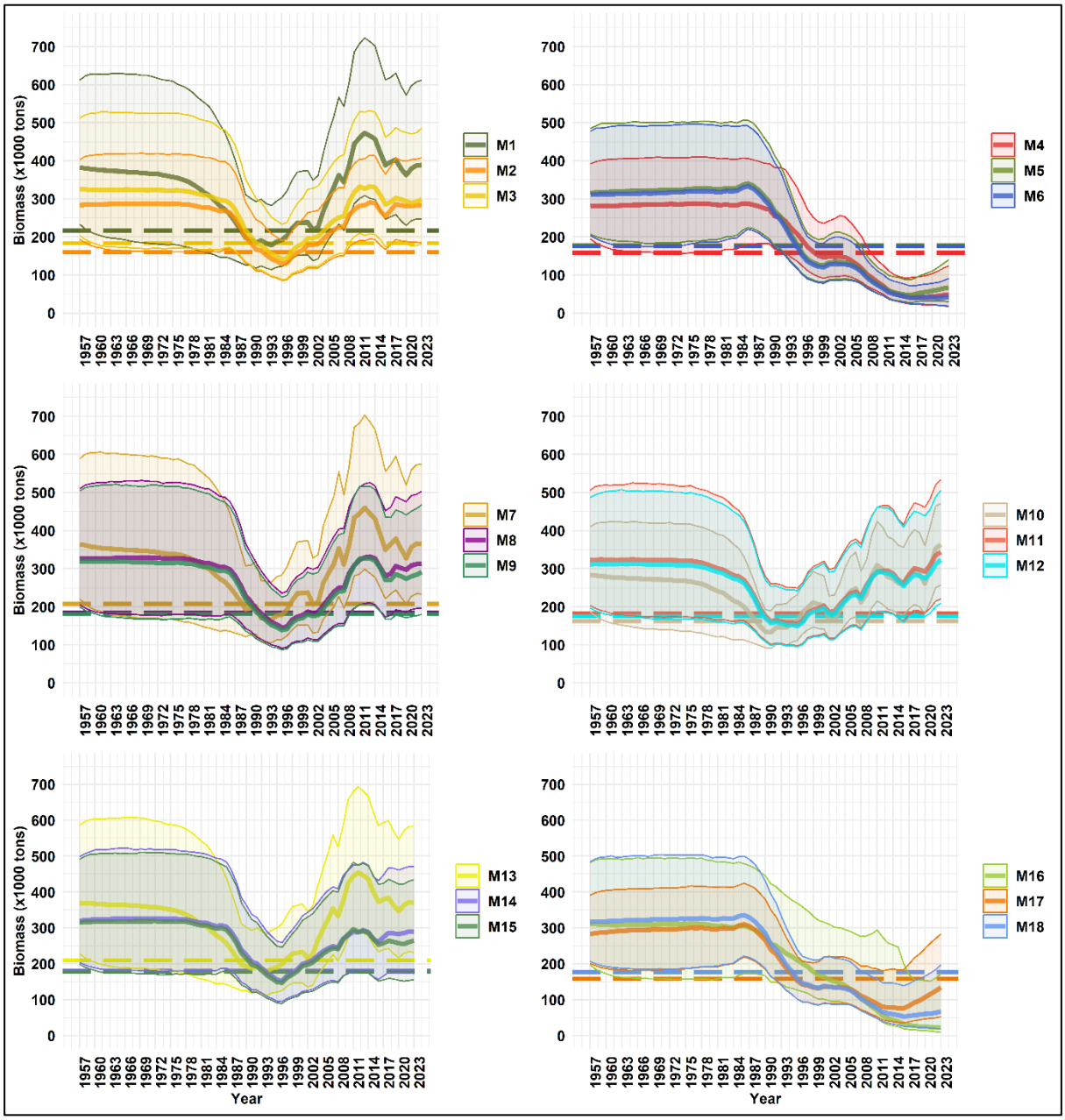

Figure 25. Biomass (B) trend of the models M1-M18 (SW Atlantic stock). The solid line corresponds to the mean and the shaded area to the 95% credible interval. Dashed lines represent the B_{MSY} for each model. The catch, abundance indices and priors of the models (M#) are described in Table 2.

One general trend is the biomass recovery estimated after the 1990s for the models including the finfish licences CPUEs (Figure 25). In general, the trend was guided by the finfish

licences CPUE, even when combined with Argentine CPUEs and SAI, although when combined with those indices, the biomass was estimated lower. This is evident for the pooled finfish licences CPUE (M1-M3), where the recovery was higher when only that CPUE was included (M1), and less high when combined with the Argentine CPUEs and with the SAI. This trend was also valid for the models including the finfish CPUEs by nation flag (M7-M9) and when the pooled finfish licence CPUE was combined with the calamari (Loligo) licence CPUE (M13-M15). However, when the finfish CPUE was standardised by licence, a very similar pattern was observed when including them only and when including them in combination with Argentine CPUE and with SAI (Figure 25, M10-M12), with an increasing biomass trend.

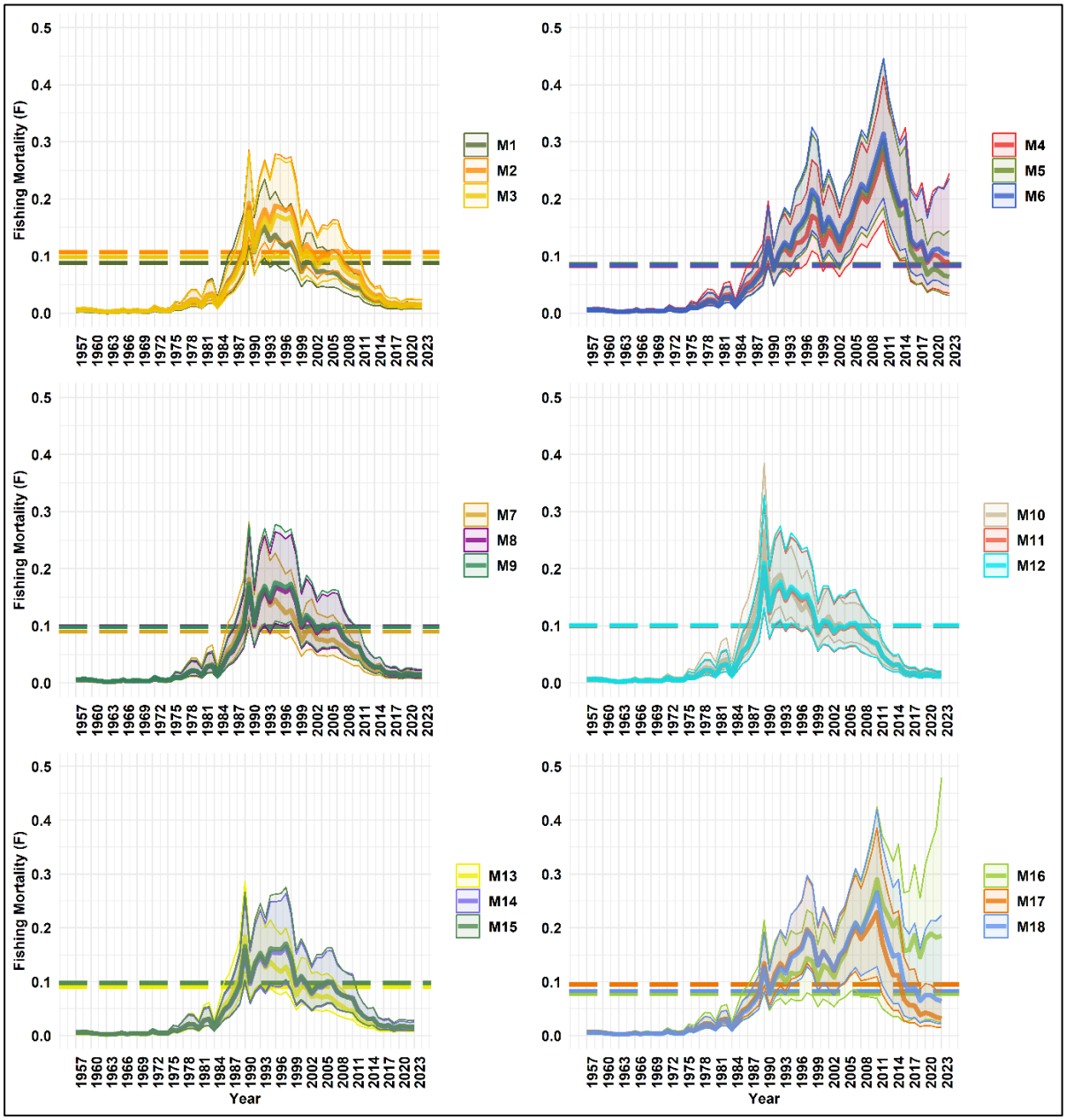

Figure 26. Fishing mortality (F) trends of the models M1-M18 (SW Atlantic stock). The solid line corresponds to the mean and the shaded area to the 95% credible interval. Dashed lines represent the F_{MSY} for each model. The catch, abundance indices and priors of the models (M#) are described in Table 2.

An opposite trend was estimated when the selected CPUE was the calamari (Loligo) licence, be it alone or in combination with the Argentine CPUE and SAI (Figure 25, M4-M6) and when the SAI, the Argentine CPUE or their combination where included (Figure 25, M16-M18). In these models, instead of a recovery after the mid-1990s, the decreasing trend continues until the end of the time-series, placing the estimated biomass at the end of the time-series below the B_{MSY}. In the model that includes only the Argentine CPUE (M17) a slight recovery is observed for the final years of the time-series, but still below B_{MSY} (Figure 25).

The fishing mortality estimates (Figure 26) show similar pattern for almost all the models, with a trend to increase above F_{MSY} in the 1990s, and to decrease below F_{MSY} in the mid-2000s. This general trend slightly deviates for models M4-M6 and M16-M18, where the final decrease in fishing mortality is less steep, ending either above F_{MSY} (M4, M6, and M16) or just below F_{MSY} (M5, M17, and M18; Figure 26).

In the case of the FI share of the stock, the biomass estimates at the start of the time series were proximate to the B_{MSY} in most models (M19, M21, M22, M23, M25, M26) or above B_{MSY} (M20, M24). In models where the estimations commenced in proximity to the reference point, the trend exhibits a brief decline in biomass during the 1990s, followed by a subsequent recovery to levels exceeding the carrying capacity (Figure 27). Those models were associated with the different combinations of finfish licence CPUEs or with the pooled finfish licences CPUE in combination with calamari (Loligo) licence CPUE (M21) and with SAI (M25) or the three CPUEs together (M26). In the models where the initial biomass was estimated above the B_{MSY}, the biomass had a declining trend, falling below the reference point at the end of the time series (Figure 27). Those models used only the calamari (Loligo) licence CPUE (M20) or the SAI (M24).

The fishing mortality rate for the FI share of the stock fluctuated around F_{MSY} until 2015, and declined afterwards for the models including the CPUE associated with finfish licences to levels below F_{MSY} (Figure 28). In the models not associated with finfish licences CPUE (M20, M24), the fishing mortality follows a period of fluctuation below the reference point until 2005, when it shows an increasing trend, exciding the F_{MSY} (Figure 28).

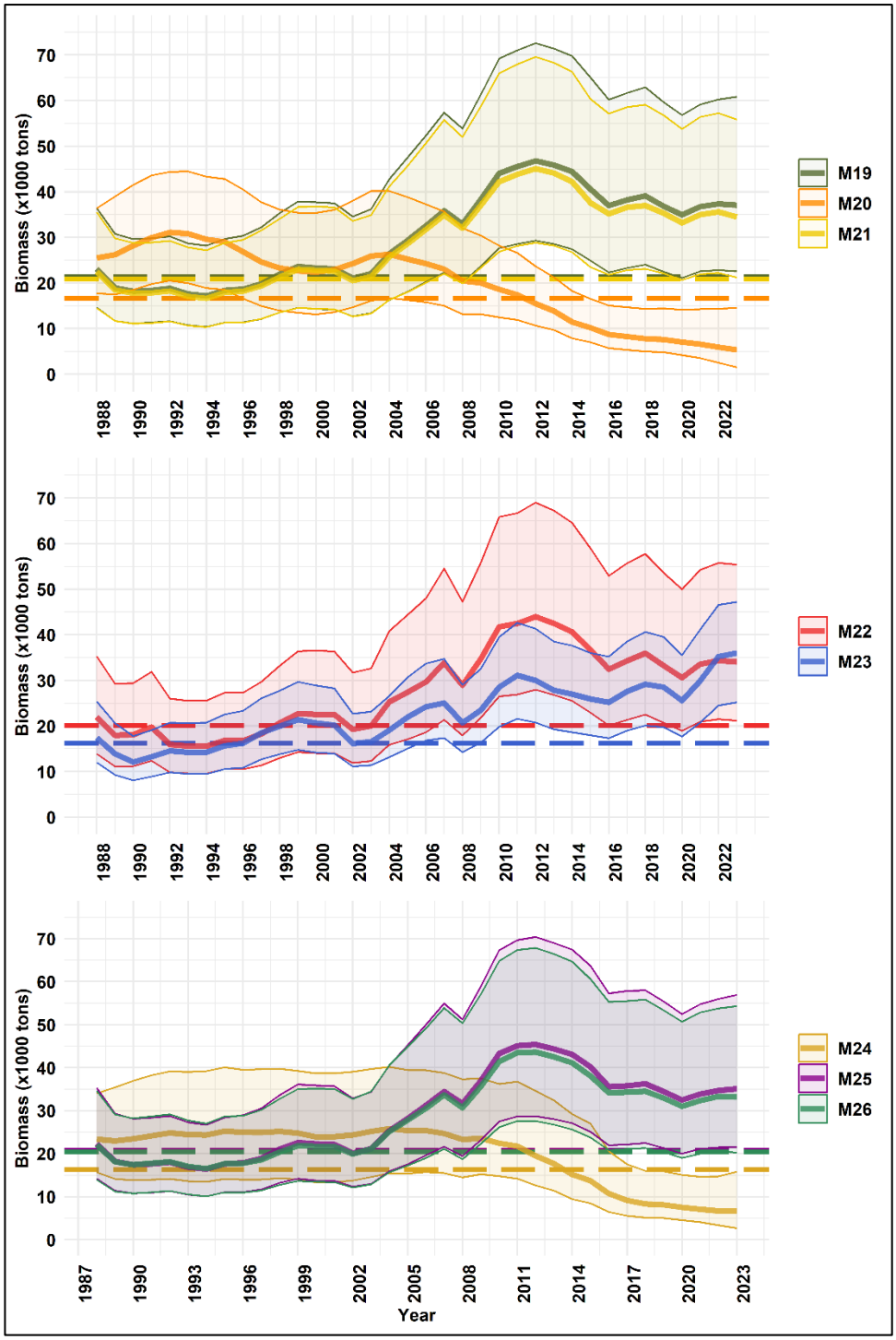

Figure 27. Biomass (B) trend of the models M19-M26 (FI share of the stock). The solid line corresponds to the mean and the shaded area to the 95% credible interval. Dashed lines represent the B_{MSY} for each model. The catch, abundance indices and priors of the models (M#) are described in Table 2.

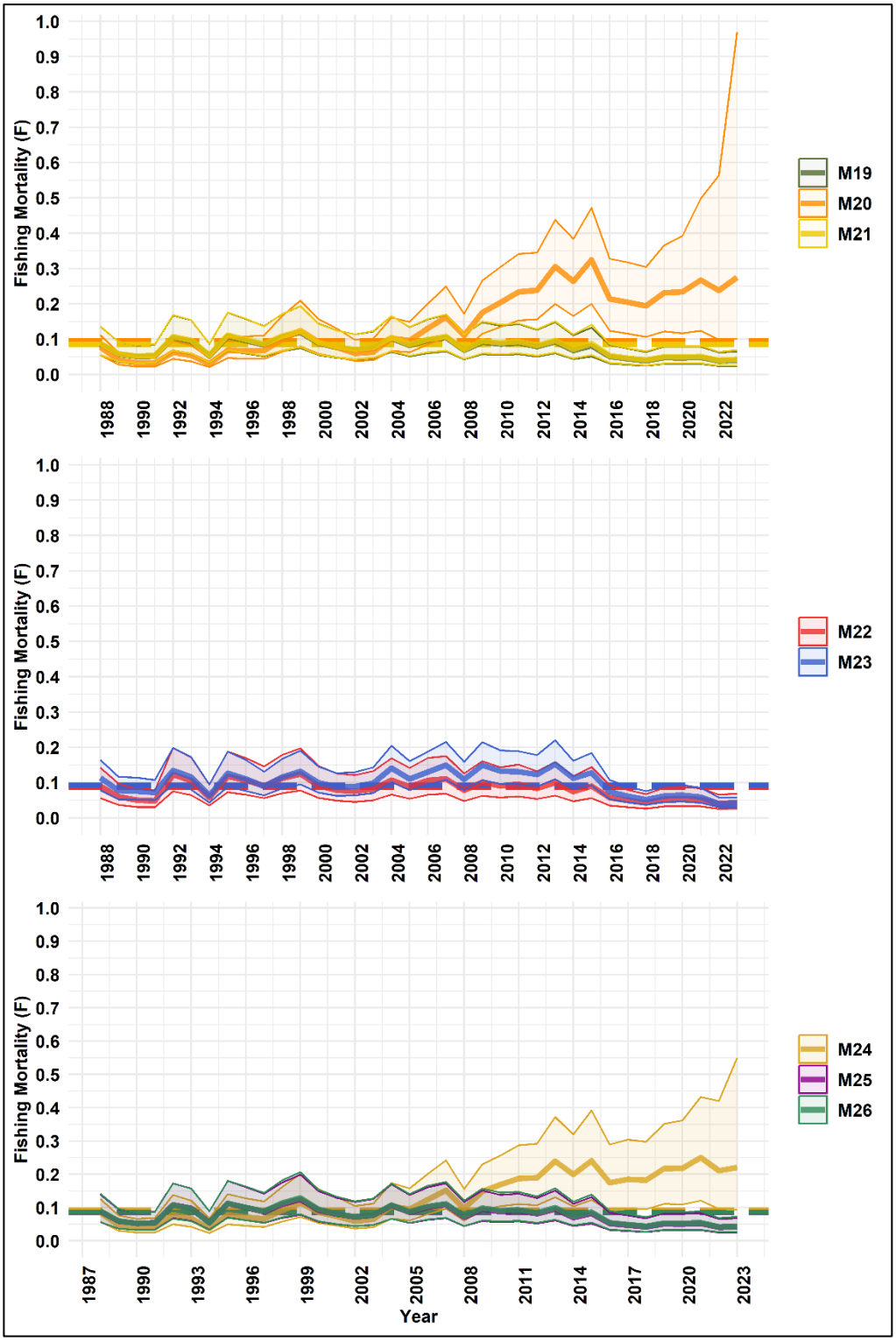

Figure 28. Fishing mortality (F) trends of the models M19-M26 (FI share of the stock). The solid line corresponds to the mean and the shaded area to the 95% credible interval. Dashed lines represent the F_{MSY} for each model. The catch, abundance indices and priors of the models (M#) are described in Table 2.

Stock status trends

The different tested models provided two major interpretations of the trend of the kingclip stock. For the whole SW Atlantic stock, a general estimated trend for the early years is initial under-exploitation and under-fishing, followed by an estimated over-exploitation and over-fishing in mid-1980s to mid-1990s (Figures 29, 30). Then, the trend changes according to the CPUE index used to fit the model. For the models that included one or more finfish related CPUE indices, the models estimated a return to an under-exploited and under-fished state (Figure 29, M1-M3, M7-M9; Figure 30, M10-M15). However, for the models that did not include a finfish-related CPUE index, although the models estimate a decrease in fishing mortality over the last 10-15 years, the estimations led to an under-fished but still over-exploited scenario for models M5, M17, and M18 (Figures 29, 30), and to an over-fished and over-exploited scenario in models M4, M6, and M16 (Figures 29, 30).

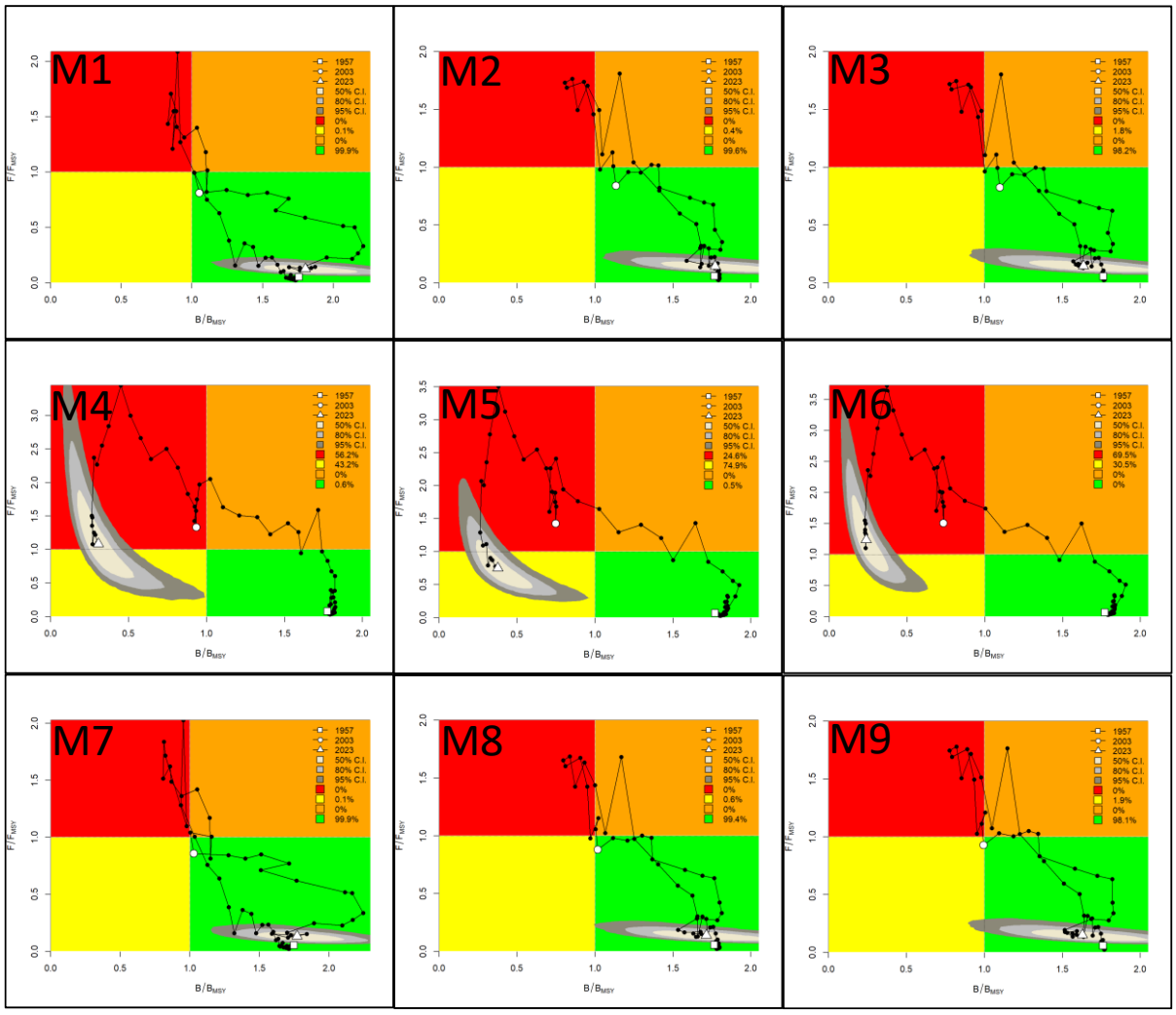

Figure 29. Kobe plots showing the estimated trajectories of B/B_{MSY} and F/F_{MSY} for the models M1-M9, SW Atlantic stock. Different grey shaded areas denote the 50%, 80%, and 95% credibility interval for the terminal assessment year. The probability of terminal year points falling within each quadrant is indicated in the figure legend.

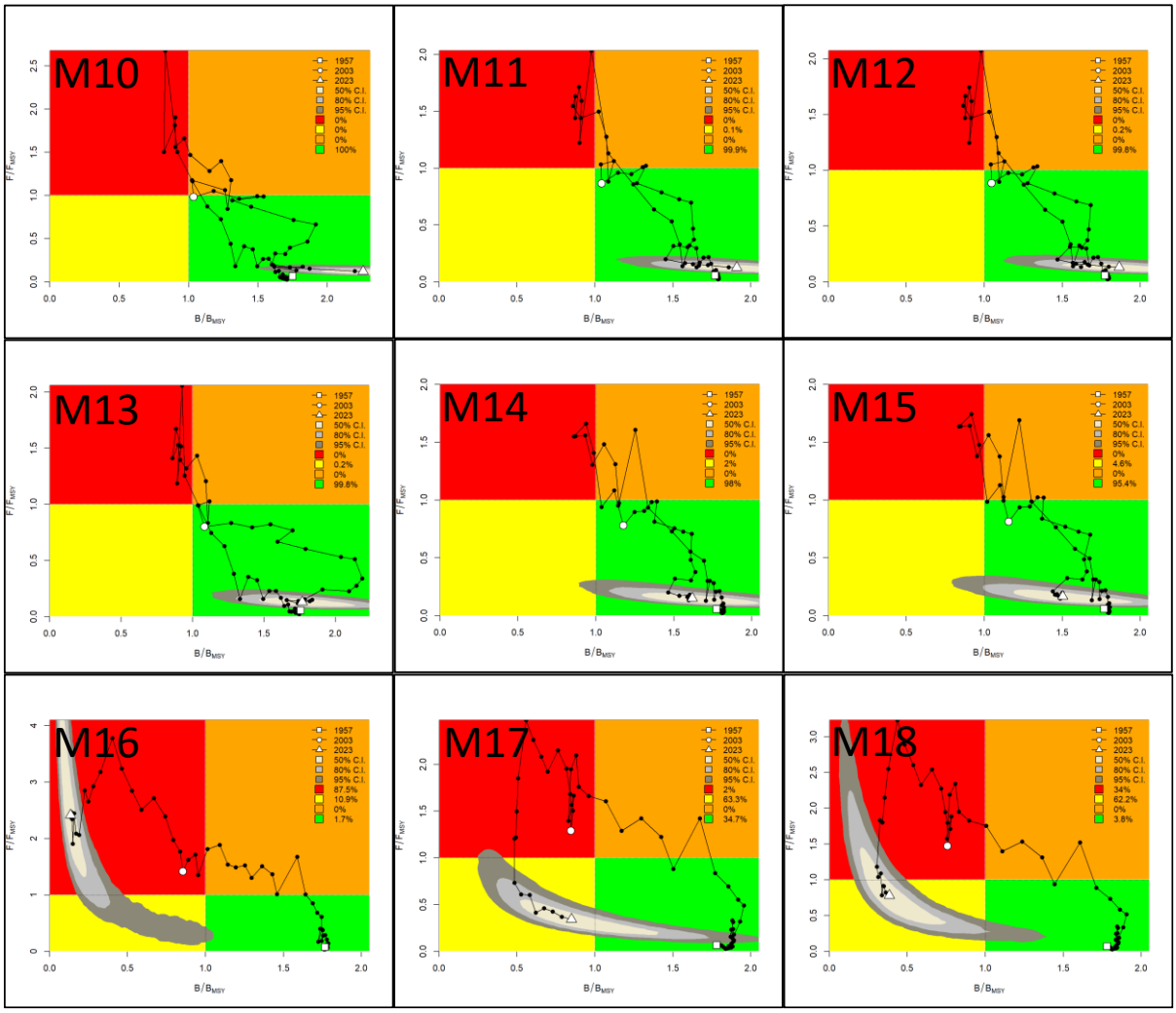

Figure 30. Kobe plots showing the estimated trajectories of B/B_{MSY} and F/F_{MSY} for the models M10-M18, whole SW Atlantic stock. Different grey shaded areas denote the 50%, 80%, and 95% credibility interval for the terminal assessment year. The probability of terminal year points falling within each quadrant is indicated in the figure legend.

The trend for the models that included the FI share of the stock started with a fishing mortality close to F_{MSY} and with a biomass, depending on the model, close to B_{MSY} (M19, M21-M23, M25, M26) or in an under-exploited state (M20, M24). After a period of over-fishing and over-exploitation in all models (Figure 31), some of them returned to a state of under-exploitation and under-fishing (M19, M21-M23, M25, M26). All those models included a finfish related CPUE. In the models that did not include a finfish related CPUE (M20, M24) the current state of the resource shows over-fishing and over-exploitation (Figure 31).

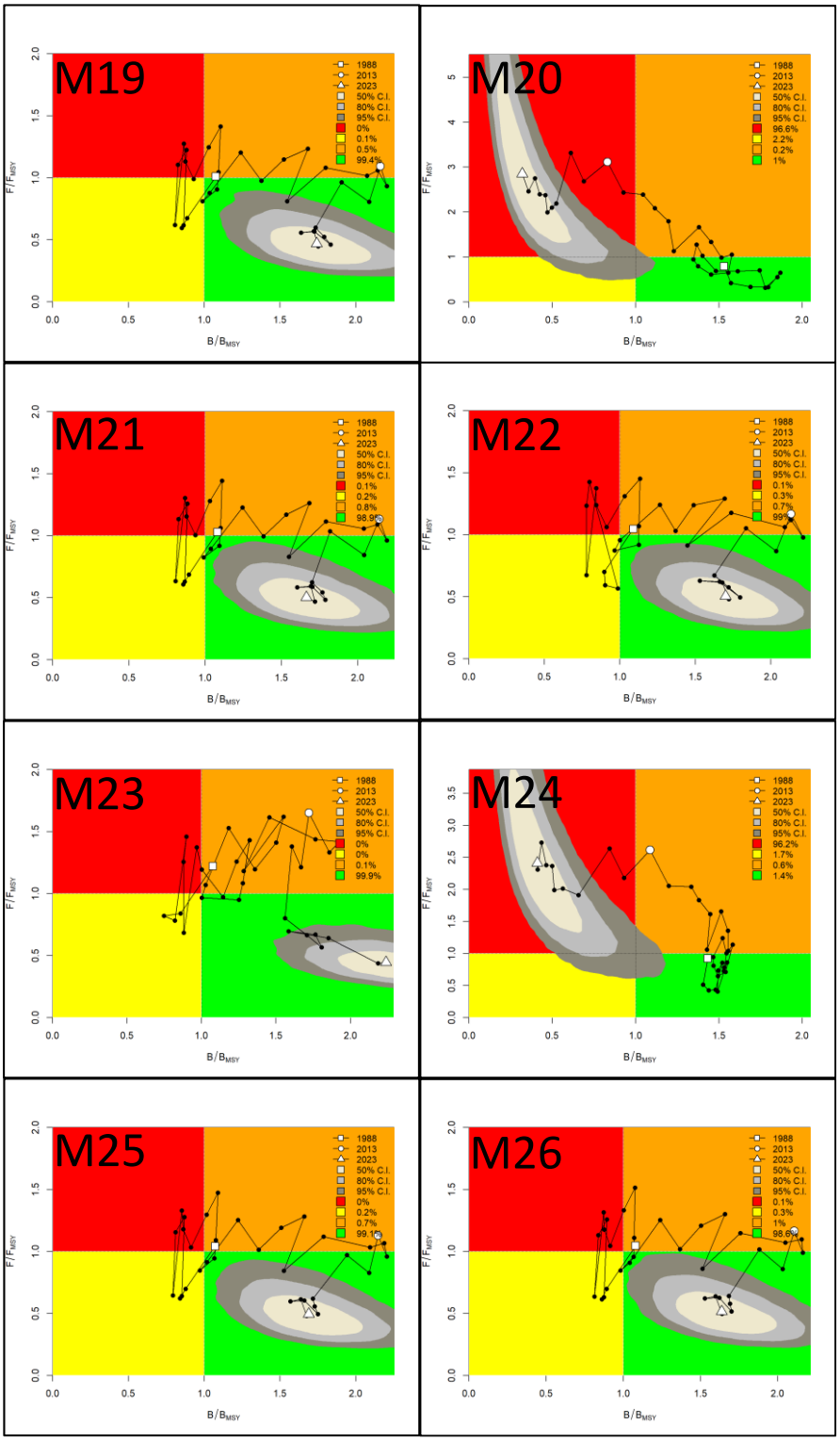

Figure 31. Kobe plots showing the estimated trajectories of B/B_{MSY} and F/F_{MSY} for the models M19-M26 (FI share of the stock). Different grey shaded areas denote the 50%, 80%, and 95% credibility interval for the terminal assessment year. The probability of terminal year points falling within each quadrant is indicated in the figure legend.

Discussion

CPUE selection and standardisation

Different data subsets led to different trends in the commercial CPUE. When the finfish licences were included, a similar trend pattern was observed for the pooled finfish licences CPUE, for the Spanish flag vessels CPUE, and for the CPUE of the licences AY. The trend showed a pattern of increase in the CPUE until around the year 2011, with a posterior decrease but to a higher level than the one at the beginning of the temporal series. This increase in the CPUE was related to an increase in the catch in those years. The similarity between the three mentioned abundance indices could be because the finfish licences are dominated by Spanish flag vessels and the majority of them operate with the A (Y) licence. However, the licence that was historically associated with the largest kingclip catches and had the largest CPUE in the recent years is the licence W (Z). For this licence, the abundance index showed almost a constant increase over time. It is possible that the trend observed for the A (Y) licences has a higher weight (more data) when the CPUE includes all the finfish licences pooled, leading to a similar trend, and that most of the vessels correspond to the Spanish nation flag.

The CPUE corresponding to the calamari (Loligo) licences (C, X) shows a different trend, with a steep decrease in the CPUE after the year 2007. It is difficult, with the available information, to conclude if this corresponds to a real decrease in the kingclip abundance inside the “Loligo box”, or is a result of changes in the way the fleet operates. For example, a change in the fishing strategy by the captains, avoiding the aggregation sites of the kingclip, could lead to a decrease in the catch of the species without decreasing the effort targeting the calamari (Loligo), that is the objective of these licences.

The survey abundance index (SAI) also showed a decrease in the abundance of kingclip after the year 2015. In general, abundance indices derived from the surveys are preferred over the fishery-based indices in stock assessment, as they are designed in a robust scientific manner that minimises bias. Furthermore, the standardisation of these indices can enhance the precision of abundance estimations (Zimney & Smart, 2022). In the case of the FI waters, while the fishery-independent abundance index may be more reliable than the fishery-dependent indices, the short time series of the former is insufficient. A long timeseries is always preferable for detecting trends in the abundance of a resource. This highlights the importance of maintaining continuity in surveys, ensuring consistency in the sites and effort employed. The decline in the fishery-independent abundance index of the kingclip over time in this report aligns with the findings reported for the assumed same stock in Argentine waters (Irusta *et al.*, 2016; Di Marco, 2022).

When standardising the indices, in all cases the AIC favoured the most complex models. In general, all the standardization models for each CPUE showed the same trend differing only in the scale, and mostly following the trend of the nominal CPUE. The AIC tends to give a lower value to more complex models, especially when increasing the degrees of freedom. For this reason, some authors recommend the utilization of other selection criteria (Shono, 2005), like

the Bayesian Information Criteria (BIC). During the model selection process the BIC was also evaluated (not shown), and the results were similar to those of the AIC.

The standardisation of CPUE is influenced by a number of factors, including the biology of the species, the structure (and changes) of the fishery, and, most importantly, data availability (Hoyle *et al.*, 2024). For example, when the species tend to aggregate for some periods, as is the case for the kingclip in the non-reproductive season (Irusta *et al.*, 2016), a number of zeros in the CPUE could be wrongly considered as true zeros, as the trawling was not conducted in the area of the aggregation of the species and they should be treated as false zeros, excluding them from the standardisation (Hoyle *et al.*, 2024). Also, if there is an upgrade in some aspects of the fleet, like power or storage capacities, this could lead to an increase in the abundance index that is not related to an increase in the abundance of the stock. At the present, no detailed information exists for the FI waters for the determination of these factors, and in this report only the available information was used to construct the standardised abundance indices.

The current state of knowledge of the kingclip fishery in FI waters does not permit a definitive conclusion as to whether the observed increase in fishery-dependent abundance indices of the finfish licences over time is a genuine reflection of an actual increase in the abundance of the resource or if it is an artefact resulting from an improvement in the quality of catch reports over time. The introduction of a more accurate reporting system could be a significant factor in the observed increase in catch, particularly for bycatch species such as kingclip. It is not uncommon for underdeveloped fisheries to exhibit a tendency to underreport catch (Belhabib *et al.*, 2014, 2016). This could have been a factor in the fisheries of the FI waters at the initial stage of the time series. Furthermore, Pauly & Zeller (2016) demonstrated that reported catches are often significantly lower than the actual catches in marine fisheries. As fisheries develop, compliance controls may become more rigorous, leading to more accurate reporting of catches. This could explain the observed increase in abundance indices, rather than reflecting a genuine increase in the stock abundance. As stated above, another factor that could influence the CPUE estimation is the catchability of the vessels. If the fleet is upgraded and the catchability of the vessels increases, it could have an effect in CPUE standardisations (Feenstra *et al.*, 2019). These factors should be considered in order to increase the reliability of the CPUE standardisation. However, the lack of detailed information about related changes in reports or catchability of the vessels made such considerations in the present report impossible.

Surplus production model outcomes

The results of the SPMs showed a strong relation with the standardised CPUE included. For the whole SW Atlantic stock assessment, the biomass trend was observed as an unchanged pattern until the mid-1980s, when the total catch increased significantly. A subsequent decrease in biomass was observed. During this period, wide credible intervals are observed until the year 1988, as the model's estimates are mostly directed by the catch. Then, the trend changes accordingly to the standardised CPUE included in the model.

When a finfish related CPUE was included, that CPUE drive the biomass estimation. If the finfish related CPUE was combined with other indices (Arg, LOL or SAI), the final biomass estimation was scaled to a lower value, but still with the trend of the finfish indices. Setting the average CV for FI CPUE indices to equal the CV of the Argentine indices assigns them equal weights, levelling their importance. In the present report, the CV of the SAI was intentionally given a higher weight (mean of 0.2 vs. 0.3 for the other). This higher weight is evidenced in models M9, M12, and M15, where the biomass estimations at the end of the time-series shows the lower levels of the compared similar models. However, the short time-series of the SAI was not enough to change the general trend of the biomass, compared to the other similar models.

All the models including the finfish indices by licences, showed a similar biomass trend guided mainly by the licence W (Z) CPUE. From the three licence CPUEs, the W (Z) showed an increasing trend and a smaller standard error, compared with the A (Y) licence. Although the G licence had the smallest standard error, its lack of trend was interpreted as uninformative for the model and thus had no major effect in the models. When the Argentine CPUE and the SAI were included, the final trend was maintained and the absolute values were, although smaller, relatively similar; however, the credible intervals increased. This indicates that contradictory indices add more uncertainty to the assessment.

The models that included the calamari (Loligo) CPUE (M4-M6) showed an opposite trend to the models including a finfish related CPUE. The trend is a decrease in the biomass, to levels below the B_{MSY} with no further recovery. In those models, adding the Argentine and SAI indices to the assessment does not changes the trend, as the three indices are not contradictory and are consistent with a decrease of the CPUE with time. In these cases, the credible intervals are narrower also due to the lack of contradiction. This trend is also similar to the trend of models M16-M18 that included the SAI and the Argentine CPUE. The model including only the SAI (M16) shows the wider credible intervals, possibly related with the short time series of this index, present only since 2010. In the case of the model only with the Argentine CPUE (M17) an increasing trend is observed at the end of the time-series where the lack of CPUE made the model rely only on the catch, resulting in wide credible interval. Even so, the biomass levels did not reach the B_{MSY}. The model that includes both, Argentine CPUE and SAI, shows a similar pattern to the one with only the Argentine CPUE until the year 2011, where the final increase is not estimated. This could be related to the higher weight given to the SAI CV that is influencing the estimations only at the end of the timeseries due to its shorter length.

Similarly, for the FI stock-share different trends are observed depending on the abundance index included. These models (M19-M26) included only the FI catch and the fishery dependant abundance indices encompass all the catch period. The trend for the finfish CPUE related models shows a general pattern of a great increase in biomass towards the year 2012, with a slight decrease afterwards. This trend is observed clearly in models M19 and M22, where the finfish CPUE indices are included (pooled finfish, or by nation flag), but also is observed for the models M21 (pooled finfish in combination with calamari (Loligo) CPUEs), and for M25 and M26, were the polled finfish CPUE was in combination with the SAI, and both the calamari (Loligo) CPUE and

the SAI. This remarks the weight given in the models to the finfish licences, probably as a combination of the smaller standard error compared with the calamari (Loligo) CPUE and the longer length of the CPUE time-series compared with the SAI. When including in the model only the calamari (Loligo) CPUE (M20) or only the SAI (M24), the trend is similar to the trend of the SW Atlantic stock, with a constant decrease in biomass since the mid-2000s. The trend for the models including finfish CPUE by licence (M23), shows a trend of constant increasing biomass, similar to the trend observed for the SW Atlantic stock, guided mainly by the W (Z) licence CPUE that is the one with the smallest standard error and including a contrast in the CPUE time-series. All these results highlight the importance of the abundance index employed for the assessment, as an index that does not reflect the actual abundance of a stock could lead to misleading results and interpretations (Hoyle *et al.*, 2024).

The Kobe plots shows the trajectory of the stock since the beginning of the time-series, relating the biomass in the form of B/B_{MSY} with the fishing mortality in the form of F/F_{MSY} for each year. For the whole SW Atlantic stock (M1-M19), a clear period of overfishing ($F/F_{MSY}>1$) in the 1990s led to an overexploited period ($B/B_{MSY}<1$). After this period, the behaviour of the models depended on the included abundance indices, with the estimations returning to an under-fished and under-exploited state over the last 10-15 years for the models including indices with an increasing trend, or the permanence in the state of overexploitation when including indices with a decreasing trend. This behaviour of the models was consistent between the SW Atlantic stock and FI share of the stock. It should be highlighted again that the only difference between the models compared was the abundance index included, with the catch time-series and the priors remaining identical (although different for the whole and the FI share stock assessments).

It is noteworthy that the estimated MSY for all models including only the FI share of the stock was between 1,825 and 1,503 tons, regardless of the relative state of the fishery with respect to B_{MSY}. The MSY is a theorical value that is related to r and K in the form: MSY = rK/4 (Beverton & Holt, 1957). In the tested models the prior information for r and K was relaxed by design to let the data influence the posteriors. Even so, the estimated values of MSY did not vary much (~300 tons). The values estimated are close to the 1,675 tons set as the Total Allowable Catch (TAC) in the previous assessment (Ramos & Winter, 2022), derived by applying ICES Advice Rules Category 5 (average of the catches of the previous three completed years); a method recommended by the independent finfish fishery review (MEP, 2020). However, depending on the SPM considered, and the state of the stock relative to the reference point, these levels could be considered sustainable or, in the case of an overfished/overexploited estimate (M20, M24), lead to the stock depletion. It needs to be clear that the MSY concept is commonly regarded as a target for the populations, however some authors highlight the importance of regarding it as a limit, instead of a target (Mace, 2001).

When considering the goodness of fit and the Deviation Information Criterion for model selection, the models that included the pooled finfish licences showed the best combined statistics (M1, M19). However, given the uncertainty about the true state of the stock, and the low reliability of all the indices, it is difficult to base the assessment on a single model. Although

the RMSE is a good measure of how precisely the model predicts the response, there is no guarantee that a model with a higher goodness-of-fit score adequately reflects the population dynamics of the stock (Winker *et al.*, 2018). In some occasions, the fisheries-dependent input data could be sampled in a biased way and not representative of the process they are meant to measure. In addition, misreporting of catches can introduce data conflicts in the stock assessment models (Carvalho *et al.*, 2021). Because of the complexity of the kingclip biology and its fisheries, it is difficult to determine whether a model better reflects the current state of the stock based solely on statistics that rely on the fit of an index to the model.

Management remarks

In the past, most of the kingclip catch in SW Atlantic was taken by Argentine vessels. However, this has changed in the recent years. The Argentine government has imposed restrictions on fishing for this species since 2012 (Irusta *et al.*, 2016; Di Marco, 2022). However, there is no evidence of stock recovery and the biomass is still estimated to be below the reference limits (Di Marco, 2022). The Argentine CPUE included in this report shows a decreasing period until the late 1990s, a steady medium period until the late 2000s, and a steady low period since 2009. As fishing restrictions were imposed since 2012, it is difficult to determine whether the steady period of low CPUE is due to the low kingclip abundance or to the restriction measures imposed.

Presently, the catch of the Falkland Islands and the catch of Argentina are similar (Table A1). Given that the portion of the stock that reaches the FI waters is just a fraction of the whole stock, similar and precautionary measures could be considered by the FIG in order to contribute to the recuperation of the stock. One of the measures could be to avoid trawling in areas with high kingclip aggregations (Di Marco, 2022). For this purpose, a fine-scale identification of these spots should be carried out. After the sensitive areas are identified, a trawling restriction could be suggested in order to protect the population. Another and more immediate measure would be to remove the kingclip as a target species from the licences and to include it as a by-catch species, with regulations similar to those in rays.

The SPMs strongly rely on informative CPUE indices, which proved questionable for the kingclip in FI waters. Thus, other assessment methods are recommended to be explored. These alternatives include length-based methods such as (but not restricted to) Length Based Spawning Potential Ratio (LB-SPR; Hordyk *et al.*, 2015), length-based Bayesian Biomass estimations (LBB; Froese *et al.*, 2018) or Length Based Indicators (LBI; Froese, 2004). Some of these methods were explored by Ramos & Winter (2019) and results showed the biomass to be below the reference points. An update of these methods and a comparison of the present study results with those of other methods could lead to a better interpretation of the current status of the stock and therefore to a better management strategy. Final recommendations should be based on both approaches.

Even though it is assumed that the FI stock is shared with Argentina, it is not clear whether the Chilean stock is a separate one. Genetic studies of the Chilean stock showed no differences between the northern and the southern areas (Canales-Aguirre *et al.*, 2010). However, when life-history parameters (Wiff *et al.*, 2011) or otolith morphometry (Wiff *et al.*, 2019) are evaluated, different stock differentiation is evidenced. Given the complexity of the Chilean coast (open sea and fjords), it is possible that more than one stock exists (Wiff *et al.*, 2019). However, given the proximity of the southern portion of the Chilean stock to the Southwest Atlantic stock, a regional delimitation stock study could be of interest for a better management strategy.

Recommendations for the future of stock management must therefore be consistent with clear objectives. It is impossible to fish all species at (or close to) the MSY (Pikitch, 1989), and it needs to be considered that species with vulnerable life-histories, such as kingclip, could be progressively depleted and lost from the fishery (Roberts *et al.*, 2024). Fishing less of this species can also contribute to a better ecosystem functioning. For this purpose, besides reducing exploitation rates, other measures should be adopted, such as shifting trawls to places with lower catch of the species. This could lead to produce higher population sizes, increase CPUE and cause less damage to habitats and non-target species (Roberts *et al.*, 2024).

Final considerations

This report serves as a milestone in the assessment of kingclip using a Bayesian framework surplus production model. However, the results of this report suggest that at least some of the commercial CPUE indices may be unrepresentative of the underlying kingclip biomass, while the survey abundance indices suffer from the short time-series.

If only the Falkland Islands share of the stock is included in the exercises, the MSY values are close to the TAC set for the species. This again raises a red flag, as this could be a sustainable catch or a catch that could lead to stock depletion and, eventually, its collapse depending on the chosen model. For example, in the worst scenario (M20), the estimation of the model for the present biomass (B_{2023}) is close to 5,300 tons. In this scenario, catch values close to 1,500 tonnes corresponds to 1/3 of the total biomass estimated. The TAC should therefore be treated with caution.

Identification of the areas with high aggregations at fine-scale of the species is of primary interest, and a second step would be to include restrictions for the trawling inside those areas. For this purpose, trawl by trawl catch information is vital. Identification of trawls with high kingclip catch (>30% of the trawl) and the location of the areas where they occur consistently may shed light about the location of the aggregation areas in the FI waters.

Other protection measures are also recommended for kingclip due to its vulnerability. An easy and fast management measure could be to remove the kingclip from the target species for the finfish licences and consider it in the same way as other by-catch species (e.g. 10% by-catch limit). Size limits should also be considered, to avoid the catch of juvenile individuals.

Complementing this assessment with other assessment methods, such as length-based methods, is of particular interest.

References

Akaike, H. (2011). *Akaike's information criterion*. International Encyclopedia of Statistical Science (Springer), 25-25.

Arkhipkin A., P. Brickle, V. Laptikhovsky, A. Winter. (2012). Dining hall at sea: feeding migrations of nektonic predators to the eastern Patagonian Shelf. *Journal of Fish Biology* 81: 882–902. DOI: 10.1111/j.1095-8649.2012.03359.x

Baker L. L., R. Wiff, J. C. Quiroz, A. Flores, R. Cespedes, M. A. Barrientos, V. Ojeda, C. Gatica. (2014). Reproductive ecology of the female pink cusk-eel (*Genypterus blacodes*): evaluating differences between fishery management zones in the Chilean austral zone. *Environmental Biology of Fish*. 97, 1083-1093. DOI: 10.1007/s10641-013-0199-2

Belhabib, D., V. Koutob, A. Sall, V. W. Y. Lam, D. Pauly. (2014). Fisheries catch misreporting and its implications: The case of Senegal. *Fisheries Research*, 151, 1-11. DOI 10.1016/j.fishres.2013.12.006

Belhabib, D., A. Mendy, S. Yevewo, N. T. Broh, A. S. Jueseah, N. Nipey, W. W. Boeh, N. Willemse, D. Zeller, D. Pauly. (2016). Fisheries catch under-reporting in The Gambia, Liberia and Namibia and the three large marine ecosystems which they represent. *Environmental Development*, 17, 157-174. DOI: 10.1016/j.envdev.2015.08.004

Belleggia, M., C. D. Álvarez, E. Pisani, M. Descalzo, E. Zuazquita. (2023). Prey contribution to the diet of pink cusk-eel *Genypterus blacodes* (Forster, 1801) revealed by stomach content and stable isotopic analyses in the southwestern Atlantic. *Fisheries Research*, 262, 106660. DOI: 10.1016/j.fishres.2023.106660

Beverton R. J. H., S. J. Holt. (1957). On the Dynamics of Exploited Fish Populations. Ministry of Agriculture, Fisheries and Food. Fishery Investigations, London, Series II, XIX. 533pp.

Canales-Aguirre C. B., S. Ferrada, C. E. Hernández, R. Galleguillos. (2010). Population structure and demographic history of *Genypterus blacodes* using microsatellite loci. *Fisheries Research*, 106, 102-106. DOI: 10.1016/j.fishres.2010.06.010

Carvalho, F., A.E. Punt, Y.J. Chang, M.N. Maunder, K.R. Piner. (2017). Can diagnostic tests help identify model misspecification in integrated stock assessments? *Fisheries Research*, 192, 28–40. DOI: 10.1016/j.fishres.2016.09.018

Carvalho, F., H. Winker, D. Courtney, M. Kapur, L. Kell, M. Cardinale, M. Schirripa, T. Kitakado, D. Yemane, K.R. Piner, M.N. Maunder. (2021). A cookbook for using model diagnostics in integrated stock assessments. *Fisheries Research*, 240, 105959. DOI: 10.1016/j.fishres.2021.105959

Cordo, H. D. (2001). Evaluación del abadejo (*Genypterus blacodes*) en el Atlántico sudoccidental, por medio de modelos de producción dinámicos. *Revista de Investigación y Desarrollo Pesquero*, 14, 79-93.

Cordo, H. D., L. Machinandiarena, G. J. Macchi, M. F. Villarino. (2002). Talla de Primera Madurez del Abadejo (*Genypterus blacodes*) en el Atlántico Sudoccidental. *INIDEP Informe Técnico*, 47/02, 1-5.

Cordo, H. D. (2004). Abadejo (*Genypterus blacodes*). Caracterización biológica y estado del recurso. *El Mar Argentino y sus Recursos Pesqueros*, 4, 237-253.

Di Marco, E. (2022). Evaluación del efectivo de abadejo (*Genypterus blacodes*) en el Atlántico sudoccidental (período 1980-2021). Captura biológicamente aceptable para el año 2022 y provisoria para el año 2023. *Informe Tecnico Oficial INIDEP* Nº 035/22, 39pp.

Feenstra, F., R. McGarvey, A. Linnane, M. Haddon, J. Matthews, A. E. Punt. (2019). Impacts on CPUE from vessel fleet composition changes in an Australian lobster (*Jasus edwardsii*) fishery. *New Zealand Journal of Marine and Freshwater Research*, 53(2), 292-302. DOI: 10.1080/00288330.2018.1556166

Froese, R. (2004). Keep It Simple: Three Indicators to Deal with Overfishing. *Fish and Fisheries*, 5, 86-91. DOI: 10.1111/j.1467-2979.2004.00144.x

Froese, R., N. Demirel, G. Coro, K. M. Kleisner, H. Winker. (2017). Estimating fisheries reference points from catch and resilience. *Fish and Fisheries*, 18(3), 506-526. DOI: 10.1111/faf.12190

Froese, R., D. Pauly. Editors. (2024). *FishBase*. World Wide Web electronic publication. www.fishbase.org, (02/2024)

Froese, R., Winker, H., Coro, G., Demirel, N., Tsikliras, A. C., Dimarchopoulou, D., Scarcella, G., Probst, W. N., Dureuil, M., and Pauly, D. A new approach for estimating stock status from length frequency data. *ICES Journal of Marine Science*, 75: 2004-2015.

Hastie, T., R. Tibshirani. (1986). Generalized Additive Models. *Statistical Science*, 1(4), 297-310.

Horn, P. L. (1993). Growth, age structure and productivity of ling, *Genypterus blacodes* (Ophidiidae), in New Zealand waters. *New Zealand Journal of Marine and Freshwater Research*, 27, 385-397.

Hordyk, A., K. Ono, S. Valencia, N. Loneragan, J. Prince. (2015). A novel length-based empirical estimation method of spawning potential ratio (SPR), and tests of its performance, for small-scale, data-poor fisheries. *ICES Journal of Marine Science*, 72: 217-231. DOI: 10.1093/icesjms/fsu004

Hoyle, S. D., R. A. Campbell, N. D. Ducharme-Barth, A. Grüss, B. R. Moore, J. T. Thorson, L. Tremblay-Boyer, H. Winker, S. Zhou, M. N. Maunder. (2024). Catch per unit effort modelling for stock assessment: A summary of good practices. *Fisheries Research*, 269, 106860. DOI: 10.1016/j.fishres.2023.106860

Irusta, C. G., E. Pisani, R. Castrucci, M. Simonazzi. (2016). Análisis de la pesquería comercial de abadejo y estado de explotación del recurso. Sugerencias de medidas de manejo. *Informe Técnico Oficial INIDEP* No. 33/16, 21pp.

Mace, P. M. (2001). A new role for MSY in single-species and ecosystem approaches to fisheries stock assessment and management. *Fish and Fisheries*, 2, 2-32. DOI: 10.1046/j.1467-2979.2001.00033.x

MEP. (2020). Annex 3: Review of Finfish Stock Assessments. Report for Falkland Islands Government. MacAlister Elliot & Partners Ltd. 47 p.

Pella J.J., P.K. Tomlinson. (1969). A generalized stock production model. *Inter-American Tropical Tuna Commission Bulletin*. 13, 421-458.

Pauly, D., D. Zeller. (2016). Catch reconstructions reveal that global marine fisheries catches are higher than reported and declining. *Nature Communications,* 7:10244. DOI: 10.1038/ncomms10244

Pikitch, E. K. (1989). Objectives for biologically and technically interrelated fisheries. *Fishery Science and Management: Objectives and Limitations*, 28, 107-136.

Plummer, M. (2003). JAGS: a program for analysis of bayesian graphical models using gibbs sampling. In: *3rd International Workshop on Distributed Statistical Computing* (DSC 2003). Vienna, Austria.

Posit team. (2023). RStudio: Integrated Development Environment for R. *Posit Software, PBC, Boston, MA*. URL http://www.posit.co/.

R Core Team. (2022). R: A language and environment for statistical computing. *R Foundation for Statistical Computing, Vienna, Austria*. URL https://www.R-project.org/.

Ramos J. E., A. Winter. (2019). Stock assessment of Kingclip (*Genypterus blacodes*) in the Falkland Islands, 2017-2018. *Fisheries Department, Directorate of Natural Resources, Falkland Islands Government*. Stanley, Falkland Islands. 31 pp.

Ramos J. E., Winter A. (2021). Stock assessment of kingclip (*Genypterus blacodes*) in the Falkland Islands. SA–2021–KIN. *Fisheries Department, Directorate of Natural Resources, Falkland Islands Government*. Stanley, Falkland Islands. 10 p.

Ramos J. E., A. Winter. (2022). Stock assessment of kingclip (*Genypterus blacodes*) in the Falkland Islands. SA–2022–KIN. *Fisheries Department, Directorate of Natural Resources, Falkland Islands Government.* Stanley, Falkland Islands. 41 p.

Ramos J. E., A. Winter. (2024). February bottom trawl survey biomasses of fishery species in Falkland Islands waters, 2010–2024. SA-2024-04*. Fisheries Department, Directorate of Natural Resources, Falkland Islands Government.* Stanley, Falkland Islands. 82 p.

Roberts, C., C. Béné, N. Bennett, J. S. Boon, W. W. Cheung, P. Cury, O. Defeo, G. De Jong Cleyndert, R. Froese, D. Gascuel, C. D. Golden, J. Hawkins, A. J. Hobday, J. Jacquet, P. Kemp, M. E. Lam, F. Le Manach, J. J. Meeuwing, F. Micheli, T. Morato, C. Norris, C. Nouvian, D. Pauly,

E. Pikitch, F. P. Amargos, A. Saenz-Arroyo, U. R. Sumaila, L. Teh, L. Watling, B. C. O'leary. (2024). Rethinking sustainability of marine fisheries for a fast-changing planet. *npj Ocean Sustainability*, 3(1), 41. DOI: 10.1038/s44183-024-00078-2

Sammarone, M. (2019). Distribución, estructura de longitudes y abundancia del abadejo (*Genypterus blacodes*) en el área reproductiva patagónica. Periodo 2000-2012. *Informe Investigación INIDEP* Nº 63/2019. 19 p.

Sammarone, M. (2023). Distribución, rendimientos y condición reproductiva del abadejo (*Genypterus blacodes*) en la plataforma argentina (43º S-48º S) en invierno y verano entre 2000-2012. *Marine and Fishery Sciences*, 36(1), 53-74. DOI*: 10.47193/mafis.3612023010105*

Schaefer, M. B. (1954). Some aspects of the dynamics of populations important to the management of the commercial marine fisheries. *Inter-American Tropical Tuna Commission*, 1 (2), 27-56

Shono, H. (2005). Is model selection using Akaike's information criterion appropriate for catch per unit effort standardization in large samples? *Fisheries Science*, 71, 978-986. DOI: 10.1111/j.1444-2906.2005.01054.x

Simpson G. (2024). *gratia: Graceful ggplot-Based Graphics and Other Functions for GAMs Fitted using mgcv*. R package version 0.9.2, https://gavinsimpson.github.io/gratia/.

Thorson, J. T., A. A. Maureaud, R. Frelat, B. Mérigot, J. S. Bigman, S. T. Friedman, M. L. D. Palomares, M. L. Pinsky, S. A. Price, P. Wainwright. (2023). Identifying direct and indirect associations among traits by merging phylogenetic comparative methods and structural equation models. *Methods in Ecology and Evolution*. DOI: 10.1111/2041-210X.14076

Villarino, M. F., M. Renzi. (1997). Validación de los anillos de crecimiento del abadejo manchado (*Genypterus blacodes*) como indicadores del crecimiento individual anual. *Informe Técnico Interno DNI-INIDEP* No 34/97, 14pp

Villarino, M. F. (1998). Distribución estacional y estructura de tallas del abadejo (*Genypterus blacodes*) en el mar argentino. *INIDEP Informe Técnico* 18, 1-25.

Wickham H. (2016). *ggplot2: Elegant Graphics for Data Analysis*. Springer-Verlag New York. ISBN 978-3-319-24277-4, https://ggplot2.tidyverse.org.

Wiff R., J. C. Quiroz, V. Ojeda, M. A. Barrientos. (2011). Estimation of natural mortality and uncertainty in pink cusk-eel (*Genypterus blacodes* Schneider, 1801) in southern Chile. *Latin American Journal of Aquatic Research*, 39, 316-326. DOI: 10.3856/vol39-issue2-fulltext-13

Wiff R., A. Flores, A. M. Segura, M. A. Barrientos, V. Ojeda. (2019). Otolith shape as a stock discrimination tool for ling (*Genypterus blacodes*) in the fjords of Chilean Patagonia. *New Zealand Journal of Marine and Freshwater Research*, 54 (2), 218-232. DOI: 10.1080/00288330.2019.1701047

Winker H., F. Carvalho, M. Kapur. (2018). JABBA: Just Another Bayesian Biomass Assessment. *Fisheries Research*. 204, 275-288. DOI: 10.1016/j.fishres.2018.03.010

Wood, S. N. (2017). *Generalized additive models: an introduction with R.* Chapman and Hall/CRC. 496pp. DOI: 10.1201/9781315370279

Zimney A., T. Smart. (2022). Effects of incomplete sampling and standardization on indices of abundance from a fishery-independent trawl survey off the Atlantic coast of the southeastern United States. *Fishery Bulletin*, 120 (3-4), 252-267. DOI: 10.7755/FB.120.3-4.6

Appendix

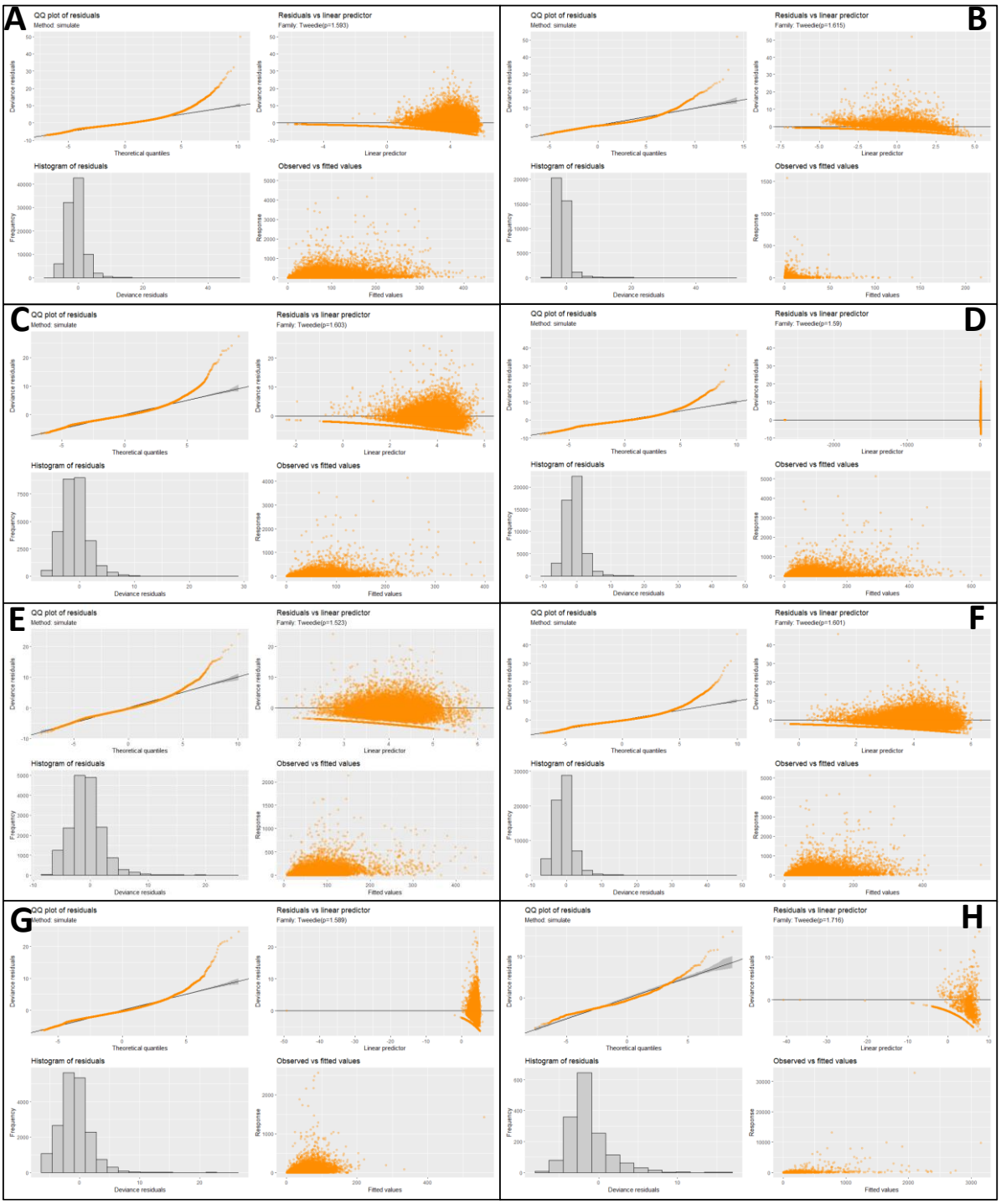

Figure A1. Residuals diagnosis of the GAM models. CPUEs standardisations used from A to H: finfish licences, Loligo licences, A-Y licences, W-Z licences, G licence, Spanish flag vessels, Falkland Islands flag vessels, survey abundance index.

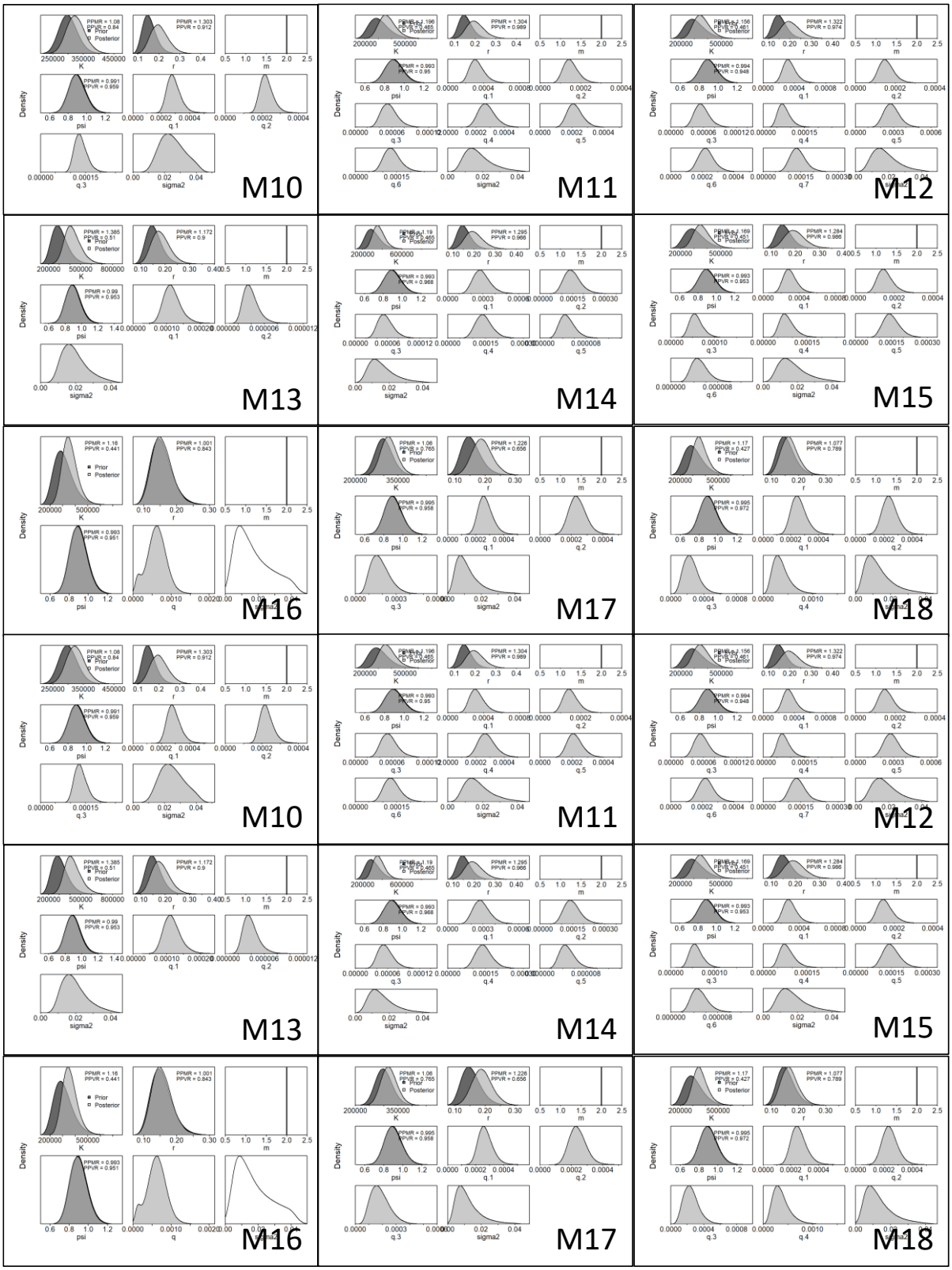

Figure A2. Priors to posteriors comparisons for the models M1-M18; SW Atlantic stock.

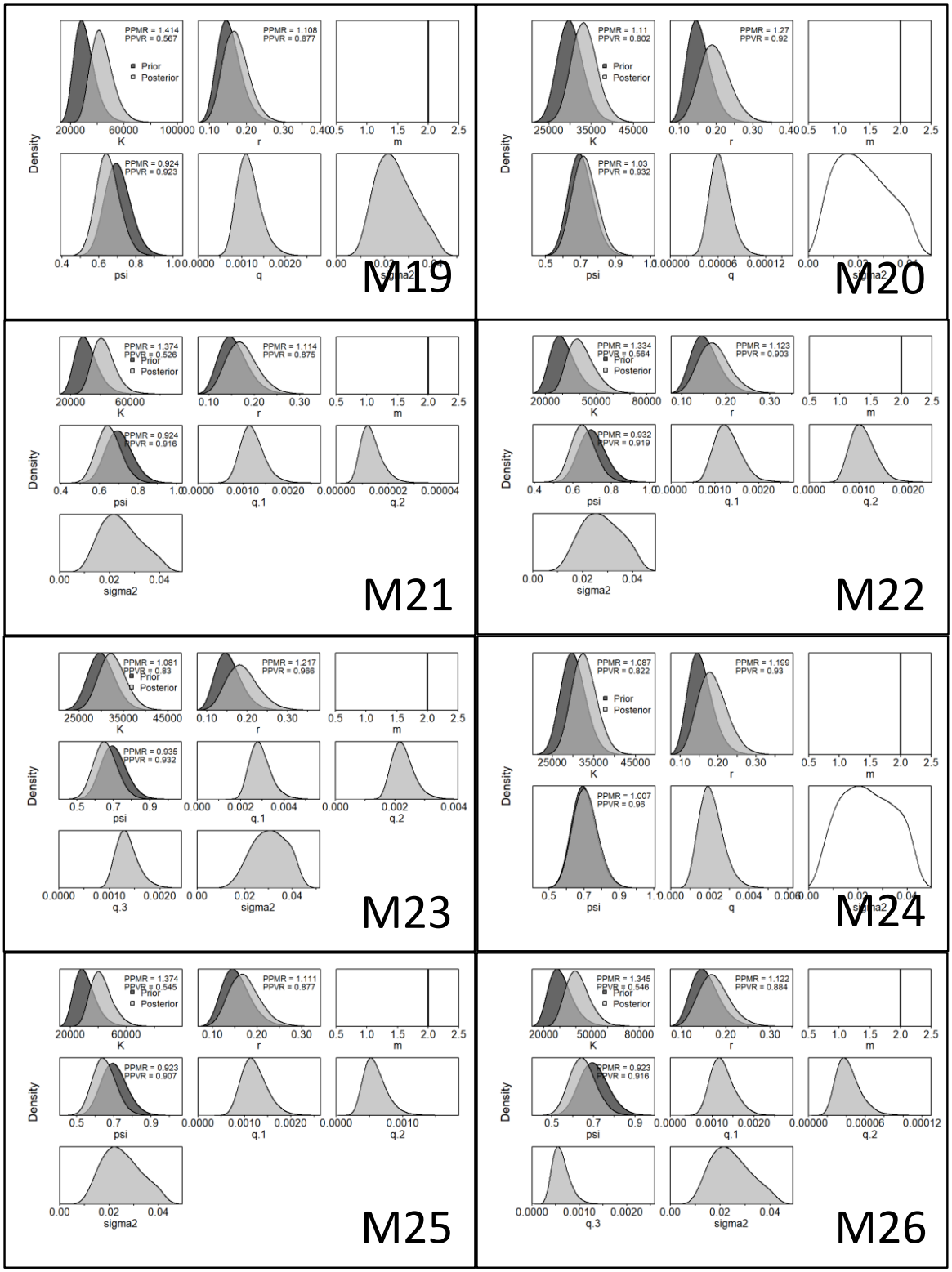

Figure A3. Priors to posteriors comparisons for the models M19-M26; FI share of the stock.

Figure A4. Run tests to quantitatively evaluate the randomness of the time series of CPUE residuals for models M1 to M18. Green panels indicate no evidence of lack of randomness of time series residuals (p>0.05) while red panels indicate the opposite. The inner shaded area shows three standard errors from the overall mean and red circles identify a specific year with residuals greater than this threshold value (3x sigma rule). Inner panels for each model correspond to a different CPUE. cpue_ff: CPUE of pooled finfish licence; cpue_LOL: CPUE of the calamari (Loligo) licences; cpue_es: CPUE of the vessels with Spanish flag; cpue_fk: CPUE of the vessels with Falkland Islands flag; cpue_AY: CPUE of vessels with A or Y licence; cpue_WZ: CPUE of vessels with W or Z licence; cpue_G: CPUE of vessels with G licence; cpue1, cpue2, cpue3: CPUEs from the Argentine fleet; sur: Survey Abundance Index.

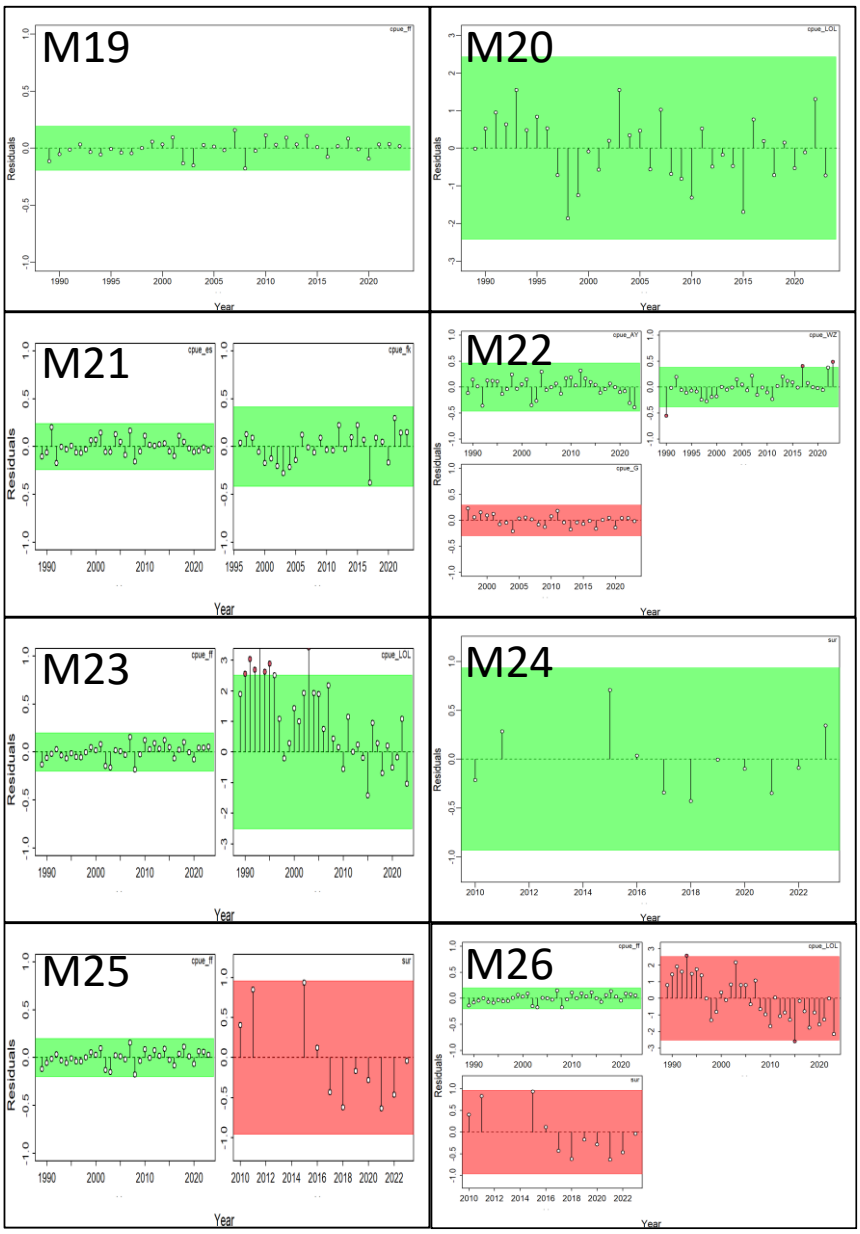

Figure A5 - Runs tests to quantitatively evaluate the randomness of the time series of CPUE residuals for models M19 to M26. Green panels indicate no evidence of lack of randomness of time series residuals (p>0.05) while red panels indicate the opposite. The inner shaded area shows three standard errors from the overall mean and red circles identify a specific year with residuals greater than this threshold value (3x sigma rule). Inner panels for each model correspond to a different CPUE. cpue_ff: CPUE of pooled finfish licence; cpue_LOL: CPUE of the calamari (Loligo) licences; cpue_es: CPUE of the vessels with Spanish flag; cpue_fk: CPUE of the vessels with Falkland Islands flag; cpue_AY: CPUE of vessels with A or Y licence; cpue_WZ: CPUE of vessels with W or Z licence; cpue_G: CPUE of vessels with G licence; sur: Survey Abundance Index.

Table A1. Annual catch (t) of kingclip from Falkland Islands and Argentina.

Year	Argentina (t)	Falkland Islands (t)	TOTAL (t)
1957	1,779	0	1,779
1958	1,789	0	1,789
1959	1,767	0	1,767
1960	1,542	0	1,542
1961	1,240	0	1,240
1962	892	0	892
1963	689	0	689
1964	843	0	843
1965	1,008	0	1,008
1966	1,501	0	1,501
1967	937	0	937
1968	1,303	0	1,303
1969	1,188	0	1,188
1970	1,083	0	1,083
1971	1,116	0	1,116
1972	2,274	0	2,274
1973	1,504	0	1,504
1974	1,341	0	1,341
1975	1,464	0	1,464
1976	3,361	0	3,361
1977	2,948	0	2,948
1978	5,050	0	5,050
1979	6,793	0	6,793
1980	6,561	0	6,561
1981	4,346	0	4,346
1982	8,820	0	8,820
1983	9,291	0	9,291
1984	3,894	0	3,894
1985	9,208	0	9,208
1986	14,363	0	14,363
1987	15,175	674	15,849
1988	17,307	1,977	19,284
1989	21,091	1,081	22,172
1990	34,775	918	35,693
1991	18,850	960	19,810
1992	24,174	1,953	26,127

Table A1. (Cont.)

Year	Argentina (t)	Falkland Islands (t)	TOTAL (t)
1993	26,010	1,648	27,658
1994	21,725	900	22,625
1995	23,711	1,989	25,700
1996	22,095	1,789	23,884
1997	21,939	1,658	23,597
1998	25,245	2,317	27,562
1999	21,793	2,822	24,615
2000	15,183	2,061	17,244
2001	19,666	1,770	21,436
2002	17,817	1,442	19,259
2003	14,605	1,636	16,241
2004	17,125	2,694	19,819
2005	18,628	2,422	21,050
2006	20,558	3,159	23,717
2007	20,609	3,746	24,355
2008	17,559	2,263	19,822
2009	16,694	3,506	20,200
2010	16,359	3,790	20,149
2011	16,276	4,073	20,349
2012	10,113	3,688	13,801
2013	6,697	4,242	10,939
2014	5,750	3,022	8,772
2015	5,238	3,307	8,545
2016	3,299	1,867	5,166
2017	2,999	1,692	4,691
2018	3,610	1,521	5,131
2019	2,005	1,765	3,770
2020	2,932	1,647	4,579
2021	2,793	1,767	4,560
2022	1,583	1,415	2,998
2023	1,617	1,469	3,086

Table A2. Abundance indices employed in the JABBA models. CPUE_FF: CPUE from the pooled finfish licences; CPUE_LOL: CPUE from the calamari (Loligo) licences; CPUE_ES: CPUE from the Spanish nation flag vessels; CPUE_FK: CPUE from the Falkland Islands nation flag vessels; CPUE_AY: CPUE from licences A and Y; CPUE_WZ: CPUE from W and Z licences; CPUE_G: CPUE from G licence; SAI: Survey Abundance Index; CPUE1, CPUE2, CPUE3: CPUEs from the Argentine industrial fleet.

YEAR	CPUE_FF	CPUE_LOL	CPUE_ES	CPUE_FK	CPUE_AY	CPUE_WZ	CPUE_G	SAI	CPUE1	CPUE2	CPUE3
1986									115.04		
1987									111.02		
1988									92.11		
1989	19.26	1.61	20.50		35.58				85.60		
1990	19.65	2.97	21.55		40.14	15.59			68.00		
1991	20.69	4.78	30.57		38.74	29.34			77.77		
1992	22.14	3.62	17.00		29.02	39.62			68.41		
1993	19.45	8.96	19.61		45.99	30.09			54.69		
1994	18.45	2.95	19.17		45.99	28.58			53.94		
1995	20.86	4.09	21.53		49.71	32.76			43.83		
1996	20.43	2.86	20.01	18.57	40.71	33.36			33.34		
1997	21.57	0.75	21.48	21.99	51.00	32.41	31.08		28.73		
1998	25.05	0.22	25.37	24.04	72.97	33.86	28.25			26.24	
1999	28.49	0.40	30.69	22.78	59.49	39.54	33.25			27.53	
2000	27.34	1.26	30.62	20.16	62.44	38.67	30.24			27.31	
2001	28.94	0.80	33.01	21.08	67.22	45.32	30.59			37.41	
2002	20.95	1.80	23.11	16.73	32.67	34.34	20.03			40.97	
2003	21.61	7.54	23.92	16.07	36.41	36.85	21.16			31.70	
2004	30.95	2.32	36.46	21.68	73.78	49.57	20.59			28.14	
2005	33.94	2.49	36.38	25.31	59.69	51.68	30.22			32.47	
2006	36.39	0.86	34.50	35.68	69.69	51.05	34.07			34.74	
2007	47.86	3.97	50.69	35.57	76.70	69.74	33.93			30.16	
2008	31.49	0.64	31.33	28.81	52.39	39.85	25.46			25.23	
2009	42.60	0.55	41.79	40.51	79.89	52.06	27.54				20.53
2010	56.15	0.31	59.15	42.65	98.29	57.60	41.13	36.57			13.05
2011	53.26	1.82	54.63	43.29	92.09	55.15	49.93	59.00			15.88
2012	58.23	0.59	56.11	58.42	117.76	68.64	38.45				12.26
2013	53.84	0.73	55.05	43.81	94.35	76.48	31.07				18.11
2014	56.08	0.45	53.18	47.43	84.98	67.99	34.44				19.24
2015	46.54	0.12	44.02	48.49	77.50	63.34	32.30	58.15			11.48
2016	38.90	1.17	37.24	37.04	64.89	55.93	33.24	22.65			7.90
2017	44.28	0.63	48.92	25.06	76.09	92.91	31.23	13.10			14.13
2018	48.33	0.24	47.86	41.63	89.51	70.80	39.00	10.91			20.58
2019	41.51	0.57	41.25	37.06	81.53	63.65	39.86	16.34			16.58
2020	36.18	0.26	36.63	27.45	66.51	55.96	29.59	13.84			18.00
2021	43.14	0.37	40.50	48.05	79.17	63.25	41.40	10.11			
2022	43.94	1.36	43.01	42.06	73.78	114.59	48.55	12.38			
2023	42.91	0.16	41.45	42.17	69.47	130.32	46.79	18.94			

Table A3. Standard Errors (SE) employed in the JABBA models. SE_FF: SE from the pooled finfish licences; SE_LOL: SE from the calamari (Loligo) licences; SE_ES: SE from the Spanish nation flag vessels; SE_FK: SE from the Falkland Islands nation flag vessels; SE_AY: SE from licences A and Y; SE_WZ: SE from W and Z licences; SE_G: SE from G licence; SE_SAI: SE from the Survey Abundance Index.

YEAR	SE_FF	SE_LOL	SE_ES	SE_FK	SE_AY	SE_WZ	SE_G	SESAI
1989	0.109	0.707	0.063		0.293			
1990	0.113	0.708	0.073		0.300	0.209		
1991	0.104	0.725	0.065		0.298	0.159		
1992	0.103	0.721	0.064		0.300	0.157		
1993	0.107	0.719	0.066		0.303	0.160		
1994	0.108	0.716	0.067		0.314	0.160		
1995	0.107	0.726	0.060		0.312	0.159		
1996	0.108	0.731	0.064	0.212	0.316	0.160		
1997	0.109	0.742	0.064	0.203	0.304	0.161	0.120	
1998	0.107	0.741	0.058	0.209	0.300	0.161	0.082	
1999	0.107	0.737	0.057	0.207	0.300	0.160	0.083	
2000	0.108	0.786	0.059	0.208	0.299	0.161	0.090	
2001	0.108	0.732	0.060	0.207	0.300	0.161	0.086	
2002	0.108	0.722	0.060	0.207	0.300	0.161	0.086	
2003	0.108	0.769	0.060	0.207	0.300	0.160	0.094	
2004	0.108	0.734	0.060	0.207	0.298	0.160	0.098	
2005	0.108	0.713	0.058	0.206	0.297	0.160	0.125	
2006	0.106	0.712	0.054	0.204	0.296	0.160	0.086	
2007	0.106	0.707	0.053	0.205	0.296	0.160	0.084	
2008	0.106	0.707	0.053	0.205	0.296	0.160	0.081	
2009	0.106	0.715	0.053	0.205	0.296	0.160	0.081	
2010	0.106	0.719	0.053	0.205	0.296	0.160	0.079	0.034
2011	0.106	0.708	0.053	0.205	0.296	0.160	0.079	0.037
2012	0.106	0.714	0.052	0.205	0.296	0.160	0.078	
2013	0.106	0.713	0.052	0.205	0.296	0.159	0.080	
2014	0.107	0.719	0.053	0.206	0.296	0.160	0.082	
2015	0.107	0.729	0.052	0.208	0.297	0.160	0.080	0.033
2016	0.108	0.709	0.054	0.209	0.297	0.162	0.083	0.038
2017	0.108	0.713	0.056	0.212	0.296	0.165	0.087	0.033
2018	0.109	0.720	0.057	0.209	0.296	0.166	0.085	0.045
2019	0.109	0.715	0.056	0.213	0.296	0.163	0.079	0.045
2020	0.109	0.718	0.056	0.215	0.297	0.163	0.082	0.036
2021	0.109	0.716	0.057	0.214	0.296	0.164	0.082	0.035
2022	0.110	0.713	0.058	0.215	0.296	0.184	0.092	0.034
2023	0.109	0.728	0.057	0.210	0.296	0.186	0.089	0.033

Table A4. Coefficients of Variation (CV) employed in the JABBA models. CV_FF: CV from the pooled finfish licences; CV_LOL: CV from the calamari (Loligo) licences; CV_ES: CV from the Spanish nation flag vessels; CV_FK: CV from the Falkland Islands nation flag vessels; CVAY: CV from licences A and Y; CVWZ: CV from W and Z licences; CVG: CV from G licence; CVSAI: CV from the Survey Abundance Index; CV1, CV2, CV3: CVs from the Argentine industrial fleet.

YEAR	CVFF	CVLOL	CV_ES	CV_FK	CVAY	CVWZ	CVG	CVSAI	CV1	CV2	CV3
1986									0.40		
1987									0.47		
1988									0.38		
1989	0.30	0.29	0.31		0.30				0.42		
1990	0.30	0.29	0.32		0.30	0.35			0.37		
1991	0.29	0.31	0.31		0.30	0.30			0.30		
1992	0.29	0.31	0.31		0.30	0.29			0.27		
1993	0.30	0.30	0.31		0.30	0.30			0.25		
1994	0.30	0.30	0.31		0.32	0.30			0.22		
1995	0.30	0.31	0.30		0.31	0.30			0.18		
1996	0.30	0.32	0.31	0.30	0.32	0.30			0.18		
1997	0.30	0.33	0.31	0.30	0.31	0.30	0.33		0.16		
1998	0.30	0.33	0.30	0.30	0.30	0.30	0.30			0.29	
1999	0.30	0.32	0.30	0.30	0.30	0.30	0.30			0.32	
2000	0.30	0.37	0.30	0.30	0.30	0.30	0.30			0.33	
2001	0.30	0.32	0.30	0.30	0.30	0.30	0.30			0.32	
2002	0.30	0.31	0.30	0.30	0.30	0.30	0.30			0.32	
2003	0.30	0.35	0.30	0.30	0.30	0.30	0.31			0.31	
2004	0.30	0.32	0.30	0.30	0.30	0.30	0.31			0.28	
2005	0.30	0.30	0.30	0.30	0.30	0.30	0.34			0.30	
2006	0.30	0.30	0.30	0.30	0.30	0.30	0.30			0.28	
2007	0.30	0.29	0.30	0.30	0.30	0.30	0.30			0.28	
2008	0.30	0.29	0.30	0.30	0.30	0.30	0.29			0.27	
2009	0.30	0.30	0.30	0.30	0.30	0.30	0.29				0.28
2010	0.30	0.30	0.30	0.30	0.30	0.30	0.29	0.20			0.29
2011	0.30	0.29	0.30	0.30	0.30	0.30	0.29	0.20			0.29
2012	0.30	0.30	0.30	0.30	0.30	0.30	0.29				0.31
2013	0.30	0.30	0.30	0.30	0.30	0.30	0.29				0.31
2014	0.30	0.30	0.30	0.30	0.30	0.30	0.30				0.31
2015	0.30	0.31	0.30	0.30	0.30	0.30	0.29	0.20			0.32
2016	0.30	0.29	0.30	0.30	0.30	0.30	0.30	0.20			0.32
2017	0.30	0.30	0.30	0.30	0.30	0.30	0.30	0.20			0.31
2018	0.30	0.30	0.30	0.30	0.30	0.30	0.30	0.21			0.29
2019	0.30	0.30	0.30	0.30	0.30	0.30	0.29	0.21			0.30
2020	0.30	0.30	0.30	0.31	0.30	0.30	0.30	0.20			0.29
2021	0.30	0.30	0.30	0.31	0.30	0.30	0.29	0.20			
2022	0.30	0.30	0.30	0.31	0.30	0.32	0.31	0.20			
2023	0.30	0.31	0.30	0.30	0.30	0.32	0.30	0.20			

MSY reborn
1990s

by Pamela M. Mace

Up springs MSY.
No, it didn't die.
It just metamorphosed
To be better-for-those
Who wrote of its woes.

Ahead of his time was Larkin,
To him we would always harken.
But MSY has a cause,
It's the focus of many laws.

It finally discovered the key:
"Please, don't take all of me.
Just take a quarter,
Leave more in the water.
(For my son and my daughter)
You know that you ought'a."

Now MSY has found a new niche,
And all that's needed is to make the pitch
That production from the oceans is finite,
And civilized people should *not* have a pie-fight.